MAST CELLS AND INTERFERONS AS A NOVEL APPROACH TO IMMUNOTHERAPY USING A MURINE BREAST CANCER MODEL

by

Owen Crump

Submitted in partial fulfillment of the requirements

for the degree of Master of Science

at

Dalhousie University

Halifax, Nova Scotia

March 2020

TABLE OF CONTENTS

LIST OF TABLES

LIST OF FIGURES

ABSTRACT

Breast cancer has the second highest mortality in women diagnosed with cancer-related disease. Immunotherapy, a strategy targeting regulation of the immune system to combat tumour growth has demonstrated therapeutic potential. Mast cells are sentinel cells of the innate immune system, known to secrete mediators with anti-tumour properties, such as interferons (IFNs) that can enhance anti-tumour immunity or directly kill tumour cells. The feasibility of mast cell-mediated IFN delivery was examined. Mast cells were genetically modified to express a target IFN following induction. This technology was tested using mast cell-deficient mice. Local mast cell reconstitution, with control mast cells, resulted in significant breast tumour growth reduction, in wild type and mast cell-deficient animals. Mast cells modified to deliver local IFN-α1 on induction yielded no further reduction. Our findings implicate local mast cells as a potentially important therapeutic target in breast cancer while treatments using IFN delivery require further optimization.

LIST OF ABBREVIATIONS AND SYMBOLS USED

ACT	Adoptive cell transfer
ANOVA	Analysis of variance
APC	Allophycocyanin
ATCC	American Type Culture Collection
AV	Annexin V
BMMC	Bone marrow-derived mast cells
BSA	Bovine serum albumin
BV	Brilliant Violet
CBMC	Cord blood-derived mast cells
CD	Cluster of differentiation
Cpa3	Carboxypeptidase A3
CTLs	Cytotoxic T lymphocytes
CTLA-4	Cytotoxic T-lymphocytes-associated protein 4
CXCL	Chemokine C-X-C motif ligand
Cy7	Cyanine 7 conjugate
DC	Dendritic cells
ddPCR	Droplet digital PCR
DMEM	Dulbecco's Modified Eagle's Medium
dsRNA	Double-stranded RNA
ECM	Extracellular matrix
ER	Estrogen receptor
FBS	Fetal bovine serum
FcεRI	Fc epsilon receptor I
FITC	Fluorescein isothiocyanate
FVD	Fixable viability dye
GAS	Gamma-activated response element
GFP	Green fluorescent protein
Gusb	glucuronidase beta
H&E	Hematoxylin and eosin
HCl	Hydrochloric acid
HER-2	Human epidermal growth factor receptor 2
HK	Hello kitty
Hprt	Hypoxanthine-guanine phosphate
Ifit1	Interferon induced protein with tetratricopeptide repeats 1
IFN	Interferon
IFNAR1	Interferon alpha receptor 1
IFNAR2	Interferon alpha receptor 2
IFNλR1	Interferon lambda receptor 1
IgE	Immunoglobulin E
IL	Interleukin
IL10Rβ	IL-10 receptor beta
IMF	Immunofluorescence
IRF	Interferon regulatory factor
ISG	Interferon-stimulated gene

ISGF3	Interferon-stimulated gene factor 3
ISRE	Interferon-stimulated response element
JAK	Janus kinase
LB	Lysogeny broth
LF3000	Lipofectamine 3000
LTB_4	Leukotriene B4
mAbs	Monoclonal antibodies
Mcl-1	Induced myeloid leukemia cell differentiation protein 1
MDSCs	Myeloid-derived suppressor cells
MHC	Major histocompatibility complex
mRNA	Messenger RNA
Mx1	MX dynamin like GTPase 1
NK	Natural killer
PAMPs	Pattern-associated molecular patterns
PBS	Phosphate buffered saline
PD-1	Programmed cell death protein 1
PE	Phycoerythrin
PerCP	Peridinin chlorophyll-A protein
PFA	Paraformaldehyde
PR	Progesterone receptor
PRRs	Pattern recognition receptors
RIG-I	Retionoic acid-inducible gene I
RPMI	Roswell Park Memorial Institute
RSV	Respiratory syncytial virus
RT-qPCR	Real time quantitative polymerase chain reaction
SOCS	Suppressor of cytokine signaling
STAT	Signal transducer and activator of transcription
Tbp	TATA-box binding protein
Th	T helper cells
TLR	Toll-like receptors
TME	Tumour microenvironment
TNBC	Triple negative breast cancer
TNF	Tumour necrosis factor
T_{regs}	Regulatory T cells
TYK	Tyrosine kinase
WT	Wild type
VEGF	Vascular endothelial growth factor
Ywhaz	Tryptophan 5-monooxygenase activation protein zeta
α	Alpha
β	Beta
ε	Epsilon
γ	Gamma
xg	Gravity
κ	Kappa
λ	Lambda
ω	Omega

ζ	Zeta
°C	Degrees Celsius
g	Grams
ng	Nanogram
µg	Microgram
mg	Milligram
µL	Microlitre
mL	Milliliter
µM	Micromolar
mM	Millimolar
N	Normal
U	Units

ACKNOWLEDGEMENTS

I would like to thank my supervisor Dr. Jean Marshall for her guidance and mentorship throughout my duration as a Master's student. Dr. Marshall provided me with my first opportunity to explore scientific research and with her support and encouragement has helped to kickstart my journey in the immunology field and taught me with patience and poise. I would also like to thank Dr. Ian Haidl for his involvement in this project. His mentorship during my Master's thesis played a pivotal role in shaping the direction of the project and in developing individual experiments. I would also like to thank my committee members Dr. Brent Johnston and Dr. Chris Richardson for their respected feedback and contributions to this research.

I would also like to acknowledge members of the Marshall lab, both past and present for their assistance on this research. In particular, Dr. Liliana Portales-Cervantes, Dr. Dihia Meghnem, Dr. Ava Vila-Leahey, Bassel Dawod, Stephanie Legere, Edwin Leong, Dr. Barakat Alrashdi, and Mark Hanes should be recognized for their insight into this project and their assistance with various experiments and data interpretation. I would also like to thank all of the laboratory technical staff from the Marshall lab, including Maria Vaci, Nong Xu, and Alexander Edgar for their assistance in this project. I also want to acknowledge members of Dr. Shashi Gujar's lab, Dr. Barry Kennedy and Youra Kim, for their collaborations in the use of the ID8 ovarian cancer model highlighted in this thesis. I would also like to thank the Flow Cytometry CORES facility members Derek Rowter and Mary Ann Trevors for their assistance with data acquisition, and all the of staff at the Charles Tupper Animal Care Facility.

Finally, I would like to thank all of my friends and family in Halifax and Toronto for their endless support throughout the past two years. To my parents and roommates, thank you for providing endless encouragement and positivity throughout this process. You and all of my co-workers provided the proper atmosphere to motivate me to accomplish this research and to thoroughly enjoy my first experience in a scientific research setting. This research would not have been possible without you.

CHAPTER 1: INTRODUCTION

1.1 Cancer, the anti-tumour immune response, and immunotherapy

1.1.1 Cancer statistics on a global scale

Cancer continues to be a major global health threat and was the second leading cause of death in 2018, killing 9.6 million people across the world[1]. Cancer incidence and mortality continue to grow rapidly worldwide, with 1 in 5 men and 1 in 6 women estimated to develop the disease over their lifetime, and 1 in 8 men and 1 in 10 women estimated to die from the disease as reported by GLOBOCAN in 2018[2]. The Canadian Cancer Society estimated that 1 in 2 Canadians would be diagnosed with cancer in their lifetime and 1 in 4 would succumb to the disease[3]. The World Health Organization has suggested that incidence rates are expected to climb by 70% over the next two decades[4]. The five most common types of cancer, as recorded in 2018, are lung, breast, colorectal, prostate, and non-melanoma skin cancer, while cancers causing the highest number of deaths were lung, colorectal, stomach, liver and breast cancer[1]. In 2018, Canadian women and men were commonly diagnosed with breast cancer and prostate cancer, respectively, and the Canadian Cancer Society reported the collective five-year survival rate for a cancer diagnosis was 63%[3]. The development of cancer can be affected by socioeconomic factors, sex, age or genetic predisposition. Current research continues to focus on identifying links between these factors to identify prevention and treatment options[4]. A key step in identifying more targeted treatment methods is to further understand and elucidate the cellular and biological processes in a growing tumour.

1.1.2 Inflammatory response to nascent tumour development

In the biological development of cancer, multiple genetic mutations can accumulate in a single cell that results in the formation of an abnormal tumour cell, which can be characterized by alterations in cell surface proteins[5]. Tumour cells can release these antigens into the bloodstream or a local tissue site that may be recognized by the immune system, which consists of the innate and adaptive immune compartments. The innate immune system, known for its rapid response to pathogen invasion, consists of subsets such as neutrophils, macrophages, dendritic cells (DCs), eosinophils, basophils, mast cells, and natural killer (NK) cells. Some innate immune cells, such as NK cells, are important effector cells in early tumour clearance, recognizing abnormalities in tumour cell surface protein expression, characterized by a lack of the universally expressed major histocompatibility complex I (MHCI) or other inhibitory proteins. NK cell activation occurs in response to this "missing self" phenotype, resulting in release of cytotoxic mediators that result in tumour cell death[5]. Other innate immune components, such as DCs, may take up tumour-associated antigens at the local tissue site and present processed antigens to activate members of the adaptive immune system, consisting of B and T cells, found at distal lymph node sites[6]. Activation of these adaptive immune cells forms highly specific anti-tumour responses, as activated cytotoxic T lymphocytes (CTLs) migrate to the site of tumour formation and infiltrate the tumour bed to elicit killing of individual cancer cells, mediated by recognition of the tumour-specific antigens presented on MHCI[6]. Tumour cell death releases more tumour-associated antigens that increase the breadth and depth of the anti-tumour inflammatory response[6]. Many tumours are likely prevented from developing through these mechanisms. However, despite

immune surveillance, macroscopic tumours still develop in the presence of a functioning immune system and with detectable immune infiltrate residing inside the tumour[7]. Current evidence suggests the adaptive immune system effectively eliminates highly immunogenic tumour cells, while non-immunogenic tumour cells, differentiated through greater genomic instability, are positively selected, cause further DNA mutation, and subsequently grow into a larger mass, a process coined as immunoediting[7,8]. This leads to the tumour's resistance to immune destruction, which has been widely accepted as a biological hallmark of cancer[9].

1.1.3 Immunosuppressive environment of growing tumours

In the early 2000's, there were thought to be six biological hallmarks of cancer cells that differentiated them from normal healthy cells: sustained proliferative signaling, resistance to growth inhibitory signals, resistance towards cell death, induction of angiogenesis (formation of new blood vessels), replicative immortality and activation of invasion and metastasis[10]. Research in the last decade has expanded this list of hallmarks after further identifying the interplay between tumour cells and other cellular players and multi-cellular networks that form the tumour microenvironment (TME) of macroscopic tumours. The cellular components include immune cells, adipose cells, neuroendocrine cells, and fibroblasts, while multi-cellular components include the extracellular matrix (ECM) and blood and lymphatic networks[11]. The immune system normally functions to identify and eliminate nascent tumours as previously discussed. However, tumour cell evasion of the immune response, local hypoxia, and necrosis can result in chronic

inflammation that can, conversely, contribute to tumour progression, and this has more recently been considered as another biological hallmark of this disease[9].

Chronic cancer-associated inflammation at the tumour site can exacerbate tumour progression[12]. Many immune cell subsets infiltrating the TME are known to exhibit immunosuppressive functions. Some innate immune cell types, such as macrophages and neutrophils, polarize towards immunosuppressive M2 and N2 phenotypes, respectively, which are primarily pro-tumorigenic, as exemplified through secretion of anti-inflammatory cytokines such as interleukin (IL) -10 and transforming growth factor beta[13,14]. The ability of DCs to mediate potent anti-tumour responses through priming $CD8^+$ CTLs and NK cells to enhance their cytotoxic function is well established. Despite these actions, dysfunction of DCs in cancer has also been documented, as tumour-infiltrating DCs are defective in their differentiation and activation and are poor inducers of immune responses[15]. Other tumour-infiltrating cells, including myeloid-derived suppressor cells (MDSCs) and regulatory T cells (T_{Regs}), accumulate in growing tumours over time and function to suppress other infiltrating effector cells and induce a state of immune tolerance[16]. Other adaptive immune system components, including $CD4^+$ T helper (Th) cells, and B cells, exhibit tumour-killing abilities. B cells produce tumour-specific antibodies that bind to tumour cells to promote lysis in the presence of complement proteins, while $CD4^+$ T cells can facilitate the optimal expansion, trafficking and effector functions of CTLs[17,18]. The activation and number of local T and B cells has been associated with better prognostic outcomes in some cancers such as breast and ovarian cancer[19,20]. However, the process of immunoediting can lead to immune evasion by tumour cells and chronic inflammation at the tumour site that can upregulate

immunoregulatory pathways that inhibit adaptive immune responses. For example, tumour-infiltrating CTLs are known to express inhibitory receptors in the TME, including programmed cell-death protein 1 (PD-1) and cytotoxic T-lymphocyte-associated protein 4 (CTLA-4). These receptors bind to ligands on antigen-presenting cells or tumour cells that downregulate immune responses, leading to immune tolerance and ultimately tumour progression[5]. Because of the immunosuppressive phenotype of cancer, therapeutic research has focused on targeting immunoregulatory pathways to enhance the anti-tumour immune response and eliminate macroscopic tumours, an approach which has been successful, coined immunotherapy.

1.1.4 Immunotherapy as a treatment approach

The term immunotherapy refers to the manipulation of the immune response to treat disease. Immunotherapy has emerged within the last decade as an efficacious method of targeting and eliminating cancer cells. The clinical efficacy of immunotherapy was successfully demonstrated in a 2010 study that used anti-CTLA-4 antibodies to counteract CTL inactivation in melanoma patients, resulting in improved patient survival[21]. Research has since demonstrated that immunotherapy improves long-term patient survival compared to more common methods of treatment, such as tumour cell-targeted therapies and chemotherapy, and is most effective when used in combination with other treatment methods[22]. Immunotherapy can be classified into passive and active subcategories[23]. Passive immunotherapies use donated or laboratory-made immune system components to fight cancer cells, while active immunotherapies aim to directly stimulate the host immune system to enhance tumoricidal function[23]. Modern active

immunotherapies include injection of immunostimulatory cytokines, immunomodulatory monoclonal antibodies (mAbs), or administration of peptide- and DNA-based cancer vaccines, all of which enhance anti-tumour inflammatory response[23]. Common passive immunotherapies include tumour-targeting mAbs, oncolytic viruses, and adoptive cell transfer (ACT) therapy[23]. In ACT, circulating or tumour-infiltrating leukocytes are collected from the patient before selecting, modifying and expanding the desired immune cell type, *ex vivo*, and subsequently re-administering the modified cells to patients, often in combination with other immunostimulatory adjuvants to enhance the anti-tumour immune response[23,24]. CTLs and NK cells are most commonly used in ACT therapies as the major effector cells in tumour clearance due to their potent effects[24,25]. DCs are also targeted in ACT therapies, which can involve pulsing these cells with tumour-specific antigens or tumour lysates before re-administeration to patients to elicit a targeted immune response through activation of $CD4^+$ and $CD8^+$ T cells[26]. ACT has shown promising results in a wide variety of cancer types, including metastatic melanoma, renal cell carcinoma and lung cancer[27-28].

Immunotherapies, while effective, are not without disadvantages, and further research is needed to optimize cost of treatment and identify broad biomarkers that can be targeted across multiple tumour types[29,30]. Patient response to immunotherapy is often unpredictable, and is tumour- and patient-specific, with a minority of patients showing effective results[29]. Even the most common forms of immunotherapy, such as anti-PD-1 or anti-CTLA-4 mAbs, have shown only a 15-25% response rate in patients with various tumour types in human clinical trials[29]. The worldwide cost of immunotherapies is also high, as the use of anti-PD-1 mAb (nivolumab) in renal cell carcinoma patients was $2.7

billion in 2014[30]. Additionally, systemic administration of some immune adjuvants, such as IL-2, can result in life-threatening toxicity from potent stimulation of the immune system, which can result in sepsis-like syndrome and cytokine storms[31]. These findings reinforce the requirement for further investigation to optimize cost, maximize therapeutic efficacy while minimizing toxicity, and to elucidate undiscovered tumour biomarkers.

1.1.5 Mouse models of cancer

To further define the intricacies surrounding the cellular interactions between the immune system and tumours, mouse models can be used as a host for transplantable tumours. Mice possess many physiological and molecular similarities to humans and these models provide many advantages to cancer research[32]. The growth of solid tumours in mice replicates several facets of tumorigenesis that cannot be assessed in cell cultures, such as angiogenesis and metastasis[32]. In syngeneic murine cancer models, tumour cell lines derived from specific tissue sites can be implanted into the same site in live mice to assess tumour growth in that specific tissue microenvironment in animals of a matching genotype[33]. Characteristics of tumour progression in syngeneic models depend on a number of factors including, the number of cells injected, the site of implantation, and the inocula[33]. This study primarily focused on three syngeneic mouse models derived from C57BL/6 mice: E0771 mammary adenocarcinoma, ID8 ovarian cancer, and B16-F10 melanoma. The E0771 model is a model of breast cancer that has not been as well characterised as more frequently used models. The literature reports both triple negative breast cancer (TNBC) or estrogen receptor (ER) positive subtypes[34,35]. In our laboratory, *in vitro*, this cell line does not demonstrate ER expression. The model is applied via

subcutaneous injection to the mouse mammary fat pad, forming a solid mass that has metastatic potential, although these results are similarly controversial[35,36]. The B16-F10 model, a variant of the parent B16 melanoma cell line, is a metastatic model established via subcutaneous injection into the skin[37]. The ID8 model is derived from spontaneous transformation of mouse ovarian surface epithelial cells through multiple passaging of normal cells *in vitro*[38]. These cells are injected into the peritoneum of mice to form primary tumours with the ovarian stroma, with tumour foci formed throughout the peritoneum, causing extensive ascites collection in the peritoneal cavity over time[38]. These tumours models can be applied in genetically engineered mouse models to determine the role of a specific immune cell type, cytokine or protein in cancer pathogenesis[39]. Genetically engineered mouse models were utilized in this study that exhibit a loss-of-function phenotype through an inversion in the gene c-kit, resulting in depletion of mast cells.

1.2 Interferons

1.2.1 Introduction to interferons

Interferons (IFNs) are a group of secreted cytokines known for their potent anti-viral activity. IFNs can be subcategorized into 3 distinct types: type I, II, and III[40]. Type I IFNs consist of 17 subtypes in humans and 18 in mice, consisting of multiple IFN-α subtypes (13 in humans, 14 in mice), and a single IFN-β, IFN-ε, IFN-κ, IFN-ω (found in humans) and IFN-ζ (found in mice) subtypes[40,41]. Type I IFNs are categorized by their limited structural similarity and binding to a shared heterodimeric receptor, consisting of two subunits, IFN-α receptor 1 (IFNAR1) and IFN-α receptor 2 (IFNAR2)[40,41,42]. Expression

of the type I IFN receptor is ubiquitous across all cell types[40]. Type II IFN has one member, IFN-γ, which is primarily secreted by activated NK and T cells, possessing potent immunomodulatory effects and distinguished by low sequence similarity to other IFNs[40,43]. IFN-γ binds to a ternary homodimer receptor complex, consisting of two chains of IFN-γ receptor 1 and two chains of IFN-γ receptor 2[43]. The IFN-γ receptor complex displays broad tissue expression patterns in humans and can be found on immune, epithelial and endothelial cells[44]. Type III IFNs consist of 4 subtypes of IFN-λ, -λ1, -λ2, -λ3, and -λ4, found in humans, while only two functional subtypes, IFN-λ2 and IFN-λ3, are known in mice[41,45,46]. IFN-λ cytokines bind to the type III IFN receptor consisting of two heterodimeric receptor subunits, IFN-λ receptor 1 (IFNλR1) and IL-10 receptor β (IL10Rβ), a subunit shared with the IL-10 family[45]. Expression of the type III IFN receptor is not ubiquitous, found only on the surface of epithelial cells (e.g. lung, intestinal, hepatocytes and in many epithelial-derived cancers) and a select subset of immune cells, most notably, neutrophils and DCs[40]. Due to the limited tropism of type III IFNs, and their efficiency of controlling viral infection at specific sites, exemplified in the gastrointestinal tract, this subtype is thought to provide protection at mucosal surfaces[40,47]. While Type I and III IFNs are genetically distinct and utilize different receptors, they were initially assumed to be redundant due to similar signalling pathways[41]. Current research continues to elucidate major differences in the regulation, signaling, and function of type I and III IFNs.

1.2.2 Type I and III IFN receptor binding, signaling and pathway regulation

IFNs can be produced in response to a broad range of pathogens and play a key role in combatting the spread of infection by stimulating and controlling inflammation, which is particularly well described in the context of viral infection. After pathogen infection, viral-sensing pattern recognition receptors (PRRs), including toll-like receptors (TLRs), retinoic acid-inducible gene (RIG-I) type receptors and NOD-like receptors, can recognize numerous viral pathogen-associated molecular patterns (PAMPs) (e.g. DNA, double-stranded RNA (dsRNA), single-stranded RNA) to induce production of IFNs[48]. The binding of PAMPs to PRRs leads to activation of the transcription factors, such as nuclear factor kappa-light-chain-enhancer of activated B cells and IFN regulatory factor 3 (IRF3), to produce IFN-β[49]. Type I IFNs can act in an autocrine, paracrine, or systemic manner when binding to the type I IFN receptor to induce further IFN production[40]. A visual representation of the type I and III IFN signaling pathways are shown in **Figure 1.1**.

Type I IFNs bind the type I IFN receptor with high affinity to the extracellular component of IFNAR2 subunit, before binding to the IFNAR1 subunit, which induces a conformational change to the intracellular component of the receptor subunits[40]. IFNAR engagement activates the Janus kinase (JAK) – signal transducer and activator of transcription (STAT) pathway[50]. During canonical signaling, intracellular receptor-associated kinases, including tyrosine kinase 2 (TYK2) and JAK1 that are associated with IFNAR1 and IFNAR2 respectively, phosphorylate STAT1 and STAT2 proteins after IFN binding[50]. These phosphorylated proteins dimerize and form a transcription complex with IRF9 known as IFN-stimulated gene factor 3 (ISGF3), which translocates into the nucleus

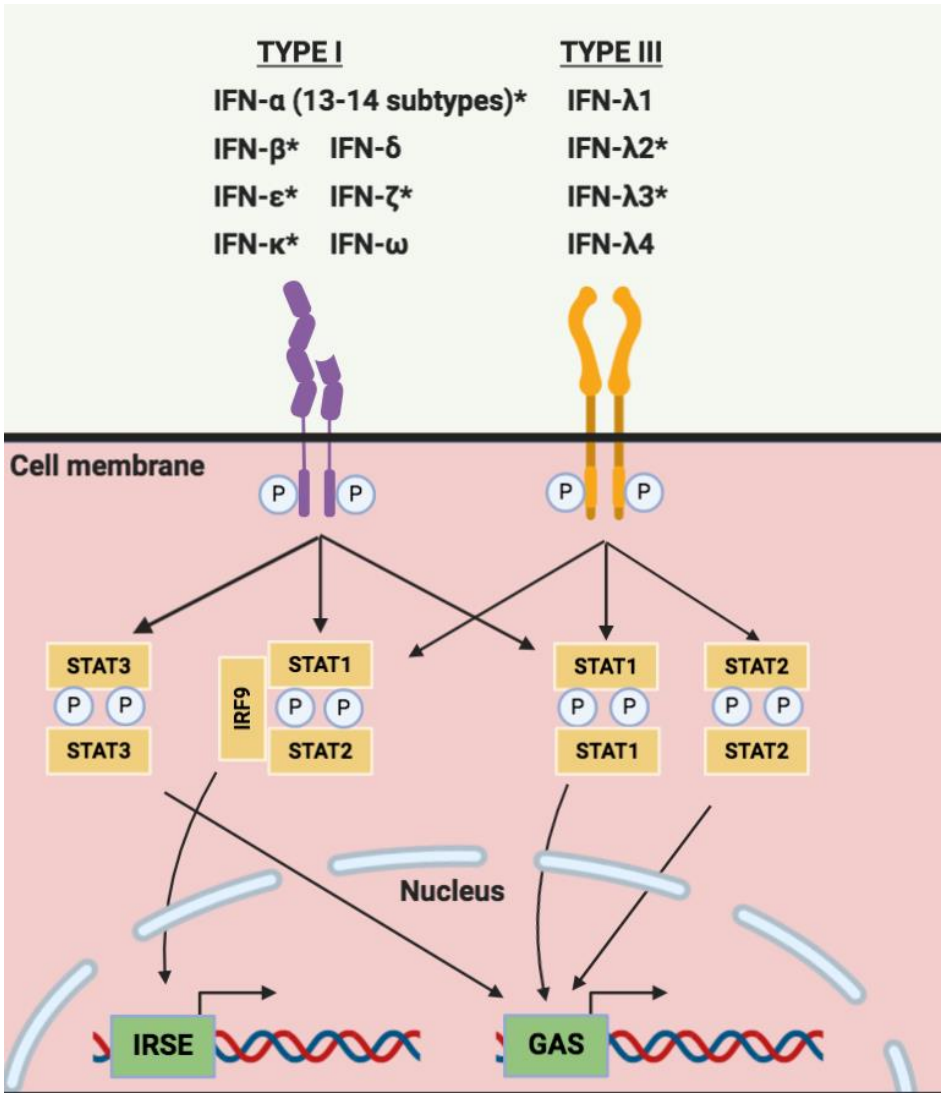

Figure 1.1. Overview of Type I and III IFN Signaling Pathway. The type I IFN pathway is initiated by type I cytokines binding directly to the extracellular portion of IFNAR2, triggering its dimerization with IFNAR1 to initiate an intracellular signaling cascade. Binding of the IFN induces a conformational change to JAK1 and TYK2, associated with IFNAR2 and IFNAR1 respectively, which phosphorylate STAT1 and STAT2 proteins. These phosphorylated STAT proteins dimerize and form a transcription complex with IRF9, known as ISGF3. This transcription complex translocates to the nucleus to bind to ISRE and activate a subset of genes known as ISGs, many of which possess pro-inflammatory and anti-tumour functions. Alternatively, STAT proteins may form homodimers once phosphorylated and translocate to the nuclear to bind to the GAS promoter to induce a different subset of inflammatory response genes. STAT1, STAT2, and STAT3 have been suggested to form homodimers in this manner. During type III IFN signaling, JAK1 and TYK2, which are associated with IFNλR1 and IL10β respectively, signal through the same downstream pathway as type I IFNs. Each cytokine in the respective type I and III IFN families are compiled above the receptor as documented in humans, with the asterisks depicting IFNs shared in the mouse immune system[52].

to bind to IFN-stimulated response element (ISRE)[50]. This activates the production of a subset of genes known as IFN-stimulated genes (ISGs), which encode proteins that can restrain viruses by several mechanisms, including inhibition of viral transcription, translation, and replication[50]. Alternatively, the type I IFN pathway may also phosphorylate STAT1 or STAT3, which can form homodimers and bind to the gamma-activated response element (GAS) to induce an alternative subset of inflammatory response genes[51,52].

Type III IFNs are also known to signal through the same JAK-STAT system as the type I IFNs. IFN-λ binds with high affinity to IFNλR1, which recruits the low affinity receptor, IL10Rβ, to form the ternary signaling complex, resulting in the phosphorylation of STAT1 and STAT2 and recruitment of IRF9 to form ISGF3 to begin transcription of ISGs[41]. Type III IFNs can also form STAT1 homodimers that signal through the GAS promoter and largely induce the same subset of ISGs as type I IFNs[53,54]. While type I and III IFNs are known to share signaling pathways, there are subtle differences that contribute to their unique functions. Key differences between type I and III IFN responses are highlighted by their kinetics, in which type I IFNs induce rapid and more potent ISG induction than type III IFNs, although type III IFNs elicit more sustained induction[55,56]. These differences in kinetics between type I and III IFNs have been theorized to be determined by differential activation of promoter-binding response elements, leading to more potent ISG induction[57]. For example, type I IFNs, but not type III IFNs, induced significant IRF1 expression in human hepatocytes, which was associated with significant upregulation of chemokine C-X-C motif ligand (CXCL) 9, CXCL10, and CXCL11 gene expression[57]. The site of PAMP engagement has also been

documented to initiate either type I or III IFN responses, exemplified by TLR4, which initiates a type I IFN response when binding PAMPs in endosomes and producing type III IFNs when engaged at the plasma membrane[58,59]. Given that type III IFN receptors are found on epithelial cells and at mucosal barriers, this group is thought to act as a first-line defence that is less inflammatory and concentrated at anatomic barriers, while type I IFNs act primarily as an systemic inflammatory response once this first defence is surpassed[60].

Considering that IFNs, especially type I, can induce potent or sustained inflammatory responses, the pathway is tightly regulated to prevent collateral damage to host tissue. Type I IFN signaling can also be directly regulated through internalization and degradation of IFNAR1, while recycling IFNAR2 back to the plasma membrane after endocytosis[61,62]. No direct degradation of IFNλR1 has been reported, however IL10Rβ levels can be modulated through internalization and degradation[63]. Receptor expression levels can also be modulated by viral infection, as rotavirus is known to downregulate expression of both type III IFN receptor subunits in a lysosomal-dependent manner[64]. Regulation of the IFN response can also be mediated through the JAK-STAT pathway. The suppressor of cytokine signaling (SOCS) 1 and SOCS3 proteins are potent negative regulators of the IFN pathway, often interacting with TYK2 to prevent its phosphorylation[65]. Binding of SOCS1 to TYK2 leads to its destabilization and subsequent downregulation of IFNAR1[66]. Additionally, SOCS1 regulates the type III IFN pathway by reducing phosphorylated STAT1 expression[67]. SOCS proteins are ISGs, produced in response to IFN induction and are considered a negative feedback mechanism for the pathway[67]. IFN-α signaling causes more rapid and transient upregulation of SOCS1 compared to IFN-λ1, which may contribute to the shorter

induction kinetics observed in type I IFN signaling[68,69]. Research has suggested that some negative regulators of IFN pathways have more potent effects on type I IFN signalling than type III. The negative regulatory protein ubiquitin specific protease 18 has been suggested to impair type I IFN signaling, but was dispensable for type III IFN signaling under normal conditions[69]. The IFN pathway is also heavily regulated regarding ISG expression, which is mediated through numerous associated transcription complexes. STAT1-6 can produce numerous combinations of homo- and hetero-dimers that can bind several STAT binding elements found at one or both of the ISRE and GAS promoter regions, allowing for selective expression of ISGs[40]. Heavy positive and negative regulation of the IFN pathway is critical for controlling the inflammatory response and ISG expression signatures are likely dependent on tissue site, dose, and duration of signaling.

1.2.3 Role of type I and III interferons in cancer and some of their differences

Aside from the potent antiviral activity elicited by IFNs, these cytokines have been well-documented for their anti-tumour functions. Both type I and III IFNs can be cytotoxic to tumour cells through induction of programmed cell death, known as apoptosis, and inhibition of cell proliferation and growth, mediated directly through binding to the respective IFN receptor on the tumour cell surface[70,71]. IFN-α and IFN-β are both known to induce pro-apoptotic ISGs, such as STAT2, phosphoinositide-3-kinase, and TNF-related apoptosis inducing ligand death receptors, which result in tumour cell death[72,73]. Of the type I IFNs, IFN-β binds with higher affinity to IFNAR compared to IFN-α, and therefore can induce anti-proliferative and apoptotic effects at a lower dose[74]. Type I

IFNs have also shown anti-angiogenic functions when binding to tumour cells, as tumour vessels have been observed to undergo necrosis and halt production of angiogenic growth factors like vascular endothelial growth factor (VEGF)[75,76]. Type I IFNs are also known to induce upregulation of MHCI molecules on the surface of tumour cells, making them more susceptible to T cell-mediated killing[77]. IFN activation also enhances the cytotoxic activity of effector immune cells to indirectly mediate tumour killing, which will be reviewed below. The anti-tumour effects of type I IFNs are so well-documented that many human clinical trials utilize IFN-α, which has been successfully used to treat many tumour types, including follicular lymphoma, melanoma, and Kaposi sarcoma[78]. Despite these successes, IFN-α-based therapies have been associated with significant side effects and toxicities, which has been attributed to its ubiquitous receptor expression[79]. This associated toxicity has created interest in using IFN-λ as a therapeutic target to determine if its limited receptor expression will coincide with a reduction in clinical side effects.

Similar to type I IFNs, IFN-λ has shown direct killing of tumour cells through induction of apoptosis. Treatment of human colorectal adenocarcinoma cells with IFN-λ mediated G_1/G_0 phase cell cycle arrest and activated apoptosis-associated proteins, a finding that correlated with type III IFN receptor expression[71]. Another group that transfected the B16 melanoma cell line with a DNA vector constitutively expressing IFN-λ2 observed a significant increase in survival rates when tumours cells were transplanted into mice[80]. IFN-λ has similarly exhibited anti-angiogenic effects in the B16 melanoma model and enhanced the cytotoxic ability of neutrophils, macrophages, NK cells and T cells in mouse models of fibrosarcoma[80,81]. IFN-λ has demonstrated therapeutic efficacy in numerous tumour models, including melanoma, lung adenocarcinoma, hepatoma,

colon cancer, prostate adenocarcinoma, and breast cancer[78]. A comparative study between IFN-α and IFN-λ in a mouse model of hepatoma showed that they similarly increased survival rates of implanted mice[82]. Combining IFN-α/λ therapies in the same mouse hepatoma model significantly increased survival rates compared to either IFN alone[83]. While IFN-λ therapies do show promise and potentially contain more benefits than currently available IFN-α therapies, more research is needed to push treatment into clinical trials.

1.2.4 Immunomodulatory effects of IFNs on immune cell subsets

As previously mentioned, type I and III IFNs can enhance activation and cytotoxic function of many different immune cells against tumours, acting on both innate and adaptive immune compartments. In innate immunity, type I IFNs are known to enhance NK cell cytotoxicity and drive upregulation of effector molecules, such as TNF-related apoptosis inducing ligand, which enhance tumour cell killing[84]. Type I IFN stimulation of macrophages also favours polarization towards a pro-inflammatory M1 phenotype[85]. With regards to DCs, type I IFNs can upregulate expression of co-stimulatory molecules, such as CD80, CD86, and MHC molecules, enhancing their ability to process and present antigen to T cells[86]. Type I IFN stimulation of DCs also induces migration to draining lymphatics and enhanced chemokine production[87]. Type I IFNs were shown to enhance cross-presentation activity of CD8α+ DCs, which enhanced tumour-specific priming of infiltrating CTLs and mediated tumour resistance *in vivo*[88]. Mice lacking IFNAR displayed increased tumour growth compared to wild type (WT) mice[88]. In T cell immunity, type I IFNs can act on both CD4+ and CD8+ T cells to polarize development to

favour a Th1 phenotype and reverse commitment to Th2 polarization[89]. Th1 cells are important in mediating cytotoxic responses towards tumour cells. Studies have shown that type I IFNs can enhance the effector function of anti-tumour $CD8^+$ T cell populations and promote survival signaling[90]. The direct effects of type I IFNs on B cells in the context of cancer is still under investigation. However, these cytokines are known to enhance antibody production during viral infection[91].

Similar to type I IFNs, type III IFNs stimulate innate and adaptive immune cells, although the expression pattern of the type III IFN receptor on immune subsets requires further characterization. As a result, the immunomodulatory effects on individual populations remain to be further uncovered. Type III IFNs are known to regulate neutrophil function, preventing their production of reactive oxygen species and neutrophil extracellular traps, limiting tissue damaging effects without changing neutrophil cytokine production[92,93]. Both conventional and plasmacytoid DCs show lower expression levels of IFNλR1, but respond to IFN-λ by upregulating co-stimulatory molecules CD80 and CD86 and increasing production of TNF and IL-12[93,94]. IFN-λ also promotes Th1 polarization through modulation of antigen-presenting function by DCs, as $IFN\lambda R1^{-/-}$ mice showed a reduced ability for Th1 development[95]. Some innate immune cells, such as macrophages, are not well characterized in their expression of IFNλR1 and there is currently little evidence to suggest these cells respond to IFN-λ by ISG induction[96]. Other populations, such as NK cells, express low levels of IFNλR1, but do not show any induction of ISGs nor phosphorylation of STAT1 in response to IFN-λ[83,97]. Despite the absence of a direct response, IFN-λ presence in the TME can enhance NK cell immunity indirectly through upregulating NKG2D-binding ligands, to promote NK cell-mediated

killing[98]. Human and murine T cells have also been reported to express IFNλR1, however there is a lack of evidence demonstrating downstream signaling[99]. T cells can be modulated indirectly by IFN-λ through priming of DCs[88]. Human B cells express significant levels of IFNλR1 and respond to IFN-λ by phosphorylating STAT1 and upregulating ISG transcription[100,101]. IFN-λ-primed B cells exhibit enhanced TLR-mediated cytokine production[101]. While further effort is required to uncover the effects of type III IFNs on the immune system, current research suggests that these cytokines activate multiple immune subsets, making them an attractive target for development of immune therapies that counteract the immunosuppressive TME. The expression patterns of type I and III IFNs on innate and adaptive immune cells is highlighted in **Figure 1.2**.

1.3 Mast cells

1.3.1 Introduction to mast cells

Mast cells have been investigated in the context of cancer and examined for their role in numerous types of human cancer[102]. However, mast cells remain largely un-utilized in the context of immunotherapy and their biological functions in the TME have not been fully described. By gaining a better understanding of the biological actions of mast cells in a tumour setting, we can potentially utilize their anti-tumorigenic functions to reduce or eliminate tumour growth.

Mast cells are an important part of the innate immune system that originate from pluripotent progenitor cells of the bone marrow and differentiate along the hematopoietic lineage[103]. Mast cells briefly transit through the blood as immature precursors before moving into vascularized tissue sites where they undergo maturation to form resident

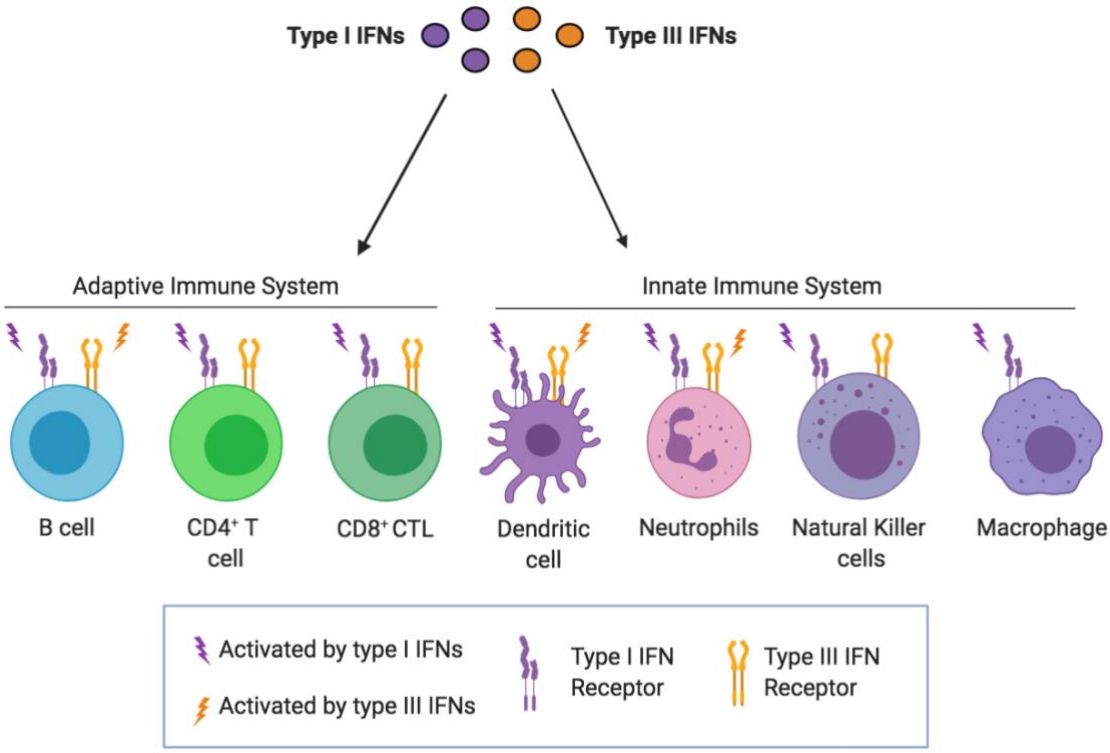

Figure 1.2. Type I and III IFN receptor expression patterns on members of the innate and adaptive immune system and their responses. The type I IFN receptor is ubiquitously expressed across all members of the innate and adaptive immune system listed above and is known to elicit pro-inflammatory functions. These functions can include polarization of effector cells towards an anti-tumour phenotype (e.g. macrophages and $CD8_+$ CTLs), upregulation of activation and co-stimulatory markers (e.g. DCs) or enhancing cytotoxic functions (e.g. NK cells). Characterizing expression of the type III IFN receptor on immune cells is currently still under investigation, however B cells, $CD4_+$ and $CD8_+$ T cells, DCs, neutrophils and NK cells are known to express both receptor subunits. Although this expression has been documented, only neutrophils, DCs, and B cells have been observed to respond to IFN-λ signaling or elicit responses to type III IFNs. Neutrophils and DCs are best characterized in their responses to type III IFN stimulation, as they decrease secretion of tissue-damaging reactive oxygen species, and increase cytokine production in response to IFN-λ, respectively.

populations[104,105,106]. These populations are often found in tissues exposed to the external environment, including the gastrointestinal tract, the skin and the respiratory epithelium, and are closely associated with blood vessels[105]. Mature mast cells possess 50-200 cytoplasmic granules that store inflammatory cytokines, such as tumour necrosis factor (TNF), histamine, and neutral proteases, most notably tryptase and chymase[103,107]. Heterogeneity amongst mast cell populations reflects the tissue microenvironment in which they reside, however human mast cells can be broadly categorized into three different subtypes: those possessing tryptase only, chymase only, or both tryptase and chymase[108]. Murine mast cells can be divided two major subsets: mucosal mast cells, preferentially expressing mouse mast cell protease-1 and -2, and connective tissue mast cells that express mouse mast cell protease-4, -5, -6, and carboxypeptidase A (Cpa3)[109]. These represent extremes of a spectrum of mast cell phenotypes found in different tissue microenvironments. Despite this heterogeneity, all mast cells are characterized by their expression of CD117 and high affinity immunoglobulin E (IgE) receptors, such as Fc epsilon receptor I (FcεRI)[105]. CD117, also known as c-kit, is a surface receptor that binds stem cell factor, a growth factor essential for mast cell development and survival[105,108]. Other cytokines such as IL-3 promote mast cell growth and survival in cultures *in vitro*[110]. Mast cells are also known sources of a variety of pro- and anti-inflammatory mediators, which can be subcategorized into two different classes: pre-formed mediators stored in their cytoplasmic granules and mediators synthesized *de novo* after activation. Mast cells can immediately release pre-formed mediators from their cytoplasmic granules *en masse* into the local tissue microenvironment through the process of degranulation or induce selective release of individual granules through the process of piecemeal

degranulation[111]. Complete degranulation can have largely untargeted downstream effects due to the release large amounts of diverse mediators that can elicit a variety of responses[111]. Alternatively, activated mast cells secrete specific cytokines, chemokines, and lipid mediators *de novo* in the absence of degranulation, which are produced and released over the course of hours[112]. Due to their localization at mucosal sites and their wide breadth of secreted mediators, mast cells are known initiators of inflammation after pathogen invasion and function to mobilize other innate and adaptive immune cells to the site of infection and/or draining lymph nodes to mediate pathogen clearance[111].

1.3.2 Mast cells as immune sentinels

As key initiators of an inflammatory response after pathogen invasion, mast cells express numerous PRRs, such as TLRs, NOD-like receptors, and RIG-I type receptors[113]. Murine mast cells express a wide variety of TLRs including TLR-1, -2, -4, and -6, while human peripheral blood-derived mast cells express TLR1-9[114,115,116]. These PRRs function to recognize PAMPs, leading to mast cell activation and the secretion of pro-inflammatory cytokines[113,114]. Secretion of important pro-inflammatory cytokines and chemokines, such as chemokine C-C motif ligand 2, TNF, and IL-1β, functions to recruit immune cells, such as DCs, neutrophils and Langerhans cells[117,118]. DCs were also shown to be recruited through mast cell-derived TNF in a murine model of contact hypersensitivity[119]. Other innate immune cells impacted by mast cell-derived mediators are eosinophils and NK cells, recruited by secreted eotaxin and chemokine CXCL8, respectively[117]. A summary of some known mast cell-derived mediators and their impact on innate immune cell recruitment is depicted in **Figure 1.3**.

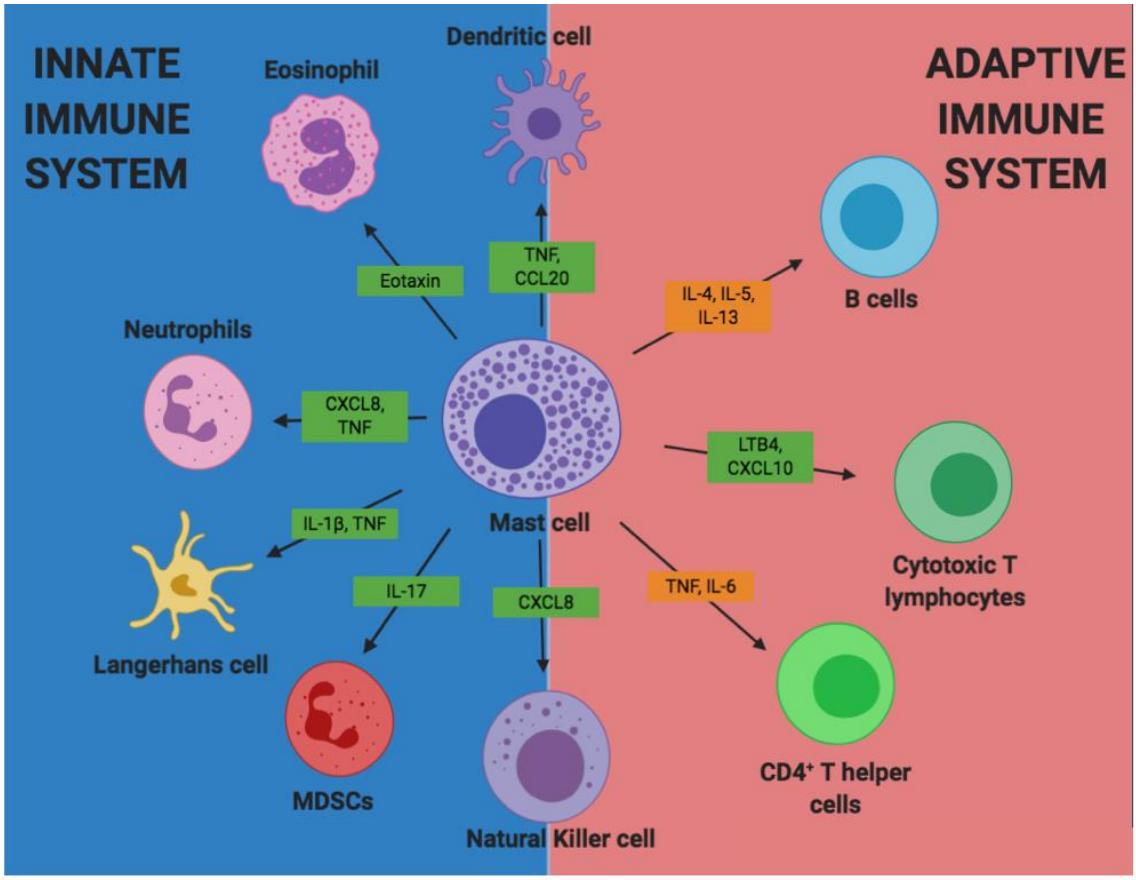

Figure 1.3. Sentinel abilities of mast cells on the innate and adaptive immune system. Mast cells are known to recruit members of the innate immune system (left), such as DCs, eosinophils, neutrophils, Langerhans cells, MDSCs and NK cells through a variety of their secreted mediators (highlighted in green), some of which overlap in their cellular targets. In the adaptive immune system (right), only CTLs are known to be recruited by mast cell-derived mediators, but other adaptive immune cells such as B cells and CD4+ Th cells are known to be activated by mast cells (highlighted in orange).

The role of mast cells as immune sentinels also impacts the adaptive immune system. Mast cell secretion of lipid mediators, such as leukotriene B4 (LTB_4), induces migration of $CD8^+$ CTLs during allergic inflammation and is important for mast cell-mediated activation of these cells[120,121]. Mast cell recruitment of $CD4^+$ T cells is not well-documented, although the literature shows that mast cells have indirect downstream impacts on T_{reg} recruitment through mast cell-mediated recruitment of MDSCs in hepatoma tumours, which increased T_{reg} infiltration by MDSC-derived IL-17[122]. Evidence to define the role of mast cells in B cell recruitment is similarly lacking, however mast cell-derived IL-4, IL-5, and IL-13 are known to drive B cell differentiation, activation and antibody release[108,123]. In addition to recruitment of adaptive immune cells, mast cells have a documented role in antigen presentation and can activate $CD4^+$ and $CD8^+$ T cells and T_{regs}[120,124,125]. Mast cell-mediated antigen presentation has been documented in human peripheral blood-derived mast cells and murine BMMCs, noting that human mast cell-mediated antigen presentation induces a pro-inflammatory IL-22$^+$ and IFN-y$^+$ expressing phenotype in $CD4^+$ T cells[126,127]. A brief overview of the interactions between mast cells and cells of the adaptive immune system is summarized in **Figure 1.3**.

Given their extensive interaction with innate and adaptive immune cell subsets, mast cells as immune sentinels can be critical for clearance of bacterial, parasitic, and viral pathogens. The protective effects of mast cells have been documented in numerous bacterial infections, including *Klebsiella pneumonaie* infection of the lungs, *Pseudomonas aeruginosa* infection of the skin, and *Escherichia coli* infection of the peritoneum and bladder[128,129,130]. In some bacterial infections, mast cell-derived mediators

were shown to be critical for survival in mice, often by promoting recruitment of neutrophils[131]. During parasitic infections, such as *Leishmania major*, mast cells promoted neutrophil, macrophage, and DC recruitment, providing systemic protection after mast cell reconstitution at sites of infection[132]. Mast cells increased DC populations and yielded downstream effects on T cell activation, shifting polarization to a protective Th1 phenotype[132]. The role of mast cells in viral infections is more enigmatic. However, mast cells express viral sensors, such as TLR3, which can detect dsRNA viruses[111,133]. TLR3-induced mast cell activation has been shown to induce $CD8^+$ T cell recruitment to infected sites and produce anti-viral cytokines such as IFNs[116,133]. Other viral sensors expressed by mast cells include TLR7, melanoma differentiation-associated protein 5, and RIG-I. Mast cells respond to numerous viruses including cytomegalovirus, Newcastle Disease virus, respiratory syncytial virus (RSV), influenza A virus, reovirus and dengue virus[134,135,136,137]. Although further investigations into the role of mast cells in anti-viral immunity are still required, existing research suggests mast cells are important in viral recognition and mobilization of anti-viral effector cells.

1.3.3 Mast cells as a source of interferons

IFN responses are crucial for viral clearance and while mast cell-mediated IFN production requires more extensive investigation, there is evidence implicating mast cells as a source of several different IFNs. Primary human cord blood-derived mast cells (CBMCs) produce IFN-α2 in response to RSV infection *in vitro*[136]. Human CBMCs responded to reovirus by upregulating messenger RNA (mRNA) of all types of IFN-α and IFN-β, suggesting they produce a diverse range of type I IFNs[138]. Human mast cells

also produced IFN-α and IFN-β mRNA and protein in response to stimulation with polyinosine-polycytidylic acid (a mimic of viral dsRNA), RSV, influenza virus, and type I reovirus, which was independent of degranulation[116]. IFN-α production was detected in murine BMMCs activated using polyinosine-polycytidylic acid, which was found to be TLR3-dependent[116]. In two separate studies, CBMCs produced IFN-α2, IFN-β, and IFN-λ1 in response to reovirus infection *in vitro*, which was enhanced by priming with IL-4 or during IgE crosslinking [139,140]. Currently, there is no evidence to suggest that mast cells produce IFN-γ, although IFN-γ promotes survival and activation of mast cells[141]. Research identified mast cells as an early source of IFNs, implicating their potential contribution to controlling viral infection and other diseases impacted by IFNs. Continued research into the mast cell IFN response may identify methods of harnessing this response in a therapeutic context.

1.3.4 Pro- and anti-tumour actions of mast cells in cancer

Within the TME, mast cells have been documented to possess both pro- and anti-tumorigenic functions. Mast cells can infiltrate the tumour stroma and directly participate in tumour rejection through secretion of cytotoxic mediators, such as IL-1, IL-4, IL-6, and TNF[142,143,144]. Given the ability of mast cells to act as immune sentinels, they can indirectly mediate tumour rejection through recruitment of cytotoxic innate and adaptive immune cells, creating immunologically "hot" tumours[145]. Mast cells can interact directly with T_{regs}, and skew their function towards a pro-inflammatory phenotype, which is mediated through OX40/OX40L axis[146]. In certain types of cancer, such as breast and ovarian cancer, increased mast cell populations at the tumour site are correlated with

longer survival time in humans[147,148]. Other mast cell-derived mediators, such as tryptase, can initiate fibroblast recruitment, leading to tumour fibrosis and slowing of tumour growth[148,149]. While mast cells are capable of driving tumour resistance, these cells have been well-documented in their contribution to tumour progression. Mast cells can directly promote tumour growth through angiogenesis, which supplies the tumour with oxygen and essential nutrients[150]. Mast cell-derived mediators such as VEGF, transforming growth factor beta, and CXCL8 help initiate angiogenesis[102,150]. Mast cell-derived proteases, such as matrix metalloproteinase 9, tryptase, and chymase, contribute to degradation of the ECM in the TME and promote tumour invasion and metastasis[102,151]. Many mast cell mediators associated with degranulation, such as histamine, have been implicated in promoting tumour cell proliferation[152]. The sentinel function of mast cells can also recruit immunosuppressive cell subsets, such as MDSCs, to the tumour site, leading to subsequent recruitment of T_{regs} that enhance the immunosuppressive environment of the tumour[122]. The contribution of mast cells to tumour growth is tumour type- and site-dependent[102]. Preliminary research has suggested that localization of mast cells relative to the tumour (e.g. peritumoural, intratumoural or in draining LN) may influence their functional effects on tumour growth[153,154]. The micro-localization of mast cells and their activation status are likely critical in determining their impact on tumour progression. **Figure 1.4** depicts some of the pro- and anti-tumour functions of mast cell-derived mediators.

1.3.5 Targeting and manipulating mast cells for immunotherapy

While therapeutically targeting mast cells for cancer immunotherapy has been

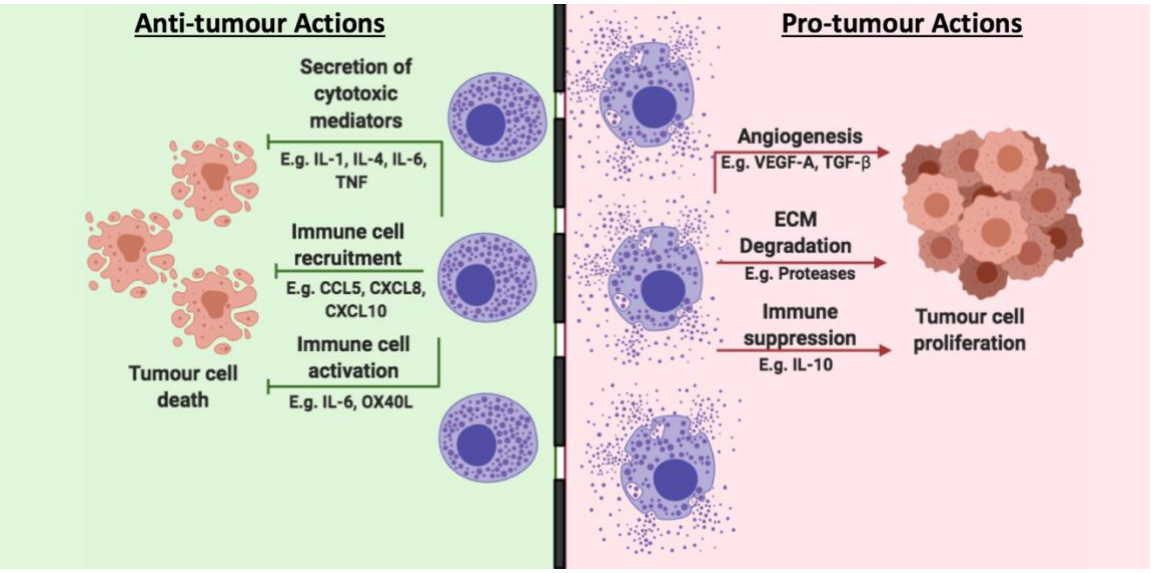

Figure 1.4. Pro- and anti-tumour functions of mast cells. The dual role of mast cells in cancer has been documented. They possess anti-tumour functions (left), including their secretion of cytotoxic mediators, recruitment and activation of immune cells to enhance anti-tumour immunity, which contribute to tumour cell death. Many of these functions have been associated with the activation status of mast cells. Conversely, mast cell-derived mediators can contribute to tumour progression (right). These mediators, often associated with mast cell degranulation, can mediate angiogenesis, ECM degradation that may ultimately promote metastasis, and immune suppression mediated by the release of anti-inflammatory mediators. Reproduced with permission from the author[156].

investigated, many studies have focused on inhibiting the pro-tumorigenic features of mast cells. While mast cells do have many pro-tumorigenic functions, this approach generated controversial results. During one study, mast cell depletion using a c-kit inhibitor (imatinib) resulted in accelerated in tumour growth in mice challenged with 4T1 mammary adenocarcinoma[155]. Other targeted approaches that used pharmacologic inhibition of mast cell degranulation effectively reduced tumour size in experimental pancreatic cancer and human xenograft thyroid cancer models in mice, when treated with a Bruton tyrosine kinase inhibitor (PCI-32765) and sodium cromoglycate, respectively[157,158]. Another study utilizing mast cell-deficient mouse models showed that mast cells was critical for promoting prostate tumour growth, although their absence resulted in a higher incidence of early and aggressive neuroendocrine tumour growth[159]. Therefore, the decision and approach to target mast cells in cancer immunotherapy is very likely dependent on tumour type and how it interacts with mast cells. Given the abundance of mast cells in the tumour periphery and their ability to secrete distinct profiles of mediators, another more novel approach to mast cell immunotherapy may be to enhance their anti-tumorigenic features[156]. This alternate strategy would elicit mast cell activation to produce cytotoxic mediators and induce anti-tumour immunity. Other studies determined that TLR2-mediated activation of mast cells reversed their pro-tumorigenic role in a murine melanoma model and reduced tumour growth via the production of IL-6[160,161]. Other methods of targeting the sentinel abilities of mast cells have also been shown to be effective, such as the TLR7 agonist (imiquimod), which activated production of mast cell-derived chemokine C-C motif ligand 2 resulting in plasmacytoid DC recruitment and reduction of melanoma

tumours[162]. These studies provide evidence that reversing the pro-tumorigenic actions of mast cell by enhancing their anti-tumour functions shows promise for mast cells in immunotherapy. Mast cells possess radioresistant features and are known to survive the cytotoxic effects of gamma radiation, maintaining their ability to respond to innate and adaptive immune activation signals, making them an ideal target for immune therapy in combination with standard radiation treatments[163].

1.4 Rationale

It has been well-documented that mast cells are important sentinel cells for the immune system, and their role in mobilizing other innate and adaptive cells is critical for pathogen clearance. Mast cells also act as important effector cells in certain types of cancer, including breast cancer, ovarian cancer, and melanoma. Research from our group has shown that mast cells can be activated to produce both type I and III IFNs, cytokines that are currently of great interest in cancer immunotherapies given their potent anti-tumour effects mediated directly on tumour cells and indirectly through enhancement of anti-tumour immunity. Considering mast cells can be found in high number and in close proximity to the tumour and possess radioresistant features, they are an ideal candidate for novel immunotherapeutic approaches involving delivery of IFNs.

To determine the feasibility of a mast cell-derived IFN immunotherapy approach, we used a system developed by Dr. Ian Haidl to genetically modify mast cells to overexpress either a type I or III IFN using a lentiviral transduction system. In this approach, an IFN gene was inserted into a DNA vector downstream of an inducible tetracycline promoter (**Figure 1.5**). This tetracycline "ON" system will only produce the

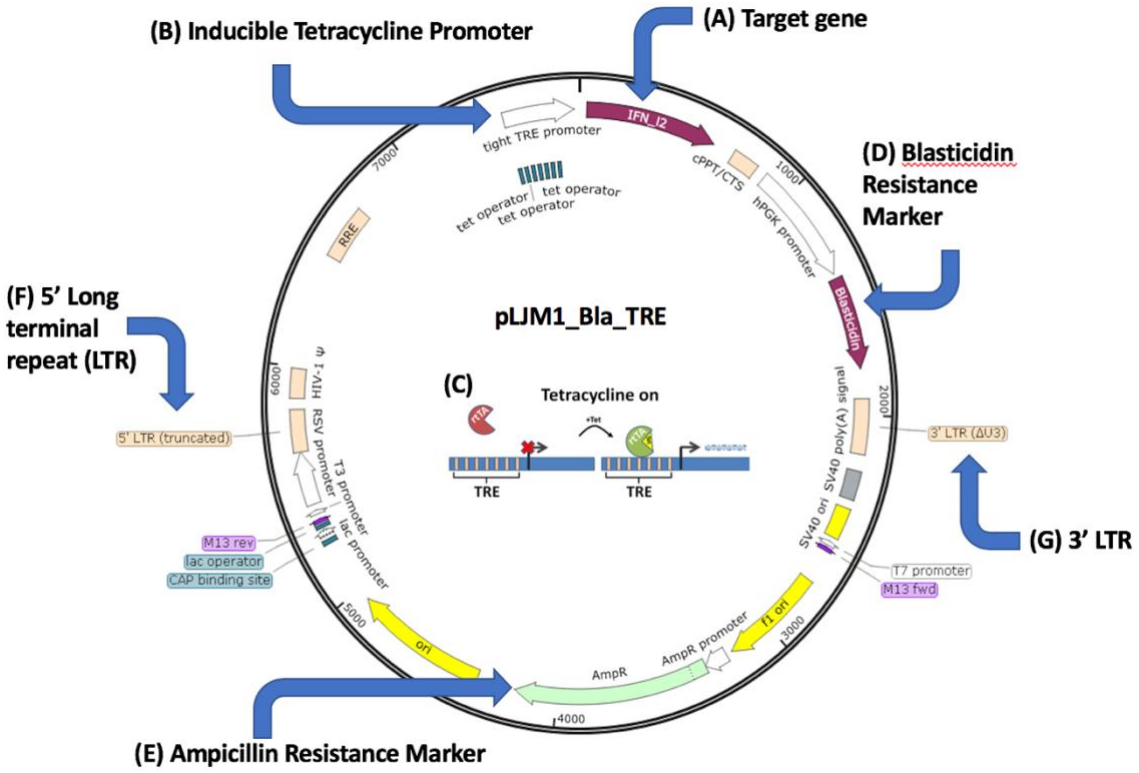

Figure 1.5. The DNA Vector, pLJM1_Bla_TRE, utilized to genetically modify mast cells for inducible IFN production. Genetic modification of target cells to express inducible IFN is accomplished by 1) transduction of the DNA vector using a 3rd generation lentiviral system, 2) selection of successfully transduced cells and 3) expansion of positively-selected cells in culture. The target gene (**A**) is found downstream of a tetracycline response element (**B**) that functions as a tetracycline "ON" system. Tetracycline "ON" systems function through a reverse tetracycline-controlled transactivator protein modified from an earlier established tetracycline "OFF" system. The "ON" system was created through the mutation of a tetracycline repressor, which is fused with the C-terminal domain of virion protein 16, a transactivator domain of herpes simplex virus, to form the reverse tetracycline repressor. Cells that express the essential reverse tetracycline-controlled transactivator protein can induce production of the downstream target gene in the presence of tetracycline or another derivative (**C**). Other markers important in the modification process include a blasticidin resistance marker (**D**), used to select for successfully transduced cells *in vitro* and an ampicillin resistance marker **(E)** used to select transformed bacteria during the cloning process of the DNA vector prior to transfection and transduction. The 5' LTR (**F**) and 3' LTR (**G**) regions are used by this lentivirus system to insert the DNA vector into target cell genomes.

target IFN in the presence of tetracycline or a derivative, allowing for selective type I or III IFN production to avoid the certain toxicities likely to occur with sustained IFN production. This project investigated utilizing either type I or III IFNs in this inducible tetracycline system, since each type of IFN possesses advantages. Type I IFNs are expected to elicit more potent and rapid responses that can bind to all components of the TME given ubiquitous type I receptor expression. However, this may result in more associated toxicities and may invoke more potent negative regulatory mechanisms than type III IFNs. Utilizing type III IFNs is expected to elicit less potent, but more sustained inflammatory responses and that are associated with less neurotoxic side effects due to limited type III receptor expression. Current mast cell-associated immunotherapies focus primarily on counteracting their pro-tumorigenic features through population depletion or inhibition of degranulation. Activated mast cells can produce many anti-tumour effector cytokines and are natural producers of IFNs. This approach to immunotherapy aims to harness the anti-tumourigenic mediators produced by mast cells, an approach not previously used for cancer treatment, and determine the therapeutic efficacy of mast cell-mediated IFN-delivery. **We hypothesized that mast cell-mediated IFN delivery could effectively reduce or eliminate tumour growth in multiple tumour models.**

Before testing the feasibility of a mast cell-IFN immunotherapy, we set out to characterize type I and III IFN receptor expression and signaling in murine tumour models. After characterization and selection of models to use *in vivo*, we sought to determine how mast cells impacted tumour growth using mast cell-deficient mouse models. These models can be used to examine the impact of re-introducing mast cells into the TME in each selected model, given ACT of cultured mast cells can create mast cell

"knock-in" animals that contain mast cells at local or systemic sites depending on the method of mast cell administration. This research will help to further elucidate how mast cells impact tumour growth *in vivo* and determine whether mast cell-mediated IFN delivery can eliminate or impede tumour growth and development.

1.5 Objectives

This investigation can be summarized in 5 objectives:

1. Characterize expression and determine functionality of the type I and type III IFN receptor on mouse tumour cell lines.
2. Test susceptibility of tumour cell lines to IFN-λ-mediated apoptosis *in vitro*.
3. Clone IFN insert of choice into a vector that utilizes an inducible system and transduce the vector into mast cells
4. Characterize tumour growth in models of mast cell-deficiency and determine how their presence contribute to type I and III IFN expression and anti-tumour immunity in tumour transplant models.
5. Analyze how overexpression of IFNs in the TME affects tumour growth and survival *in vivo*.

CHAPTER 2: MATERIALS AND METHODS

2.1 Cell isolations and culturing

2.1.1 B16-F10 melanoma tumour cell line

The mouse melanoma cell line, B16-F10 (ATCC®, CRL-6475™), was maintained in complete Dulbecco's Modified Eagle's Medium (DMEM) (Gibco) supplemented with 10% fetal bovine serum (FBS) (Gibco) and 100 U/mL penicillin and 100 μg/mL streptomycin (Hyclone). Cells were split every 3-4 days as needed to maintain growth, seeding between $8.0x10^4$ – $1.2x10^5$ in a 75 cm^3 flask. Cells were cultured and used for experiments until reaching 15 passages before being discarded.

2.1.2 E0771 mammary adenocarcinoma tumour cell line

The mouse mammary adenocarcinoma cell line, E0771 (ATCC®, CRL-3090™), was maintained using complete Roswell Park Memorial Institute (RPMI) 1640 media (Gibco) supplemented with 10% FBS, 10 mM 4-(2-hydroxyethyl)-1-piperazineethanesulfonic acid (HyClone), and 100 U/mL penicillin and 100 μg/mL streptomycin. Cells were split every 3-4 days as needed, seeding between $8.0x10^4$ – $1.2x10^5$ in a 75 cm^3 flask. Cells were cultured and used for experiments until reaching 15 passages before being discarded. This cell line lacked expression of ER measured by RT-qPCR and will be classified, in this investigation, as a TNBC model.

2.1.3 ID8 ovarian tumour cell line

The mouse ovarian cancer cell line, ID8, obtained from Dr. Shashi Gujar via Edith Lord (University of Rochester, Rochester NY), was maintained in complete DMEM

supplemented with 10% FBS and 100 U/mL penicillin and 100 μg/mL streptomycin. Cells were split every 3-4 days as needed, seeding between 6.0-9.0x10^4 cells in a 75 cm^3 flask. Cells were cultured and used for experiments until reaching 15 passages before being discarded.

2.1.4 U2-OS cells

The human bone osteosarcoma cell line, U2-OS (ATCC®, HTB 96™), were transduced lentiviral vector containing either IFN-α1 or IFN-λ2 sequences as described in Chapter 2.2. Transduced cells were cultured in complete DMEM supplemented with 10% FBS and 12 μg/mL blasticidin (Invivogen). Cells were split every 3-4 days as needed, seeding between 6.0-9.0x10^4 cells in a 75 cm^3 flask. Cells were cultured and used for experiments until reaching 15 passages before being discarded.

2.1.5 Bone marrow-derived mast cells (BMMCs)

Bone marrow was isolated from the hind limbs of C57BL/6 and B6.Cg-Gt(ROSA)26Sortm1.1(CAG-rtTA3)Slowe/LdowJ (Rosa26) mice obtained from Jackson Laboratories (Bar Harbor, ME, USA). The hind limbs were flushed to collect the bone marrow and cells were centrifuged before re-suspension in endotoxin-free bone marrow culture medium, consisting of RPMI 1640, 10% FBS (Gibco), 10% WEHI-conditioned media (media produced "in house" using supernatant from WEHI-3 cells, which produce murine IL-3; cells obtained from ATCC), 100 U/mL penicillin and 100 μg/mL streptomycin and 50 μM of 2-mercaptoethanol (Sigma). Isolated cells were cultured at 0.5x10^6 cells/ml and medium was replaced every 7 days. Two hundred mM Prostaglandin

E2 (Sigma Aldrich) was added to the cultures to promote mast cell maturation. Mast cell maturity was evaluated after 6 weeks of culturing by analyzing CD117 and FcεRI expression by flow cytometry. BMMCs were considered ready for experimental use if the population was >95% $CD117^{+}$, $Fc\varepsilon RI^{+}$.

2.2 Producing IFN-transduced cells

2.2.1 Selecting DNA cloning vector and gene inserts

The DNA vector pLJM1_Bla_TRE was optimized by Dr. Ben Johnston in Dr. Craig McCormick's laboratory at Dalhousie University. This vector contains three important features: 1) an ampicillin resistance marker used for selection of transformed bacteria used to amplify the vector, 2) an inducible tetracycline response element used to control expression of the inserted gene of interest, and 3) a blasticidin resistance marker to positively select for transduced cells in culture. IFN-α1 and IFN-λ2 were selected as genes of interest to insert into pLJM1_Bla_TRE. IFN-λ2 was selected given its established use in DNA cloning and its decreased anti-viral activity compared to IFN-λ3, which may be useful in future oncolytic virus combination therapies[164,165]. **Table 2.1** outlines the amino acid sequences for the transcripts that were selected for vector cloning. The IFN-λ2 (V1) transcript utilized by Sato *et al.* displayed functional protein production after cloning[164]. A second version of IFN-λ2 containing an extended signal peptide sequence (V2), was selected to determine whether this extended sequence had any impact on protein production or functionality. Inserts were sequenced and provided in the pUC57 vector (Genewiz). IFN-α1 was selected for type I IFNs due to its reduced potency compared to IFN-β and this sequence was not used in DNA cloning to our knowledge[74].

Table 2.1 Amino acid sequences of IFN-λ2, IFN-α1, and GFP transcripts

Target Gene	Amino Acid Sequence
GFP	MVSKGEELFTGVVPILVELDGDVNGHKFSVSGEGEGDATYGK LTLKFICTTGKLPVPWPTLVTTLTYGVQCFSRYPDHMKQHFFK SAMPEGYVQERTIFFKDDGNYKTRAEVKFEGDTLVNRIELKGI DFKEDGNILGHKLEYNYNSHNVYIMADKQKNGIKVNFKIRHNI EDGSVQLADHYQQNTPIGDGPVLLPDNHYLSTQSALSKDPNEK RDHMVLLEFVTAAGITLGMDELYK
IFN-α1	MARLCAFLMVLAVMSYWPTCSLGCDLPQTHNLRNKRALTLL VQMRRLSPLSCLKDRKFGFPQEKVDAQQIKKAQAIPVLSELTQ QILNIFTSKDSSAAWNATLLDSFCNDLHQQLNDLQGCLMQQVG VQEFPLTQEDALLAVRKYFHRITVYLREKKHSPCAWEVVRAEV WRALSSSANVLGRLEEKEQKLISEEDL
IFN-λ2 V1	MLLLLLPLLLAAVLTRTQADPVPRATRLPVEAKDCHIAQFKSL SPKELQAFKKAKDAIEKRLLEKDLRCSSHLFPRAWDLKQLQV QERPKALQAEVALTLKVWENTMTDSALATILGQPLHTLSHIHS QLQTCTQLQATAEPRSPSRRLSRWLHRLQEAESKETPGCLEAS VTSNLFRLLTRDLKCVANGDQCV
IFN-λ2 V2	***MKPETAGGH***MLLLLLPLLLAAVLTRTQADPVPRATRLPVEAK DCHIAQFKSLSPKELQAFKKAKDAIEKRLLEKDLRCSSHLFPRA WDLKQLQVQERPKALQAEVALTLKVWENTMTDSALATILGQ PLHTLSHIHSQLQTCTQLQATAEPRSPSRRLSRWLHRLQEAESK ETPGCLEASVTSNLFRLLTRDLKCVANGDQCV

Note: ***Bold and Italicized font*** indicate amino acid sequence differences between V1 and V2

2.2.2 DNA cloning procedure

The undigested pLJM1_Bla_TRE vector and pUC57 vectors containing the selected IFN transcripts or green fluorescent protein (GFP) were used during the cloning process. A GFP transcript was included in the cloning process to determine transfection and transduction efficiency, which was inserted into locus instead of the IFN sequence, as a future negative control for IFN production. DNA vectors were dephosphorylated using Antarctic phosphatase (New England Biolabs) at 37°C for 1 hour to prevent spontaneous re-ligation after restriction enzyme digestion. All vectors were digested with the restriction enzymes MluI (New England Biolabs) and BamHI (Invitrogen) and incubated

at 37°C for 1 hour. Enzymatically digested vectors and gene inserts were run on a 0.8% agarose gel for 40 minutes to separate fragments, which were then imaged on an Alpha Innotech Red™ Imaging System and cut from the gel. Gels were dissolved using Buffer QG (Qiagen) and insert fragments and the pLJM1 backbone were isolated using the MinElute® Gel Extraction Kit (Qiagen) as per the manufacturer's instructions. Ligation was performed using an insert:vector ratio of 3:1, adding DNA ligase (New England Biolabs) and incubating at room temperature for 7 minutes, then on ice for 2 minutes. The ligation mixture was then added to an *E. coli DH5A* (New England Biolabs) suspension in lysogeny broth (LB) and mixed thoroughly before incubating on ice for 30 minutes. *E. coli* were subsequently heat shocked by submerging tubes in 42°C water bath for 30 seconds and placed back on ice for 5 minutes. Super optimal broth with catabolite repression (ThermoFisher Scientific) was added to the vector-bacteria mixture and spun on a rotating drum in a 37°C incubator overnight. Transformed bacteria were then streaked on LB agar containing 100 μg/mL ampicillin and incubated at 37°C overnight. Resistant colonies were then picked at random from the bacterial lawn, 8 per insert, and added individually to LB broth containing 100 μg/mL ampicillin before incubating overnight at 37°C while spinning on rotating drum to allow for growth. Transformed bacteria were then lysed and DNA insert was isolated using a Midiprep kit (Qiagen), as per the manufacturer's instructions. DNA constructs isolated from bacterial lysates were run on a 1% agarose gel to determine if the ligation was successful, prior generation of lentiviral particles.

2.2.3 Transfection to produce Lentivirus

The production of lentivirus was carried out using a third generation lentiviral system, using pPAX2 as a packaging plasmid and pMD.2 as the envelope plasmid along with the individual target gene transfer vectors containing IFN-α1, IFN-λ2 V1, V2, or GFP_{166}. The transfection was performed in HEK293T cells using Lipofectamine 3000 (LF3000) (Thermofisher Scientific). HEK293T cells were seeded in 4 wells of a 6 well plate (one for each transfer vector) at $1x10_6$ cells/well and suspended in DMEM supplemented with 10% FBS and incubated at 37°C overnight to allow cells to adhere to the plate. In one tube, LF3000 was added to OPTI-MEM (Thermofisher Scientific) media (Tube A). In four separate tubes, 1.32 μg of the packaging plasmid and 0.64 μg of the envelope plasmid were added to OPTI-MEM media, before adding 1.7 μg of transfer vector, one for each insert (Tubes B, C, D, E). P3000 reagent (Thermofisher Scientific), followed by LF3000 solution from Tube A, was added to each Tube B, C, D and E, and incubated at room temperature for 15 minutes. LF3000/DNA complexes from Tubes B, C, D and E were added dropwise to individual wells on the 6 well plate containing HEK293T cells and incubated in 5% CO_2 at 37°C for 6 hours. The transfection medium was aspirated and replaced with DMEM containing 2% FBS. Transfected cells were incubated for 24 hours to generate lentivirus and viral supernatant was collected. Transfection efficiency was assessed by flow cytometry using GFP-transfected cells, with the percentage of GFP^+ cells representing the estimated transfection efficiency of cells transfected with IFN inserts. The efficiency of transfection was typically ~12%.

2.2.4 Transduction of target cells

Lentiviral supernatant was collected from each transfected well and passed through 0.45 μM filter. Polybrene (Sigma) was added to supernatant to a final concentration of 5 μg/mL before transferring the entire supernatant with lentivirus containing IFN-α1, IFN-λ2 V1, V2, or GFP onto their respective target cells, either the human U2-OS cell line or primary murine BMMCs, seeded on a 6 well plate. The plate was then covered with a lid and sealed with parafilm before centrifuging at 448g at room temperature for 2 hours. After spinning, transduced cells were detached from wells using TrypLE (Gibco), washed once with DMEM containing 10% FBS, and resuspended in this media without blasticidin, before being transferred into 25cm$_2$ flask. After 24 hours, blasticidin was added to a final concentration of 12 μg/mL to begin selection for successfully transduced cells. Transduction efficiency was measured in transduced target cells containing the GFP lentivirus. The measured transduction efficiency was typically <1% for BMMCs. BMMCs were continuously cultured in RPMI with 15% WEHI-conditioned media and 12 μg/mL blasticidin over 4 weeks to allow for positive selection and expansion of genetically modified cells. GFP-transduced cells were measured each week by flow cytometry to determine purity of modified cultures, and cells were ready for experimental use when GFP$_+$ cultures were >95%.

2.3 Characterizing IFN receptor expression in tumour cell lines

2.3.1 mRNA expression of type I and III IFN receptor

Mouse B16-F10, E0771, and ID8 tumour cell lines were cultured as described in Chapter 2.1. Cell culture media was removed and cells were detached using TrypLE for 5

minutes. The cells were subsequently washed once with phosphate buffered saline (PBS) (Gibco) and centrifuged at 300g at room temperature for 5 minutes. PBS was removed and cells were lysed using RLT lysis buffer (Qiagen) containing 3% 2-mercaptoethanol. RNA isolation from these cells and subsequent cDNA synthesis were performed as outline in Chapter 2.7. The quantity of RNA used to produce cDNA was 1600 ng for each sample. The normalized expression of *Inar1* (Qiagen), *Ifnar2* (Qiagen), *Ifnlr1* (Qiagen) and *Il10rb (*Qiagen) was measured through Real Time quantitative Polymerase Chain Reaction (RT-qPCR) as described in Chapter 2.7. Reference genes used to normalize relative mRNA expression were hypoxanthine-guanine phosphate (*Hprt*) and glucuronidase beta (*Gusb*) for this experiment. This process was repeated for 3 individual passages of each cell line.

2.3.2 Assessing functionality of IFN receptor

B16-F10, E0771, and ID8 cell lines were each seeded into 14 wells in 6 well plates with $5.0x10^4$ cells per well. E0771 cells were suspended in RPMI 1640 supplemented with 10% FBS and 10 mM 4-(2-hydroxyethyl)-1-piperazineethanesulfonic acid, while B16-F10 and ID8 cells were suspended in DMEM supplemented with 10% FBS. Each cell line was incubated at 5% CO_2 at 37°C overnight to adhere to the well. Cells were subsequently activated with recombinant murine IFN-λ2 (R&D Systems) at 1 of 5 doses: 300, 100, 33, 10, or 3.3 ng/mL, which were selected to implicate effects of IFN-λ2 through any dose-dependent observations. The doses were selected based on studies by Kotenko *et al.* and Li *et al.* who used similar doses when analyzing ISG induction on tumour cell lines *in vitro*[167,45]. Control groups included cells left unstimulated and those

stimulated with murine recombinant IFN-α (R&D Systems) at 5 ng/mL as a positive control for ISG induction. IFN-α was used at a lower dose given its potent effects on ISG induction. These treatment groups were analyzed at two timepoints, 6 and 24 hours. Cells were harvested at their respective timepoint and detached using TrypLE for 5 minutes, before washing once with PBS and centrifuging at 300g at 4°C for 5 minutes. PBS was removed and cells were lysed using RLT lysis buffer containing 3% 2-mercaptoethanol. RNA isolation and cDNA synthesis were performed as outlined in Chapter 2.7. The quantity of RNA used to produce cDNA was 350 ng for each sample. Relative expression of 3 ISGs, *Cxcl10,* MX dynamin like GTPase 1 (*Mx1*), and interferon induced protein with tetratricopeptide repeats 1 (*Ifit1*) were measured by RT-qPCR. *Hprt* and TATA-box binding protein (*Tbp*) were used as reference genes to normalize expression relative to mRNA. This experiment was repeated with 3 individual passages of each cell line.

2.3.3 Assessing induction of apoptosis

Tumour cell lines known to respond to IFN-λ2 were subsequently tested for induction of apoptosis after stimulation. B16-F10 and ID8 cells were suspended in DMEM supplemented with 10% FBS and seeded in 5 wells of a 6-well plate using $5.0x10^4$ and $2.5x10^4$ cells per well, respectively. Cells were incubated at 5% CO_2 at 37°C for overnight to adhere to the plate. The following morning, cells were stimulated with 300 ng/mL of recombinant murine IFN-λ2 for 72 hours. Some cells were left unstimulated or were treated with 12 μM camptothecin (Sigma) as negative and positive controls for apoptosis, respectively. Camptothecin inhibits binding of topoisomerase I to DNA complexes, which prevents DNA re-ligation and results in apoptosis through DNA

damage[168]. The selected dose of camptothecin was chosen through a preliminary dose response experiment, which determined that 12 μM induced apoptosis in >75% of cells after 72 hours. After incubation, cells were stained with the annexin V (AV) procedure outlined in Chapter 2.6.

2.4 Tumour growth in models of mast cell deficiency

2.4.1 Animals used

Female mice were used between the ages of 6-16 weeks of age. C57BL/6, B6.Cg-$^{KitW\text{-}sh}$/HNihrJaeBsmGlliJ (Wsh), and B6-Tg$^{(Cap3\text{-}cre)}$4Glli/J (Hello Kitty) mice were bred "in house" from stocks obtained from Jackson Laboratories (Bar Harbor, ME, USA). C57BL/6 mice were also obtained from Charles River Laboratories (Wilmington, MA, USA). Mice were housed at the Carleton Animal Facility at Dalhousie University under pathogen-free conditions. All procedures were approved by the Dalhousie University Committee on Laboratory Animals using guidelines from the Canadian Council for Animal Care.

2.4.2 Preparation and injection of ID8 cells

ID8 cells were cultured as outlined in Chapter 2.1. To prepare cells for injection, media was removed and cells were detached using TrypLE, incubating cells at 37°C for 5 minutes. Cells were removed by pipette and the bottom of each flask was washed once with DMEM to collect any residual cells, which were pooled with those previously detached, separating an aliquot for cell counting. After centrifuging at 300g at 4°C for 10 minutes, cells were washed twice with PBS, taking another aliquot to re-count cells after

both wash steps. After counting, the cell concentration was adjusted to $6x10^7$ cells/mL in PBS, before making dilutions to a final concentration of $3.0x10^7$ cells/mL. Cells were loaded into 1 mL syringe with a 25 5/8G needle and kept on ice until injection, at which time $6.0x10^6$ or $3.0x10^6$ cells were injected intraperitoneally into either C57BL/6 or Wsh mice in 100 μL volumes. Mice were monitored every 2 days for 80 days until ascites development or observed signs of morbidity.

2.4.3 Preparation and injection of E0771 cells

E0771 cells were cultured as outlined in Chapter 2.1. On the day of injection, media containing suspended cells was removed and saved, before adherent cells were detached using TrypLE, incubated at 5% CO_2 at 37°C for 5 minutes. Cells suspended in TrypLE were combined with cells in FBS supplemented media and centrifuged at 300g for 5 minutes at 4°C, after setting aside an aliquot for cell counting. Cells were washed once with PBS and centrifuged as above, resuspending at a final concentration of $2.0x10^6$ cells/mL in PBS and taking an aliquot to re-count cells prior to resuspension in Matrigel (Corning). After counting, E0771 cells for injection were washed and resuspended in Matrigel at a concentration of either $2.0x10^5$ or $5.0x10^4$ cells/100 μL, depending on the experiment. Matrigel was kept on ice during final resuspension to prevent gel polymerization during cell preparation. Pipette tips for handling Matrigel and syringes for injection were stored at -20°C prior to use. One mL syringes were loaded with cell-Matrigel suspension using a 25 5/8G needle, and kept on ice before injection. Mice were anesthetized by oral inhalant using 3% isoflurane and 2% oxygen and subsequently injected subcutaneously into the mammary fat pad adjacent from the 4^{th} nipple with either

$2.0x10^5$ or $5.0x10^4$ E0771 cells in 100 µL Matrigel. Mice were monitored every 2 days for 21 days and sacrificed at experimental endpoint, or if they showed significant signs of morbidity, greater than 15% weight loss, if tumour volume reached >2000mm^3 or if the tumour ulcerated during growth before reaching experimental endpoint.

2.4.4 In vivo reconstitution with transduced and WT mast cells

BMMCs were cultured as outlined in Chapter 2.1. On the day of injection, cells were resuspended within the culture flask and counted to determine the cell concentration. BMMCs were washed twice with saline (Braun), centrifuging at 300g at 4°C for 10 minutes. Cells were resuspended at $2.0x10^6$ cells/100uL in saline and loaded into a 1mL syringe with a 25 5/8G needle and kept on ice until injection. Mice were anesthetized by oral inhalant using 3% isoflurane and 2% oxygen and subsequently injected subcutaneously with $2.0x10^6$ cells BMMCs in saline into the mammary fat pad adjacent to the 4^{th} nipple. Injected mice were rested for 6 weeks to allow for mast cell reconstitution before experimental use. Six weeks was the selected resting time for reconstitution, after a pilot experiment showed that mast cells were detectable in the mammary fat pad by histology using an Alican blue and Safranin O stain on harvested tissues.

2.5 Recombinant IFN injection

Recombinant murine IFN-α (R&D Systems) and IFN-λ2 (Peprotech) were reconstituted under sterile conditions in PBS with 0.1% endotoxin-free bovine serum albumin (BSA) (Gibco) at stock concentrations of 50 µg/mL and 100 µg/mL, respectively. IFN-α was

diluted using PBS with 0.1% endotoxin-free BSA to a working concentration of 1 μg/100 μL and IFN-λ2 was further diluted to two working concentrations, 5 μg/100 μL and 1 μg/100 μL. The recombinant protein was loaded into 1 mL syringes with a 25 5/8G needle and kept on ice prior to injection. C57BL/6 mice were injected intraperitoneally with vehicle (PBS with 0.1% endotoxin-free BSA), 1 μg IFN-α, 5 μg IFN-λ2, or 1 μg IFN-λ2. Mice were euthanized 4 or 24 hours later by CO_2 asphyxiation and peritoneal cells were collected by lavage of the peritoneum with 3 mL PBS containing 0.5% BSA and 5 mM ethylenediaminetetraacetic acid (Invitrogen). A portion of the peritoneal lining was collected for RNA isolation as outlined in Chapter 2.7 and the peritoneal cells were stained for FACS analysis as outlined in Chapter 2.6. To measure ISG induction in the collected peritoneal lining, 350 ng of cDNA was synthesized and mRNA expression of selected ISGs was examined by RT-qPCR. mRNA expression was normalized to *Hprt* and tryptophan 5-monooxygenase activation protein zeta (*Ywhaz*) expression.

2.6 Flow cytometry

2.6.1 Staining procedure for tumours and tissue

To analyze the immune cell infiltrate in the TME of E0771 mammary tumours, mice were injected with E0771 cells as outlined in Chapter 2.4. Animals were monitored during mammary tumour growth and sacrificed on Day 14 via cardiac puncture to harvest spleen, inguinal lymph nodes and tumour. After all tissues were collected, spleens and inguinal lymph nodes were minced and filtered through wire mesh before being suspended in PBS supplemented with 2% FBS. Tumour samples were minced into smaller pieces and added to digestion buffer, which consisted of RPMI 1640

supplemented with 5% FBS, 1 mg/mL Collagenase D (Roche) and 100 μg/mL DNase I (Roche). Tumours were enzymatically digested at 37°C for 1 hour, spinning on a rotating drum, and subsequently filtered through wire mesh. Disaggregated tumour, spleen, and lymph node samples were centrifuged at 300g at 4°C for 10 minutes and resuspended in red blood cell lysis buffer (8.02 g ammonium chloride, 1 g potassium bicarbonate, and 37.2 mg ethylenediaminetetraacetic acid disodium salt dissolved in 1000 mL distilled water) and incubated at room temperature for 15 minutes. Cells were centrifuged as above and washed once with PBS, repeating the centrifugation process before resuspension in PBS. An aliquot of each sample was taken for cell counting. Samples were stained with fixable viability dye (FVD) eFluor506 (Invitrogen) at a 1:1000 dilution in PBS, incubated on ice for 15 minutes in the dark.

All subsequent centrifugation steps were performed at 300g at 4°C for 5 minutes. All samples were washed once with PBS and then once with immunofluorescence (IMF) buffer (1x PBS, 2% FBS, and 10 mM sodium azide). Tumour cells and splenocytes were resuspended in IMF buffer and split into three equal aliquots that were stained with either Panel 1, 2, or 3, as outlined in **Table 2.2**, and incubated on ice for 25 minutes in the dark. Lymph nodes were stained with Panel 1 and 3. All dilutions for each antibody can be found in **Table 2.2**. Cells stained with Panel 1 were washed once with IMF buffer and then PBS, before cells were fixed with 1% paraformaldehyde (PFA) in PBS, incubated at 4°C overnight. Cells stained with Panel 2 were washed once with IMF buffer before being resuspended in IMF buffer containing peridinin chlorophyll-A protein (PerCP) eFluor610-Stretavidin at a 1:300 dilution and incubated on ice for 15 minutes. After incubation, cells were washed once with IMF buffer, then PBS and fixed in 1% PFA in

PBS as with Panel 1. Cells stained with Panel 3 were washed with IMF buffer, after which an intracellular stain for anti-mouse phycoerythrin- (PE) Foxp3 (Invitrogen) was performed using the Foxp3 Transcription Factor Staining kit (Invitrogen) as outlined by the manufacturer at a 1:300 dilution. These cells were fixed with 1% PFA in PBS overnight at 4°C. The following morning, all tumour, spleen, and lymph node samples were washed once with PBS before final resuspension in IMF buffer. Tumour samples were additionally filtered through Cell-Strainer Cap Polystyrene tubes (Falcon) by centrifugation at 300g at 4°C for 5 minutes before acquisition. Data collection was completed at the Faculty of Medicine CORE flow cytometry facility using the BD LSR Fortessa SORP.

2.6.2 Staining procedure for peritoneal cells

To analyze the impact of recombinant IFN injection on immune infiltration in the mouse peritoneum, C57BL/6 mice were injected intraperitoneally with either saline, IFN-α, or IFN-λ2 at two different concentrations as outlined in Chapter 2.5. Peritoneal cells were centrifuged at 300g at 4°C for 10 minutes, before removing the lavage fluid, taking an aliquot for cell counting and washing cells with PBS. After washing, cells were resuspended in FVD eFluor506 diluted 1:1000 in PBS and incubated on ice for 15 minutes in the dark. Centrifugation for all subsequent steps was performed at 300g at 4°C for 5 minutes. Peritoneal cells were washed once with PBS to remove residual FVD and once more with IMF buffer prior to antibody incubation. At this stage, Fc receptors were blocked with 1 μg/mL human immunoglobulin G diluted 1:1000 in IMF buffer and incubated on ice for 15 minutes. After incubation, cells were split into two equal

volumes, one for each panel, before adding an antibody cocktail for Panel 4 or 5, outlined in **Table 2.2**. Samples were incubated on ice for 25 minutes in the dark. After antibody incubation, cells were washed once with IMF buffer and once with PBS before resuspension in 1% PFA and incubation at 4°C overnight. Cells were washed once with PBS and IMF buffer before final resuspension in IMF buffer prior to acquisition. Data collection was completed at the Faculty of Medicine CORE flow cytometry facility using the BD LSR Fortessa SORP.

2.6.3 Staining procedure for apoptosis experiment

After activating tumour cell lines with recombinant IFN-λ2 for 72 hours, as outlined in Chapter 2.3, media containing detached cells was removed and saved, before adherent cells were detached using TrypLE and incubated at 5% CO_2 at 37°C for 5 minutes. Cells suspended in TrypLE were then combined with media containing initially detached cells and an aliquot was taken for cell counting. Cells were centrifuged at 300g at 4°C for 5 minutes. Cells were washed and resuspended in PBS before transferring to an Eppendorf tube and adding FVD eFluor660 (eBioscience) diluted 1:1000 in PBS and were incubated on ice for 15 minutes in the dark. After incubation, cells were washed twice, once with PBS and once with IMF buffer, before suspending cells in IMF buffer containing anti-mouse PE-MHCI antibody (Clone: SF1-1.1.1, Invitrogen) at a 1:300 dilution. Another group of cells were stained with anti-mouse Rat immunoglobulin G2 PE antibody (Clone: m2a-15F8, Invitrogen) as an isotype control, diluted 1:300 in IMF buffer. All groups were incubated on ice for 25 minutes and subsequently washed with IMF buffer before resuspension in AV binding buffer (BD Pharminogen) containing 0.625uL/test

fluorescein isothiocynante- (FITC) AV (BioLegend). Cells were incubated for at room temperature for 20 minutes in the dark, and samples were diluted 1:2 in AV binding buffer before acquisition. AV-stained cells were acquired on the flow cytometer without fixation. Data collection was completed at the Faculty of Medicine CORE flow cytometry facility using the BD FACS Canto II.

2.6.4 Flow cytometry staining panels

The following flow cytometry panels were used to assess the effect of IFN injection on peritoneal cells or to characterize immune infiltrate of E0771 tumours (**Table 2.2**). All antibodies were originally used at a 1:300 dilution in an experiment to test enzymatic digestion of E0771 breast tumours, adjusted according to relative expression from this initial experiment.

Table 2.2. Antibodies used for Flow Cytometry Panels

Laser (excitation)	Fluoro-chrome	Marker	Immune cell subset	Dilution	Clone	Supplier	Panel
Violet (405nm)	BV421	CD21	Marginal Zone B cells	1:300	7E9	BioLegend	1
	BV421	CD117	Mast cell marker	1:300	2B8	BD Bioscience	2
	BV421	CD69	Activation of T cells	1:300	H1.2F3	BD Bioscience	3,4
	eFluor506	FVD	/	1:1000	/	Invitrogen	1, 2, 3,4,5
	BV605	CD19	B cells	1:300	1D3	BD Bioscience	1,4
	BV605	Ly6G	Neutrophil marker	1:300	1A8	BD Bioscience	2.5
	BV605	CD62L	Naïve T cell marker	1:300	MEL-14	BD Bioscience	3
	BV650	CD8	T cell marker	1:300	53-6.7	BD Bioscience	3,4

	BV650	CD11b	Neutrophils, Macrophages, Monocytes, NK cell activation marker	1:1600	M1/70	BD Bioscience	2,5
	BV650	CD23	Follicular B cells	1:300	B3B4	BD Bioscience	1
	BV786	CD23	Follicular B cells	1:300	B3B4	BD Bioscience	5
	BV786	CCR7	Effector Memory T cells	1:300	4B12	Biolegend	3
Blue (488nm)	FITC	CD3	Dump channel	1:300	145-2C11	Biolegend	2
	FITC	CD19	Dump channel	1:300	MB19-1	eBioscience	2
	FITC	CD80	Dump channel	1:300	16-10A1	eBioscience	5
	FITC	IgM	B1/B2 cells	1:300	eB121-15F9	eBioscience	4
	FITC	NK1.1	NK cells	1:300	PK136	Invitrogen	2
	PerCP	CD4	T cells	1:300	RM4-5	Biolegend	5
	PerCP	CD45	General Immune Marker	1:300	30-F11	Biolegend	1,3
	PerCP_eFluor710	FcεRI	Mast cells	1:300	MAR-1	eBioscience	2
Green (532nm)	PE-ef610	CD11b	Neutrophils, Macrophages, Monocytes, NK cell activation marker	1:1200	M1/70	eBioscience	1
	PE-eFL610	Strept-avidin	For CD45 in panel 2	1:300	/		2
	PE	NK1.1	NK cells	1:300	PK136	Biolegend	1,4
	PE	CD103	Dendritic Cells	1:300	2E7	eBioscience	2,5
	PE	Foxp3	T_{regs}	1:300	FJK-16S	Invitrogen	3

	PE-Cy7	CD3	T cells	1:300	145-2C11	Invitrogen	1,4
	PE-Cy7	F4/80	Resting Macrophages	1:300	BM8	Invitrogen	2,5
	PE-Cy7	CD25	T_{regs}	1:300	PC61	Biolegend	3
Red (628nm)	APC	CD5	B1/B2 cell marker	1:300	53-7.3	Biolegend	1,4
	APC	CD11c	Dendritic cells	1:300	N418	Biolegend	2,5
	APC	CD44	Effector and central memory T cells	1:300	IM7	Biolegend	3
	AF700	MHC II	Dendritic cells	1:500	M5/114.15.2	Invitrogen	2,5
	AF700	CD4	T cells	1:300	GK1.5	Biolegend	3
	APC eFluor 780	CD27	NK cell activation marker	1:300	LG.7F9	Invitrogen	1
	APC-Cy7	Ly6C	Inflammatory Monocytes	1:500	HK1.4	Invitrogen	2,5

2.6.5 Flow cytometry analysis

Flow cytometry data was analyzed using FlowJo (10.3) software. UltraComp beads (eBioscience) were stained with 0.5 µL of each monoclonal antibody in the above panels as a compensation control, fixing each control with 1% PFA diluted in PBS before acquisition. Cells isolated from a single spleen were used as unstained and FVD compensation controls. Half of the cells used for FVD compensation controls were heat killed by incubation at 65°C for 2 minutes, before recombining with live cells prior to FVD staining. Fluorescent Minus One controls were used to determine gating strategy for samples from Chapter 2.6.2. The gating strategy for staining of major innate and adaptive immune cell subsets can be observed in **Appendix Figure 3**.

2.7 Molecular Biology

2.7.1 RNA extraction and isolation for in vitro cell culture

Cell lines cultured *in vitro* were lysed by adding 350 μL of RLT+ Lysis Buffer (Qiagen) containing 3% 2-mercaptoethanol and vortexing vigorously. Samples were stored at -20°C until ready for isolation. RNA isolation was performed using a miRNeasy RNA Isolation Kit (Qiagen) as described by the manufacturer. Once RNA was successfully eluted at the final stage of isolation, RNA quantity and purity was assessed after 1:4 dilution of each sample in TE buffer (Qiagen) using an Epoch Microplate Spectrophotometer on Gen5 software (BioTek, Winooski, VT, USA).

2.7.2 RNA extraction and isolation for in vivo tissue

Portions of tissue from *in vivo* experiments were extracted upon mouse sacrifice and immediately suspended in Trizol (Ambion). Tissues were homogenized using a Tissueruptor (Qiagen) for 30 seconds and stored at -80°C until isolation. RNA isolation was performed using a miRNeast RNA Isolation Kit (Qiagen) as described by the manufacturer. Once RNA was successfully eluted at the final stage of isolation, RNA quantity and purity were assessed as outlined in Chapter 2.7.1, before proceeding to cDNA synthesis.

2.7.3 cDNA synthesis

cDNA was synthesized using the miScript II RT kit (Qiagen) as per the manufacturer's instructions. cDNA was transcribed from mRNA using a Biometra® T Gradient Thermocycler (Biometra). Upon completion of cDNA synthesis, cDNA was diluted 1:4

with RNase free water (Qiagen) and stored at -20°C until quantification of gene expression by RT-qPCR or droplet digital PCR (ddPCR).

2.7.4 Real time quantitative PCR (RT-qPCR)

To quantify cDNA synthesized as measure of relative expression for genes of interest, RT-qPCR was performed in 10 µL reactions using RNase free water (Qiagen), 1x SYBR® Green Supermix (BioRad), 0.25 µM or 0.5 µM RT_2 qPCR primers supplied by Qiagen or BioRad respectively, and 2 µL of sample cDNA. Reference genes selected were *Hprt*, *Tbp*, *Gusb*, and *Ywhaz,* which were used in an experiment-dependent manner based on which genes were most stable with their respective *Cq* values for cell lines or tissues. For example, in experiments with IFN-stimulation groups, *Hprt* was better used in combination with *Tbp* or *Ywhaz*, as the expression of these reference genes are known to remain stable after IFN treatment compared to *Gusb*[169]. All primers were validated to determine the optimal annealing temperature before quantifying expression. RT-qPCR was performed using a CFX96 Connect™ Real-Time C1000 Touch™ Thermal Cycler (BioRad) under the conditions outlined in **Table 2.3**. Data was analyzed with CFX Maestro™ software. Each PCR plate included duplicate wells for each sample and no template control wells were included for each primer used to determine any potential genomic DNA contamination in the reagents used. **Table 2.4** lists all primers and their sequences used throughout this investigation.

Table 2.3 Cycling Conditions for RT-qPCR

Cycle Step	Temperature (°C)	Time (Seconds)
Activation	95	120
Denaturation	95	10
Annealing	58	20
Expansion	95	10
Melt Curve	65-95	31

Notes: Steps in yellow are repeated 35X before expansion

Table 2.4. Primer sequences and annealing temperatures

Primer	Sequence	Efficiency (%)	Annealing Temp. (°C)
Cxcl10	Manufacturer's proprietary sequence	95	58
GUSB		>90	
Gusb		>90	
HPRT		105	
Hprt		100	
Ifit1		>90	
Ifna1		96	
Ifna2		85	
Ifnar1		>90	
Ifnar2		>90	
Ifnb1		96	
Ifnl2		90	
Ifnl3		>90	
Ifnlr1		>90	
Il10rb		>90	
Mx1		>90	
Tbp		>90	
Tpsb2		>90	
Ywhaz		>90	

Notes: Primers abbreviated in all capital letters represent human genes, while primers with only the first initial capitalized target mouse genes.

2.7.5 Droplet digital PCR (ddPCR)

ddPCR was used to quantify the number of mast cells in the mammary fat pad of mice used for our *in vivo* tumour experiments. ddPCR was performed in 22 µL reactions using 1x EvaGreen mix (BioRad), 0.2 µM *Tpsb2, Hprt* or *Gusb*, RNase free water, and 5.5 µL

of the appropriate cDNA. Sample cDNA was diluted 1:10 to analyze target genes and 1:100 to analyze reference genes. After mixing, 20 μL PCR mix was slowly added to wells in a DG8 cartridge (BioRad) to avoid introducing bubbles, before adding EvaGreen ddPCR oil (BioRad) to the bottom row of wells on the cartridge. The cartridge was covered using a Droplet Generator Gasket G8 and droplets were subsequently generated using a QX200TM Droplet Generator (BioRad). The emulsion was collected and droplets were pipetted into a 96-well PCR plate, which was sealed with a PX1 PCR Plate Sealer (BioRad). The plate was placed in a BioRad C1000 TouchTM thermocycler and run for 3 hours according to the cycling conditions outlined in **Table 2.4**. Droplets were read by QX200TM Droplet Reader (BioRad) and data was analyzed using QuantaSoftTM software.

Table 2.5 Cycling Conditions for ddPCR

Cycle Step	Temperature (°C)	Time (Seconds)	Ramp Speed (°C/Second)
Activation	95	300	2
Denaturation	95	30	
Annealing	58	60	
Expansion	72	60	
Melt Curve	4-90	600	

Note: Steps in yellow were repeated 49X before determining melt curves

2.8 IFN-λ2/3 enzyme-linked immunosorbent assay (ELISA)

IFN-λ2 protein concentrations were determined using a IFN-λ2/3 ELISA (R&D Systems). Antibodies were used at half the manufacturer's recommended concentration, based on pilot studies which showed these were appropriate. Each ELISA was performed over 2 days in a 96-well plate following the procedure described by the manufacturer, using undiluted samples for *in vivo* samples and *in vitro* samples diluted 1:4 – 1:100. On

Day 2, plates were read at 450 nm to measure protein absorbance using an Epoch Microplate Spectrophotometer on Gen 5 software (BioTek, Winooski, VT, USA).

2.9 Histology

To assess general inflammation of E0771 tumours grown in mast cell-deficient and -sufficient animals, hematoxylin and eosin (H&E) staining was performed on 5 μM sections of harvested tumour tissue. Tumour tissue was fixed using Carnoy's solution, containing 60% ethanol, 30% chloroform (Fisher Bioreagents) and 10% glacial acetic acid (Fisher Chemical) for 24 hours at room temperature. Tissues were processed and paraffin embedded prior to sectioning. Sections were cut using a Leica RM 2255 Microtome provided by Histology Services in the Department of Pathology and incubated at 37°C overnight to adhere to the slides. The following day, sections were deparaffinized by washing slides twice in xylene (Fisher Chemical) at room temperature for 3 minutes each. Sections were subsequently washed twice with 100% ethanol, followed by washes in 95% ethanol and 70% ethanol for 3 minutes each. Slides were briefly rinsed in water and stained with Harris' Hematoxylin (Sigma) for 3 minutes in the dark. Slides were washed in tap water for 5 minutes before differentiation using 1% acid alcohol (60% absolute ethanol, 29% distilled water, and 1% hydrochloric acid (HCl) incubated for 1 minute. Slides were rinsed in running tap water and incubated in Scott's Tap Water (3.5 g sodium bicarbonate and 20 g magnesium sulphate in 100 mL tap water) for 1 minute, followed by washing in 70% ethanol for 1 minute. Slides were counterstained with Eosin Y (Leica) for 5 seconds. Excess eosin was removed by rinsing in 70% ethanol, followed

by 95% ethanol. Slides were washed twice in 100% ethanol and twice with xylene, for 1 minute each, and subsequently mounted with a coverslip using Cytoseal (Thermofisher).

To determine the presence of mast cells in the murine mammary fat pad of different mouse models, an Alcian blue and Safranin O stain was performed on 5 μM sections of tissue. Sections were fixed, embedded, sectioned, and deparaffinized as described above. After deparaffinizing, slides were rinsed with cold tap water and incubated in 0.1 N HCl (Thermoscientific) for 5 minutes, before incubating in 1% Alcian blue 8GX (Sigma) dissolved in 0.7 N HCl overnight. After incubation, slides were rinsed in 0.1 N HCl briefly before submerging in Safranin O (Sigma) dissolved in 0.7 N HCl at room temperature for 20 minutes. Slides were rinsed in cold tap water, left to dry overnight, and subsequently mounted using DPX (Sigma). Images of slides were taken using an Olympus BX43 Upright Microscope on 100x and 400x total magnification.

2.10 Statistical Analysis

All statistical analyses were performed using GraphPad Prism 7 software (GraphPad, La Jolla, CA, USA). Data was assessed for normal distribution using a Shapiro-Wilk Normality test. If data sets passed normality, one way- or two way-analysis of variance (ANOVA) and Student's *t* tests were completed. If data did not pass normality, non-parametric Wilcoxon, Mann-Whitney or Kruskal-Wallis tests were performed. Statistical comparisons on experiments assessing tumour volume assessed the area under the curve and mean values were analyzed by ANOVA followed by Dunnett's, Friedman's or Sidak's multiple comparisons test or unpaired t tests. Survival data was assessed by Log-Rank (Mantel-Cox) Test. Data was determined as statistically significant if $p < 0.05$.

CHAPTER 3: RESULTS

3.1 Characterizing type I and III IFN receptors on tumour cell lines

3.1.1 Type I and III IFN receptor mRNA expression in tumour cell lines

IFNs can act through two general mechanisms to combat tumour growth: 1) by binding surface receptor to induce tumour cell apoptosis directly, or 2) indirectly by activating immune cells to strengthen the anti-tumour immune response. To determine which mechanism may have more impact on tumour size during mast cell-mediated IFN delivery, we performed experiments to select murine tumour models with differing expression of the type III IFN receptor. Three tumour models were characterized for type I and III IFN receptor expression *in vitro*: B16-F10 melanoma, E0771 mammary adenocarcinoma, and ID8 ovarian cancer. B16-F10 melanoma cells are known to express the type III IFN receptor and are susceptible to IFN-λ-mediated apoptosis, serving as a receptor-positive model[80]. IFN receptor expression is not well characterized in the E0771 or ID8 tumour model. The ID8 model is advantageous for mast cell research as the model has peritoneal localization. Mast cells can fully reconstitute in mast cell-deficient mice after i.p. injection[170].

To characterize type I and III IFN receptor expression in our selected tumour cell lines, RNA was isolated from 3 separate passages of B16-F10, E0771, and ID8 cells. *Ifnar1, Ifnar2, Ifnlr1,* and *Il10rb* gene expression were measured by RT-qPCR (**Figure 3.1**). All tested cell lines expressed *Ifnar1* and *Ifnar2* to varying degrees, with ID8 cells expressing the type I receptor mRNA at the highest level, which was statistically significant compared to E0771 cells for *Ifnar2* and for both cell lines for *Ifnar1* (**Figure 3.1A, B**). ID8 cells also expressed the highest level of *Ifnlr1,* however this was not

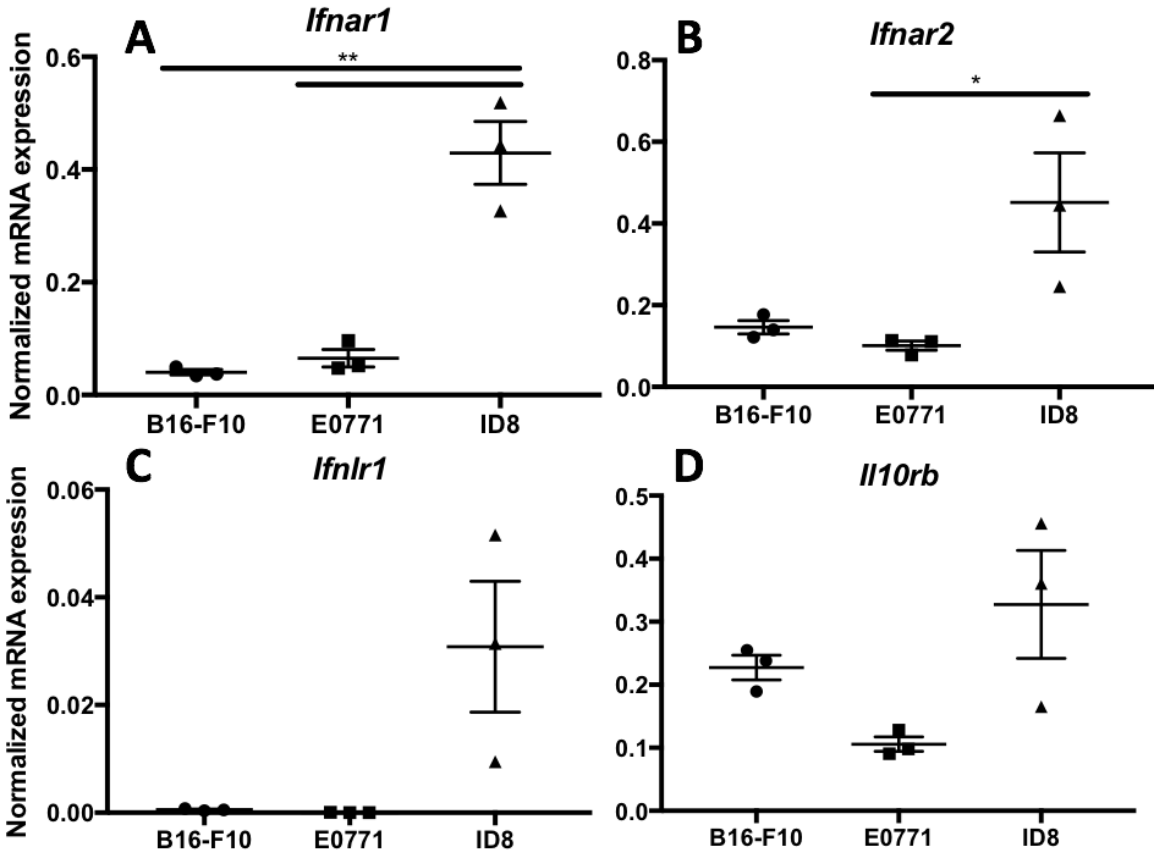

Figure 3.1: B16-F10, E0771, & ID8 tumour cell lines all express mRNA for both the type I IFN receptor subunits, IFNAR1 and IFNAR2, while only ID8 cells have detectable expression both type III IFN receptor subunits, IFNλR1 and IL10Rβ. B16-F10, E0771, and ID8 cells were harvested after 3 different passages to perform RNA isolation and analyze the level of gene expression of both receptor subunits for the type I and III IFN receptor. Expression of *Ifnar1* (**A**), *Ifnar2* **(B),** *Ifnlr1* (**C**), and *Il10rb* (**D**) was assessed by RT-qPCR. Gene expression was normalized to *Hprt* and *Gusb*. Groups were tested for normality using a Shapiro-Wilk normality test. Statistical significance was determined using an unpaired t test comparing expression in ID8 cells to expression in B16-F10 and E0771 cells independently. Data are shown as mean ± SEM. N = 3. * = $p < 0.05$, ** = $p < 0.01$.

statistically significant compared to the other cell lines (**Figure 3.1C**). Expression of *Ifnlr1* was very low in B16-F10 cells and absent in E0771 cells (**Figure 3.1C**). All cell lines expressed *Il10rb*, confirming expression of both subunits of the type III IFN receptor in ID8 cells (**Figure 3.1D**). These findings indicated that all cell lines expressed the type I IFN receptor, while only ID8 cells expressed both chains of the type III IFN receptor.

3.1.2 Determining type I and III IFN receptor functionality in tumour cell lines

Currently, antibodies to analyze protein expression of murine IFNλR1 by western blot and flow cytometry are poorly characterized. As a result, protein expression of the type I and III IFN receptors was confirmed through assessment of IFN signaling. ISG induction was measured after treatment with recombinant IFNs *in vitro*. *Cxcl10, Mx1,* and *Ifit1* were selected as read outs since these genes are upregulated in response to both type I and III IFNs[171]. B16-F10, E0771, and ID8 cell lines were treated with recombinant IFN-α (5 ng/ml) and IFN-λ2, at multiple doses (300, 100, 33, 10, and 3.3 ng/ml). Cells were harvested 6 and 24 hours post-stimulation to isolate RNA and measure ISG induction by RT-qPCR (**Figure 3.2**). An early and late timepoint were selected given the short induction kinetics of IFN-α and the prolonged kinetics of IFN-λ[56]. Unstimulated cells were used to determine baseline expression levels of each ISG. Although an upregulation in *Cxcl10* and *Mx1* expression was not observed at either time point in E0771 and ID8 cells respectively, all tumour cell lines responded to IFN-α activation through significant upregulation of at least one measured ISGs across measured time points (**Figure 3.2A-F**). Conversely, E0771 cells did not substantially upregulate any of the measured ISGs, in

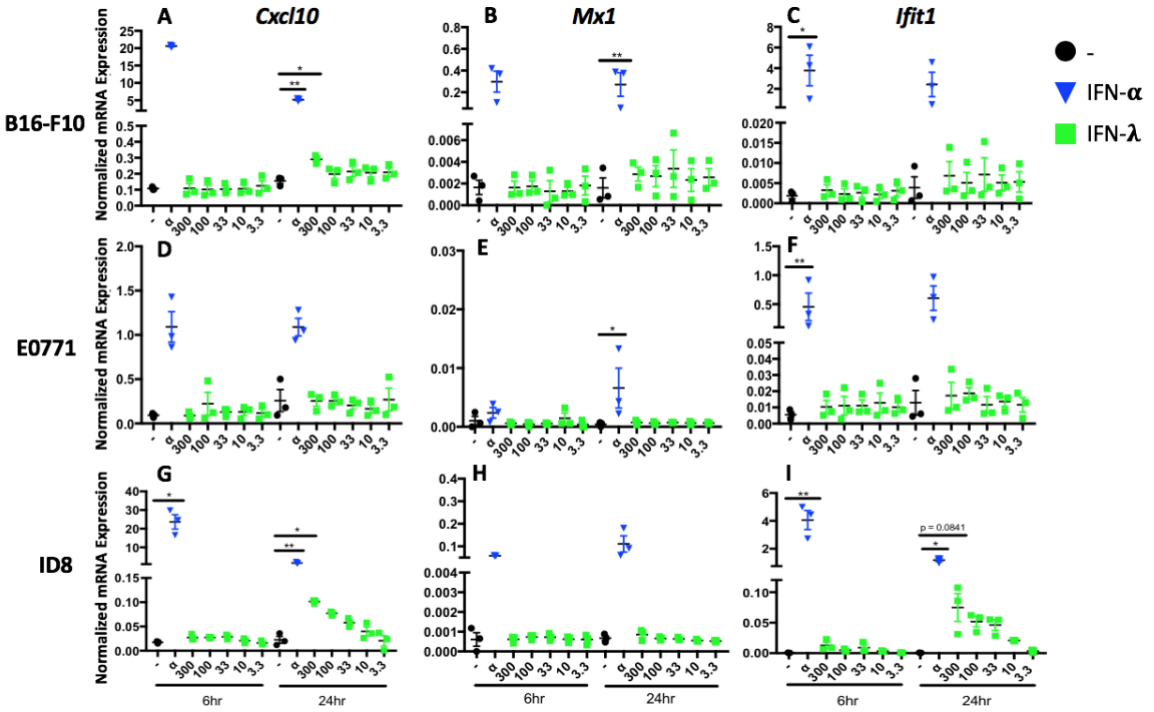

Figure 3.2: ID8 cells show upregulation of *Ifit1* and *Cxcl10* in response to IFN-λ2 stimulation after 24hrs, which is absent in B16-F10 and E0771 cells. B16-F10, E0771, and ID8 cells were left unstimulated (-), activated with 5 ng/mL IFN-α, or activated with IFN-λ2 at a range of doses: 300, 100, 33, 10, or 3.3 ng/mL. Cells were harvested at two time points, 6 and 24 hours post-activation, for RNA isolation to analyze *Cxcl10* (**A, D, G**), *Mx1* (**B, E, H**), and *Ifit1* (**C, F, I**) gene expression measured by RT-qPCR. Gene expression was normalized to *Hprt* and *Tbp*. Statistical significance was assessed by Friedman's multiple comparisons test, comparing all groups in their individual time points to the unstimulated control. Data are shown as mean ± SEM. N = 3. * = $p < 0.05$, ** = $p < 0.01$.

response to any dose of IFN-λ2 at 6 or 24 hours post-stimulation (**Figure 3.2A-F**). IFN-λ2 treatment of B16-F10 and ID8 cells showed a dose-dependent upregulation of *Cxcl10* at 24 hours, which was statistically significant at 300 ng/mL compared to untreated controls (**Figure 3.2G, I**). Interestingly, IFN-λ2 treatment of ID8 cells showed a trend towards a dose-dependent upregulation of *Cxcl10* and *Ifit1,* which was not observed in B16-F10 cells (**Figure 3.2G, I**). Unlike other measured ISGs, *Mx1* expression was not induced in IFN-λ2-treated ID8 cells at 24 hours (**Figure 3.2H**). Although not all ISGs were upregulated, the results suggest that B16-F10 and ID8 cells possess a functional type III IFN receptor, while E0771 cells do not due to their lack of response to IFN-λ2. Considering no dose-dependent upregulation was observed in B16-F10 cells treated with IFN-λ2, these results required corroboration. These results also suggest that all tumour cell lines possessed a functional type I IFN receptor.

3.1.3 Assessing IFN-λ-mediated apoptosis in tumour cells expressing the type III IFN receptor

After determining which tumour models expressed functional IFN protein receptors, we sought to determine if we could induce direct IFN-mediated apoptosis using type III IFNs *in vitro*. The cells tested included ID8 cells, which responded to IFN-λ2 *in vitro*, and B16-F10 cells, which are documented to undergo IFN-λ-mediated apoptosis, but were potentially unresponsive to type III IFNs in our previous experiments, since no dose-dependent observations occured[80]. Both tumour cell lines were treated with recombinant IFN-λ2 for 72 hours, an incubation period commonly used to assess IFN-mediated apoptosis, and cells were collected and stained for the apoptotic marker, AV, and FVD to

identify dead cells[45]. To confirm that IFN-λ signaling was occurring, expression of MHCI was also measured. Cells were counted to determine whether IFN-λ2 had any impact on cell proliferation. The frequency of late apoptotic cells (AV^+, FVD^+) and $MHCI^+$ cells were assessed by flow cytometry. Camptothecin was used as a positive control for apoptosis induction. A dose of 12 μM dose was selected as it induced cell death in ~80% of B16-F10 and ID8 cells after 72 hours (**Appendix Figure 1**).

IFN-λ2 stimulation of B16-F10 and ID8 cells did not increase the frequency of apoptotic cells compared to unstimulated controls (**Figure 3.3A, D**). Proliferation of both cell lines *in vitro* was unaffected by IFN treatment (**Figure 3.3C, F**). A trend towards an upregulation MHCI expression was observed in IFN-λ2-treated ID8 cells but not in B16-F10 cells, however this upregulation was not statistically significant (**Figure 3.3B, E**). These findings contradicted our previous data regarding type III IFN receptor expression amongst tumour cell lines, as B16-F10 cells showed no observable response to IFN treatment. Although ID8 cells express the receptor, they did not undergo apoptosis in response to type III IFN stimulation *in vitro*, even at doses as high as 300 ng/mL.

3.2 Characterizing tumour growth and IFN production in models of mast cell deficiency

3.2.1 Tumour growth kinetics of ID8 model in mast cell-deficient mice

The impact of mast cells on ovarian tumour growth is controversial, however there is evidence to suggest mast cells can hinder ovarian cancer progression[148]. To our knowledge, no previous studies have characterized survival in ID8-challenged mast cell-deficient mouse models. To address this, we used a model of mast cell-deficiency, Wsh

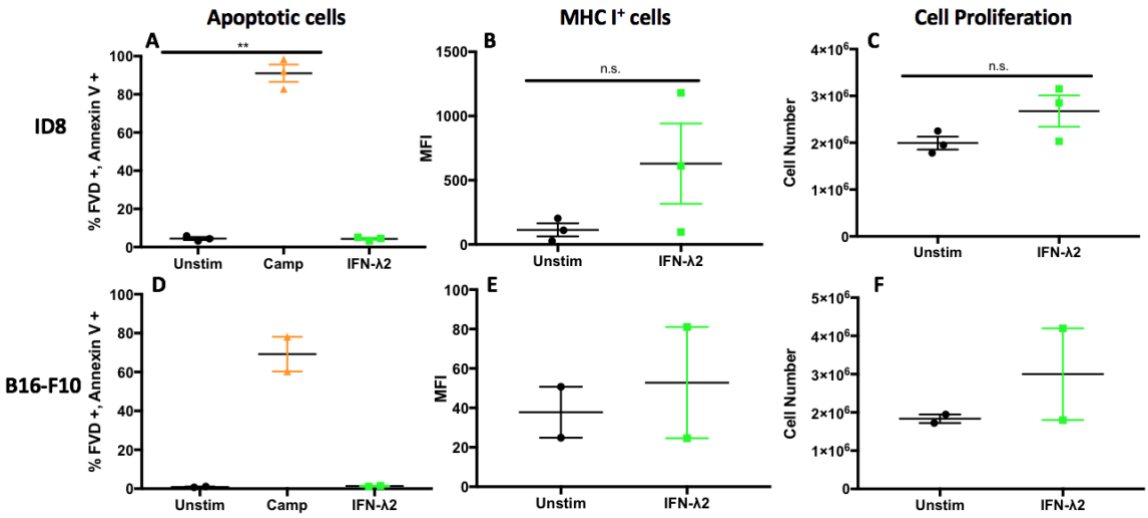

Figure 3.3: IFN-λ2 treatment does not induce apoptosis, reduce cell proliferation, or significantly upregulate MHCI expression in B16-F10 and ID8 cells *in vitro*. B16-F10 (N = 2) and ID8 (N = 3) cells were activated with 300 ng/mL IFN-λ2 for 72 hours before cells were harvested and stained with FVD and AV (**A, D**) to assess the level of IFN-mediated apoptosis by flow cytometry. Cells were also stained with an anti-MHCI antibody to confirm IFN signaling in activated cells (**B, E**)**.** Cells counts were used to assess cell proliferation (**C, F**). Controls included cells left untreated (Unstim) with IFNs to analyze the level of apoptosis occurring without cytokine activation, while another group was treated with 12 μM camptothecin (Camp) to induce significant apoptosis. Apoptotic cells are defined as FVD^+ and AV^+ cells. MHCI data is represented as the mean fluorescent intensity (MFI). Statistical significance was determined in data sets for ID8 cells. Shapiro-Wilk normality test was performed to determine normal distribution. Data sets passed normality so paired T tests were performed. Data are shown as mean ± SEM. ** = $p < 0.01$, n.s. = not significant.

mice, also known as c-Kit$^{W\text{-}sh}$ or sash mice. These mice have an inversion of c-kit, a crucial receptor involved in mast cell development and survival[172]. Female in-house bred C57BL/6 (Dal B6) and Wsh mice were injected intraperitoneally with $3.0x10^6$ ID8 cells and monitored for ascites development over the course of 80 days. Ascites is expected to develop between 30-40 days post-injection in Dal B6 mice[173]. Initially, ID8 tumours in our in-house bred mice yielded unexpected growth kinetics, with ascites development in Dal B6 mice occurring later than expected and some animals surviving to 80 days post-injection without ascites development (**Figure 3.4A**). Wsh mice exhibited shorter survival times, which was determined to be statistically significant compared to Dal B6 mice (**Figure 3.4A**). These initial results suggested that mast cell-deficiency negatively impacted overall survival.

It has been reported that microbiota can impact tumour development and growth kinetics in mice[174]. To determine if the microbiota of our in-house bred animals caused the disparity in ID8 growth kinetics observed above, female C57BL/6 mice from Charles River Laboratories (CRL B6) were injected in parallel with locally bred Dal B6 and Wsh animals to examine ascites development and overall survival. Animals were injected intraperitoneally with either the previously used dose ($3.0x10^6$) or a higher dose ($6.0x10^6$) of ID8 cells to corroborate our initial findings (**Figure 3.4B, C**). Ascites development in animals injected with the low dose of ID8 cells occurred between Day 30-40 for both strains of in-house bred animals, corroborating the reports in the literature, while CRL B6 animals showed slightly longer survival times, however this was not statistically significant (**Figure 3.4B**). This timeline of ascites development was confirmed in mice injected with the high dose of ID8 cells, with ascites development occurring between Day

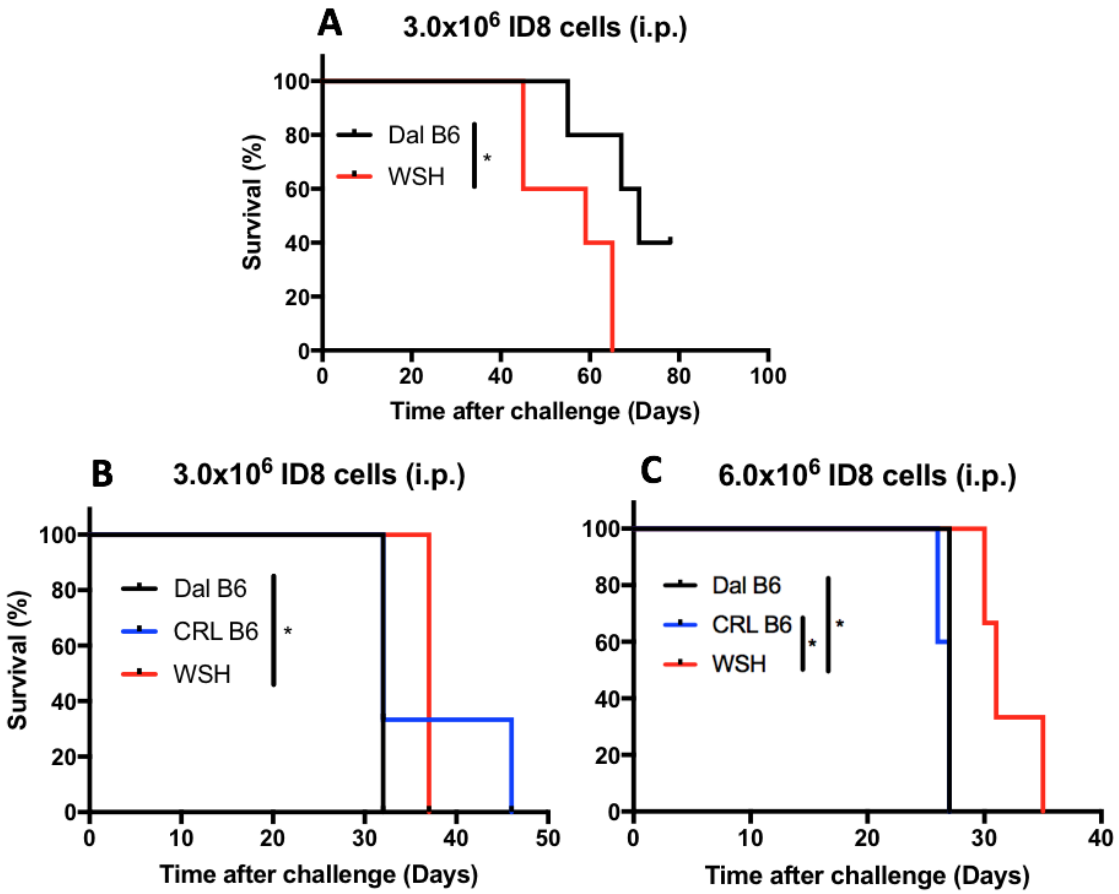

Figure 3.4: ID8 ascites development for in-house bred C57BL/6 mice and Wsh mice are inconsistent across independent experiments. In-house bred C57BL/6 mice (N = 5) and Wsh mice (N = 5) were injected intraperitoneally with 3.0x10$_6$ ID8 cells after which mice were monitored until ascites development over 80 days (**A**)**.** After this initial experiment, another set of in-house bred C57BL/6 (Dal B6, N = 3) and Wsh mice (N = 3), were injected in parallel C57BL/6 mice ordered from Charles River Laboratory's (CRL B6, N = 3). Mice were injected with two doses, the previously used dose of ID8 cells, 3.0x10$_6$ per mouse (**B**), and a higher dose, 6.0x10$_6$ per mouse (**C**), and monitored for survival over 80 days**.** Overall survival is represented through Kaplan-Meier survival curves. Data was assessed for statistical significance by Log-Rank (Mantel-Cox) Test. * = $p < 0.05$.

20-30 for both groups of C57BL/6 mice and between Day 30-40 in Wsh animals (**Figure 3.4C**). At both doses, ascites development occurred earlier for Dal B6 mice compared to Wsh mice, which was found to be statistically significant, and contradicted the earlier findings that mast cell-deficiency negatively impacted ascites development and survival (**Figure 3.4B, C**). There was no statistically significant difference in overall survival in CRL B6 mice compared to Dal B6 mice at either dose (**Figure 3.4B, C**). These findings suggested that the differences in microbiota of in-house animals and CRL C57BL/6 mice did not impact the extended survival periods and delayed ascites development observed in initial experiments, which may suggest potential technical issues related to the injection process. The experimental examination of the impact of mast cell-deficiency on ID8 tumour growth and mouse survival was inconclusive, given the contradictory findings between experiments.

3.2.2 Impact of mast cell-deficiency and mast cell-reconstitution on E0771 tumour growth

Studies on human breast cancer have depicted mast cells favourably, describing their presence as a good prognostic biomarker and attributing these cells anti-tumourigenic properties[144,147]. While mast cells may be favourable in human breast cancer, their effect on tumour growth and development in mouse mammary cancer models is not widely reported. To examine this, female C57BL/6 and Wsh mice were subcutaneously injected into the mammary fat pad with 2.0×10^5 E0771 cells suspended in Matrigel to observe tumour growth and survival over 21 days (**Figure 3.5**). Tumour volume was tracked via caliper measurements every 2 days post-injection and animals were sacrificed if tumour

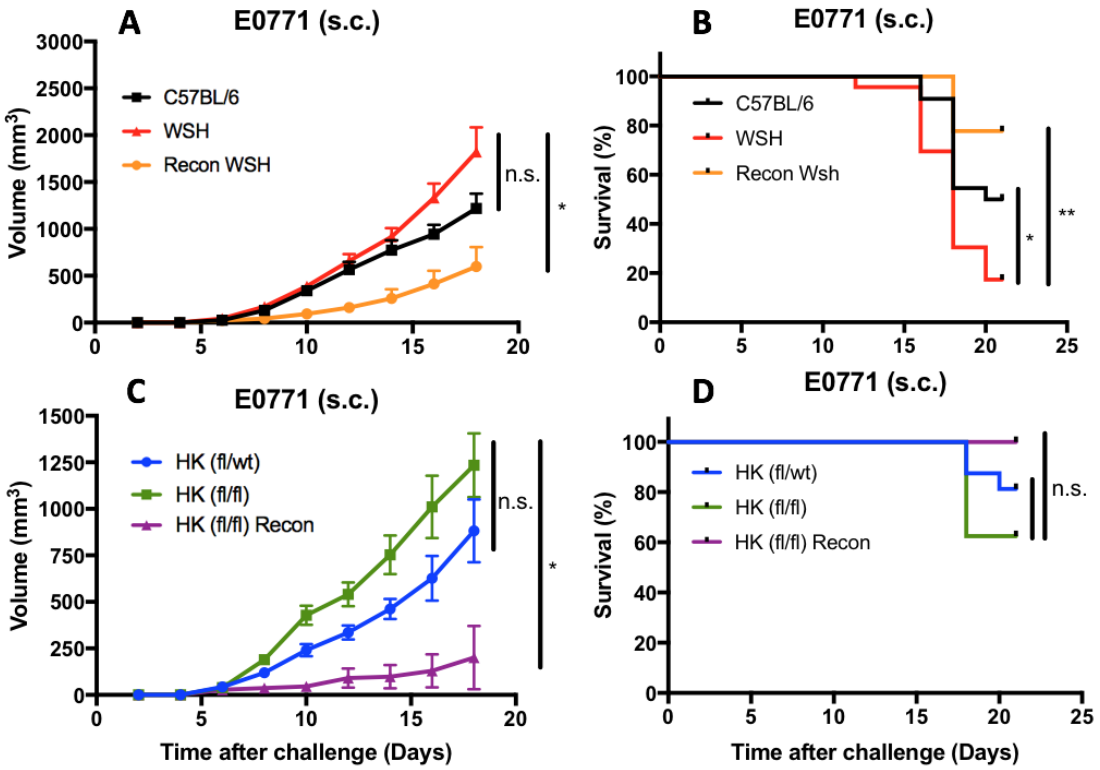

Figure 3.5: E0771 tumour progression was significantly decreased in reconstituted mast cell-deficient mice compared to WT mast cell-sufficient mice and non-reconstituted mast cell-deficient mice, resulting in significantly increased survival in reconstituted groups. Six weeks prior to injection with tumour cells, a group of Wsh mice were subcutaneously injected with 2.0x10$_6$ BMMCs in the mammary fat pad and rested to allow for reconstitution of injection site (Recon Wsh)**.** C57BL/6 mice (N = 22), non-reconstituted Wsh mice (N = 23) and Recon Wsh (N = 9) were subcutaneously injected in the mammary fat pad with 2.0x10$_5$ E0771 cells suspended in Matrigel. Tumour volume was measured by caliper measurements (**A**) and mice were monitored for 21 days to analyze survival (**B**)**.** The experiment was repeated using the mast cell-deficient, "Hello Kitty" (HK), model, injecting mast cell-sufficient HK mice (HK (fl/wt) N = 16), mast cell-deficient HK mice (HK (fl/fl), N = 8), and reconstituted HK (fl/fl) (Recon HK (fl/fl), N = 4) with E0771 cells before monitoring tumour volume and survival as above (**C, D**)**.** Statistical differences for tumour volume over the time course was determined by examining the area under the curve and comparing the mean for each condition by one-way ANOVA followed by Sidak's multiple comparisons test. Overall survival is represented through Kaplan-Meier survival curves, using Log-Rank (Mantel-Cox) Test to determine significance. Tumour volume data are shown as mean ± SEM. $p < 0.05$ = *, $p < 0.01$ = **. n.s. = not statistically significant.

volume exceeded 2000 mm^3 or if the tumour ulcerated. E0771 tumour growth appeared more aggressive in Wsh mice compared to WT controls, however tumour volumes were not statistically significant after 21 days (**Figure 3.5A**). While mast cell-deficiency appeared to have no significant impact on tumour growth, Wsh mice exhibited significantly lower survival rates compared to C57BL/6 mice (**Figure 3.5B**). This suggested that mast cell-deficiency negatively impacted survival in mice challenged with E0771 tumours. To follow-up on this finding, a group of Wsh mice were locally reconstituted with murine BMMCs derived *in vitro.* These were subcutaneously injected into the mammary fat pad (Recon Wsh) 6 weeks before E0771 tumour cell injection. Recon Wsh mice were then injected with tumour cells in parallel with age-matched C57BL/6 and non-reconstituted Wsh mice to determine how local mast cell engraftment affected tumour growth. Interestingly, local mast cell reconstitution significantly reduced E0771 tumour growth compared to control Wsh mice (**Figure 3.5A**). Local reconstitution also significantly enhanced survival of Wsh mice compared to non-reconstituted animals (**Figure 3.5B**). These findings suggested that mast cells can slow progression of mammary tumour growth in mice.

To confirm the anti-tumourigenic effects of mast cells on breast cancer growth *in vivo*, E0771 challenge was repeated using another model of mast cell-deficiency, "Hello kitty" (HK) mice. HK mice, also known as *Cpa3-Cre; Mcl-1$^{fl/fl}$* mice, are transgenic mice that use a Cre recombinase system to cause a deletion of the anti-apoptotic induced myeloid leukemia cell differentiation protein 1 (Mcl-1) gene in cells expressing Cpa3, a system that requires the Mcl-1 gene to be "floxed" by two loxP sites on both alleles to result in mast cell-deficiency[172,175]. HK mice with only one floxed allele (HK (fl/wt))

remain mast cell-sufficient, while two floxed alleles (HK (fl/fl)) and the presence of the Cre enzyme results in mast cell depletion. This mast cell-deficient mouse model occurs independently of any c-kit mutation. Female HK (fl/wt), HK (fl/fl), and mast-cell-reconstituted HK (fl/fl) (Recon HK (fl/fl)) mice were injected with E0771 cells and tumour volume and survival were measured over 21 days. HK (fl/fl) mice displayed a trend toward higher tumour volumes over 21 days compared to HK (fl/wt) mice, however this was not statistically significant (**Figure 3.5C**). Corroborating the observations using the Wsh model, Recon HK (fl/fl) mice exhibited diminished tumour volume compared to their non-reconstituted controls, which was statistically significant after 21 days (**Figure 3.5C**). Recon HK (fl/fl) mice showed a trend towards an increase in overall survival compared to both HK (fl/wt) and HK (fl/fl) groups, however this was not statistically significant (**Figure 3.5D**). Collectively, these findings observed across two models of mast cell-deficiency would indicate that mast cells mediate tumour reduction and improve survival rates after E0771 tumour challenge *in vivo*.

3.2.3 Type I and III IFN expression in the E0771 tumour microenvironment

The ability of mast cells to produce IFNs has been documented, however studies demonstrating their production *in vivo*, especially in the context of cancer, are lacking[139]. Studies characterizing IFN expression patterns in the TME are similarly scarce. To examine the expression of type I and III IFNs in the E0771 TME and the potential contribution of mast cells to this IFN expression, mRNA expression was examined in tumours from WT, mast cell-deficient and mast cell-reconstituted mice using both Wsh and HK models. Expression of major type I and III IFN-related genes, including *Ifna1,*

Ifna2, Ifnb1, Ifnl2, Ifnl3, Ifnar1, and *Ifnlr1,* was analyzed by RT-qPCR (**Figure 3.6, Appendix Figure 2**). Data was organized in blocks based on date of sacrifice to account for changes in gene expression that would occur during early and later stages of tumour growth.

Type I and III IFN expression patterns in the E0771 TME showed that *Ifnar1, Ifnb1,* and *Ifnlr1* were expressed in all mouse models (**Figure 3.6**). *Ifnar1* was expressed to the highest level of any measured gene, however no observable trends in expression between models of mast cell-deficiency were observed at any measured time point, suggesting any changes were mast cell-independent (**Figure 3.6A, C**). The E0771 TME yielded little to no expression of *Ifna1, Ifna2, Ifnl2,* and *Ifnl3* from any mouse strains across all measured time points (**Figure 3.6B, D**, **Appendix Figure 2**). *Ifnb1* and *Ifnlr1* expression fluctuated over time, however no consistent trends between our mast cell-deficient and -sufficient models were observed, suggesting that these changes were also mast cell-independent (**Figure 3.6B, D**, **Appendix Figure 2**). Important findings from these data include the expression of *Ifnar1* and *Ifnlr1 in vivo* in the E0771 TME, suggesting local cellular components would respond to IFN-α/λ overexpression. Gene expression patterns also suggest that substantial IFN-α1, IFN-α2, IFN-λ2, and IFN-λ3 cytokine production is likely absent at the tumour site. Overall, these data suggests that mast cells do not contribute to IFN expression in the TME of E0771 mammary cancer and that IFNs are generally not highly expressed nor, likely, produced during tumour growth.

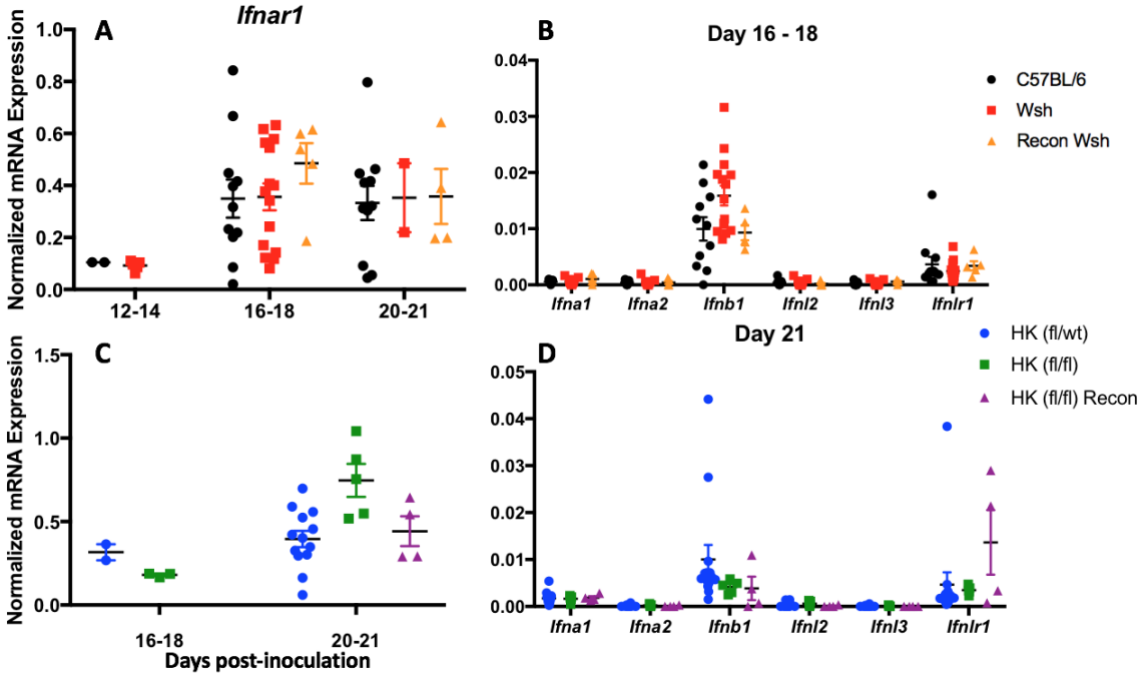

Figure 3.6: Type I and III IFN expression in the E0771 TME shows cytokine expression of *Ifnb1* and both the type I and III IFN receptors are expressed by cells in the tumour site. Six weeks prior to injection with tumour cells, a group of Wsh mice were subcutaneously injected with 2.0x10$_6$ BMMCs in the mammary fat pad to allow for mast cell reconstitution (Recon Wsh). C57BL/6 mice, non-reconstituted Wsh mice and Recon Wsh were subcutaneously injected with 2.0x10$_5$ E0771 cells suspended in Matrigel into the mammary fat pad. Mice were sacrificed when tumour volume reached above 2000mm$_3$, tumour growth obstructed mobility, mice lost more than 15% of initial body weight, or tumours ulcerated during growth. Tumours were extracted to perform RNA isolation. mRNA expression of the type I and III IFN cytokine and receptor genes *Ifnar1* (**A**), *Ifna1, Ifna2, Ifnb1, Ifnlr1, Ifnl2,* and *Ifnl3* (**B**) were assessed by RT-qPCR. This data represents IFN expression in E0771 tumours from mice sacrificed between Day 16 – 18 in B6 (N = 11), non-recon Wsh (N = 15), Recon Wsh (N = 5) groups. The experiment was repeated using HK (fl/wt) (N = 13), HK (fl/fl) (N = 5) and HK (fl/fl) Recon (N = 4) groups, assessing all aforementioned IFN genes, with the data representing mice harvested on Day 21 (**C, D**). *Ifnar1* expression is shown from mice harvested at all time points. Data are shown as mean ± SEM.

3.3 The effect of mast cell administration on E0771 tumour growth in WT mice and quantification of mast cell populations in the murine mammary fat pad

3.3.1 The impact of local mammary fat pad mast cell enrichment on E0771 tumours of C57BL/6 mice

The impact of mast cell reconstitution on E0771 tumour growth in mast cell-deficient mice suggested that mast cells possess anti-tumourigenic functions in this model of mammary cancer. Considering that increasing local mast cell number around the mammary fat pad showed a significant effect on decreasing tumour size in mice lacking mast cells, we investigated whether this would occur if mast cell numbers were locally elevated in C57BL/6 mice. Female C57BL/6 mice were administered $2.0x10_6$ WT BMMCs injected subcutaneously into the mammary fat pad (Enrich B6) to enrich the tissue with mast cells. After waiting 6 weeks for engraftment, Enrich B6 and control C57BL/6 mice were inoculated into the same mammary fat pad with E0771 cells suspended in Matrigel. Tumour growth and survival were monitored over 21 days (**Figure 3.7**). While the overall curve assessing tumour growth was comparable between the two groups, Enrich B6 mice challenged with E0771 tumours exhibited reduction in tumour growth that was statistically significant when assessed on Day 10 and 12 (**Figure 3.7A**). While mast cell enrichment showed a reduction on early stage tumour growth, mean tumour volume was comparable from Day 16 until experimental endpoint and tumour weight upon sacrifice was comparable between the two groups (**Figure 3.7A, B**). All mice survived to the humane endpoint, suggesting enrichment had no impact on overall survival. These findings suggest that mast cell enrichment of WT mice had a significant effect in early stages, but not later stages, of E0771 mammary tumour growth.

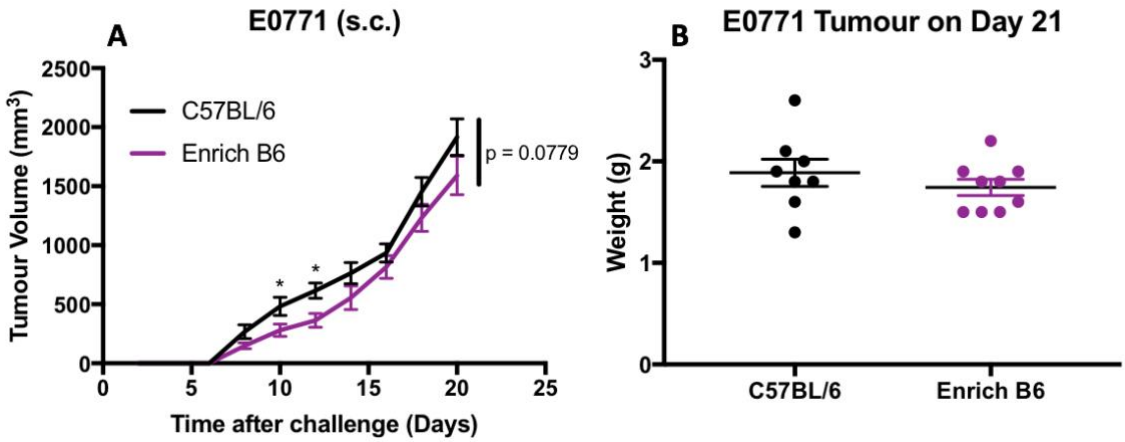

Figure 3.7: Mast cell enrichment of the mammary fat pad in C57BL/6 mice shows a transient effect on E0771 tumour growth but no difference in final tumour weight after sacrifice. C57BL/6 mice were injected subcutaneously with $2.0x10_6$ BMMCs into the mammary fat pad and rested for 6 weeks to allow for mast cell enrichment (Enrich B6). Enrich B6 and control C57BL/6 mice were injected with $2.0x10_5$ E0771 cells suspended in Matrigel into the mammary fat pad and mice were monitored for 21 days to determine overall survival and tumour volume by caliper measurements (**A**)**.** Tumours were weighed upon sacrifice (**B**). Statistical significance for tumour volume data was determined by assessing the area under the curve and comparing the area of each line by an unpaired t test. Data was also compared at individual timepoints by multiple t tests. Data are shown as mean ± SEM. $p < 0.05$ = *.

This decrease in early stage tumour growth suggested that follow-up experiments were necessary to determine if the number of mast cells residing locally in the mammary fat pad or other tissues around the injection site may influence tumour progression. These results underlined the importance of quantifying mast cell populations in the mammary fat pad of WT mice.

3.3.2 Mast cell-mediated E0771 tumour reduction is more pronounced in enriched C57BL/6 mice challenged with lower doses of tumour cells

The literature currently lacks evidence demonstrating that adoptively transferred mouse mast cells survive *in vivo*. To further confirm any potential differences in E0771 tumour growth in enriched C57BL/6 mice compared to controls, we sought to determine whether more pronounced tumour control would occur in enriched mice challenged with a lower dose of tumour cells. C57BL/6 mice were locally enriched with $2.0x10^6$ BMMCs injected into the mammary fat pad and rested for 6 weeks. Another group of C57BL/6 mice were used as an age-matched control. Mice were locally challenged with either a higher dose ($2.0x10^5$) or a lower dose ($5.0x10^4$) of E0771 tumour cells injected subcutaneously into the mammary fat pad. Tumour volume and overall survival over 21 days was assessed (**Figure 3.8**). Results showed that enriched C57BL/6 mice injected with a lower dose of tumour cells (Enrich Lo) had significantly reduced tumour volumes compared to both control mice injected with a lower dose (Control Lo) and enriched mice injected with a higher dose (Enrich Hi) after 18 days (**Figure 3.8A**). Enrich Lo mice also showed prolonged survival compared to all other mouse groups (**Figure 3.8B**). Interestingly, Enrich Hi and Control Lo mice had similar tumour volumes (**Figure 3.8A**). Enrich Hi

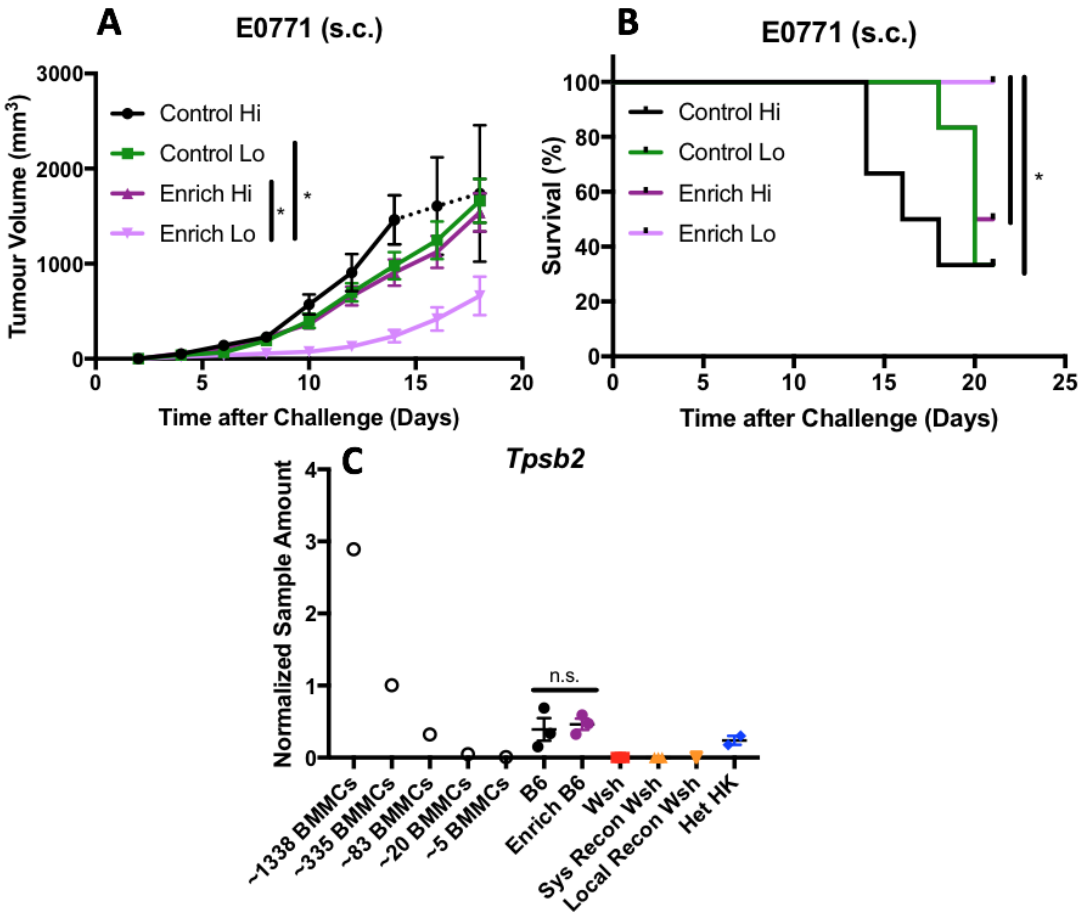

Figure 3.8 Local mast cell enrichment in C57BL/6 mice shows more pronounced E0771 tumour reduction in mice injected with a lower cell dose. Six weeks prior to tumour cell injection, C57BL/6 mice were injected with 2.0x10$_6$ BMMCs locally in the mammary fat pad (Enrich) or saline (Control). After resting for 6 weeks to allow for enrichment, Control and Enrich mice were challenged with either 2.0x10$_5$ (Hi) or 5.0x10$_4$ (Lo) E0771 cells suspended in Matrigel injected subcutaneously into the mammary fat pad. Tumour volume (**A**) and overall survival (**B**) were assessed over 21 days. Dotted lines in tumour volume data represents timepoints affected by early sacrifice of individual animals. N = 6 for Control Hi, Control Lo, and Enrich Hi, N = 7 for Enrich Lo. Another set of Control and Enrich B6 mice were sacrificed 6 weeks after mast cell enrichment to isolate RNA from harvested mammary fat pads to determine the presence of the mast cell gene *Tpsb2* by ddPCR (**C**)**.** BMMCs were harvested *in vitro* as a positive control for *Tpsb2* expression. BMMC RNA was serial diluted to create a standard curve to quantify mast cell number. Statistical significance for tumour volume was determined by calculating the area under the curve and comparing the area of each line by one-way ANOVA followed by Sidak's multiple comparisons test. Overall survival is represented through Kaplan-Meier survival curves, using Log-Rank (Mantel-Cox) Test to determine significance. Statistical significance for *Tspb2* expression compared between B6 and Enrich B6 groups was assessed for normal distribution by a Shapiro-Wilk normality test. This was followed by a Mann-Whitney test. Data are shown as mean ± SEM. * = $p < 0.05$, n.s. = not significant.

mice also showed no statistically significant differences to control mice injected with a higher dose of E0771 cells (Control Hi) after tumour challenge (**Figure 3.8A**). These results corroborated our previous data in which we showed no significant changes in tumour growth in Enrich B6 mice injected with the same dose of tumour cells compared to control mice (**Figure 3.7A**). However, our data suggests that mast cell-mediated E0771 tumour reduction is dose-dependent in C57BL/6 mice, as challenging mice with a lower dose elicited statistically significant reductions compared to Control Lo and Recon Hi mice. These data also suggest that mast cells adoptively transferred into mast cell-sufficient mice inhibit tumour growth when challenged with lower doses of E0771 cells.

3.3.3 Quantification of mast cell populations in the mammary fat pad of mouse models

Reconstitution of mast cell-deficient animals with cultured mast cells result in uneven distribution and incomplete engraftment of target tissue sites compared to WT animals[172]. Despite this, attempting local enrichment of mast cell-sufficient animals has been largely ignored as an approach in mast cell literature. The literature also lacks evidence of mast cell populations in the mouse mammary fat pad. Consequently, we wanted to confirm successful mast cell enrichment in C57BL/6 mice to help implicate mast cells in the transient mammary tumour reduction observed in Enrich B6 mice, and to determine if mast cells normally reside in the mammary fat pad in WT animals. Female C57BL/6 mice were enriched with WT BMMCs by subcutaneous injection into the mammary fat pad and examined 6 weeks later. Mammary fat pads were also harvested from control C57BL/6 mice, HK (fl/wt) mice, control Wsh mice, Wsh mice locally reconstituted in the mammary fat pad, and Wsh mice systemically reconstituted by intravenous and

intraperitoneal injection of BMMCs. RNA was isolated from mammary fat pads to quantify expression of the mast cell gene *Tpsb2* by ddPCR (**Figure 3.8C**). RNA was also harvested from 5.0x10$_6$ BMMCs cultured *in vitro* to measure *Tpsb2* expression and establish a standard curve based on the amount of RNA per BMMC.

Mammary fat pads from C57BL/6, Enrich B6, and HK (fl/wt) mice showed *Tpsb2* expression that was comparable with ~83 BMMCs (**Figure 3.8C**). There were no significant differences in expression between these three groups. *Tpsb2* expression was absent in all Wsh groups, including mice that had been systemically and locally reconstituted with WT BMMCs (**Figure 3.8C**). To confirm mast cells in the mammary fat pad, 5 μm longitudinal sections of tissue were stained with Alcian blue and Safranin O to visualize mast cells by histology (**Figure 3.9A-F**). These results confirmed the ddPCR data obtained in the C57BL/6 and Wsh mammary fat pads, depicting the presence and absence of a mast cell population, respectively (**Figure 3.9A-D**). Conversely, in the local Recon Wsh mouse group, mast cells were detected by histology, associated with the blood vessels in the mammary fat pad and infiltrating the fat pad tissue (**Figure3.9E-F**). These findings suggested that WT mice normally contain mast cell populations in the mammary fat pad. Considering different techniques gave contrasting findings in locally reconstituted Wsh mice, engraftment of mast cells in the mammary fat pad after reconstitution may be imperfect and unevenly distributed, with mast cells surviving within the mammary fat pad, although likely residing in other tissue around the injection site. The comparable *Tpsb2* expression between C57BL/6 and Enrich B6 mice also suggest that BMMCs used between C57BL/6 and Enrich B6 mice may also suggest that BMMCs used for enrichment are not infiltrating the mammary fat pad long term and

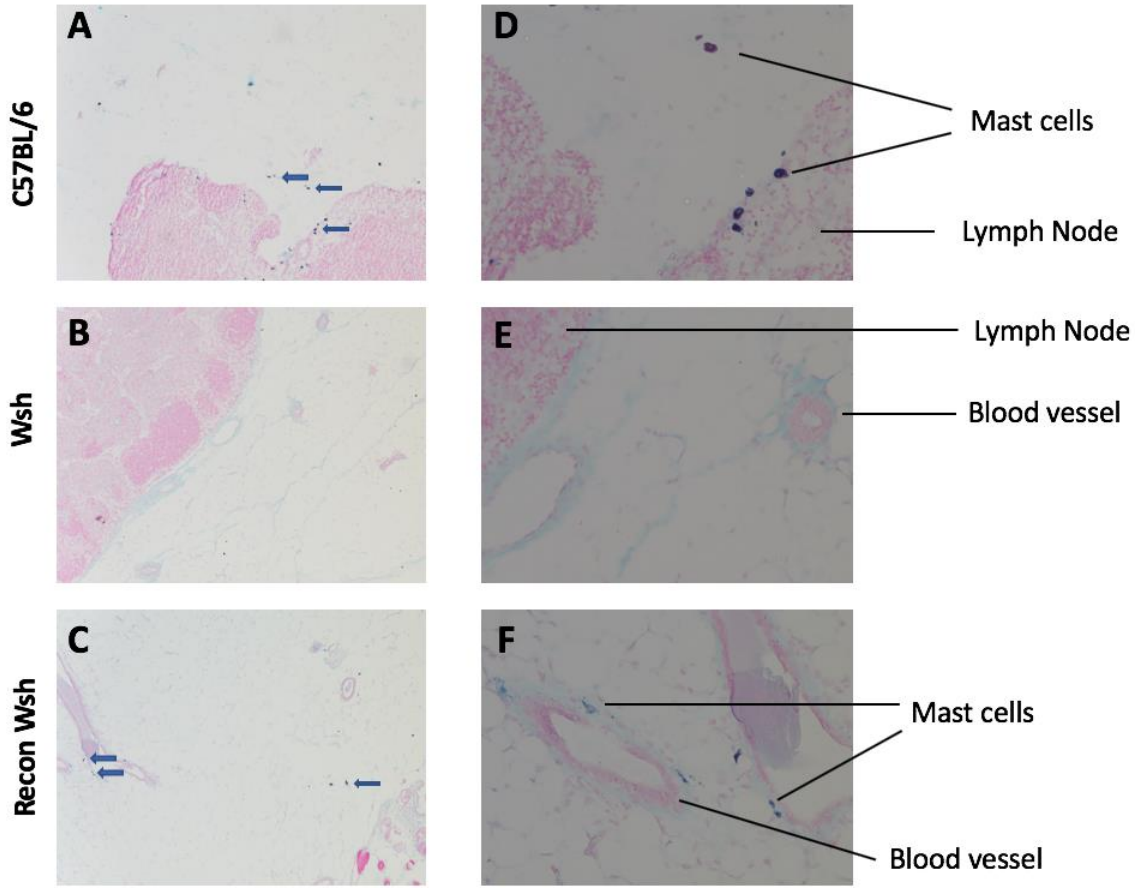

Figure 3.9: C57BL/6 mice and Recon Wsh mice have mast cells populations in the mammary fat pad. Mammary fat pads obtained from female C57BL/6, Wsh, and Recon Wsh mice were fixed in Carnoy's solution for 24 hours and paraffin embedded before 5 μM longitudinal tissue sections were cut. Sections were stained with 1% Alican blue and Safranin O to visualize mast cells granules. Mast cells were stained light blue or purple depending on granule content. Images show mast cells, blood vessels, and the inguinal lymph node throughout the mammary fat pad at 100x (**A-C**) and 400x (**D-F**) total magnification.

potentially reside in other tissues around the injection site, however this would need to be further assessed. An alternate possibility is that mast cells lose *Tpsb2* expression in this microenvironment.

3.4 The effect of mast cell reconstitution on immune cell infiltration in E0771 tumours

The sentinel abilities of mast cells are well-documented in pathogen infection and in the context of cancer, although these latter studies have characterized recruitment of immunosuppressive cell types[111,122]. Given that mast cells reduced the growth of E0771 mammary tumours, we investigated the impact of mast cell reconstitution on the infiltrating immune cell profile of the E0771 TME. To examine this, C57BL/6, Wsh, and Recon Wsh mice were inoculated with E0771 cells and tumours were monitored for 14 days before animals were sacrificed. Tumours, spleen, and inguinal lymph nodes were collected to determine the local and systemic impact by mast cells on innate and adaptive immune infiltration, as well as any changes in activation status (**Figure 3.10, Appendix Table 1 and 2**). Data was expressed in cell number/g. Tumour weight was significantly reduced in Recon Wsh compared to C57BL/6 and Wsh controls (Data not shown). Mast cell reconstitution was associated with a trend toward increased infiltration of $CD4^+$ and $CD8^+$ T cells populations, with a trend toward decreased infiltration of NK cells and B cells compared to Wsh mice, however these results were not statistically significant (**Figure 3.10A**). While this T cell infiltration was not altered, mast cell reconstitution showed a trend of enhanced activation of these cells. Recon Wsh mice showed a trend toward increased infiltrating effector memory $CD4^+$ and $CD8^+$ T cells populations, which

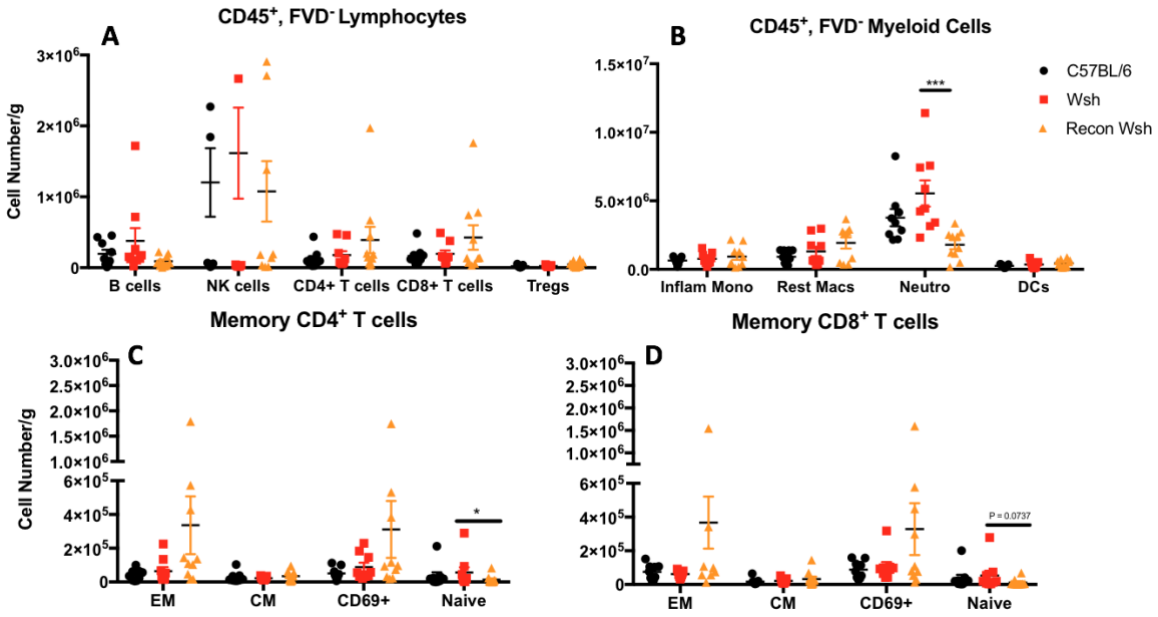

Figure 3.10: Mast cell reconstitution modifies immune infiltration in the E0771 TME, significantly decreasing the number of infiltrating neutrophils and naïve CD4+ T cells in reconstituted Wsh mice compared to control Wsh mice. Prior to tumour cell injection, 2.0x10$_6$ BMMCs were injected subcutaneously into the mammary fat pad of a group of Wsh mice (Recon Wsh), waiting 6 weeks to allow for full reconstitution. After this period, C57BL/6 (N = 9), Wsh (N = 9), and Recon Wsh mice (N = 10) were subcutaneously injected with 2.0x10$_5$ E0771 cells suspended in Matrigel. Tumour volume was monitored over 14 days. On Day 14, all mice were sacrificed, removing and weighing tumours. Tumours were enzymatically digested and stained with Panel A, B, and C as outlined in **Table 1.2,** analyzing markers for B, T, and NK cells (**A**), and myeloid cells (**B**). Central memory (CM), effector memory (EM), naïve and CD69+ T cell subsets were also further characterized for both CD4+ and CD8+ populations (**C, D**). Data are expressed in cell number/g to normalize infiltrate to tumour size. Statistical significance was determined through multiple comparisons, using a Kruskal-Wallis test comparing C57BL/6 vs. Wsh groups and Wsh vs. Recon Wsh groups. Data are shown as mean ± SEM.$p < 0.05$ = *, $p < 0.001$ = ***.

coincided with enhanced CD69 expression and a statistically significant decrease in infiltrating naïve CD4+ T cell populations and a trend towards reduced naïve CD8+ T cell populations (**Figure 3.10C, D**). Interestingly, Wsh mice showed significantly reduced CD69 expression on CD8+ T cells in the spleen compared to C57BL/6 mice, which was significantly upregulated after mast cell reconstitution (**Appendix Table 1**). These data suggested that local mast cell reconstitution had a systemic impact on CD8+ T cell activation. Wsh mice also showed significantly reduced B cell, T_{reg}, and CD8+ T cell numbers in the spleen compared to C57BL/6 mice, however reconstitution did not show any significant increase in these numbers, suggesting these results were not mast cell-dependent (**Appendix Table 1**). T cell subsets in the spleen, including effector memory CD4+ T cells, CD69+ CD4+ T cells, central memory CD8+ T cells, and naïve CD8+ T cells were also significantly decreased compared to C57BL/6 mice, however these numbers were not restored with mast cell reconstitution, suggesting the reduction was also mast cell-independent (**Appendix Table 1**). With regard to myeloid cells, Recon Wsh mice showed a numerical, but not significant, increase in infiltration of inflammatory monocytes, resting macrophages, and DCs, while neutrophil infiltration was significantly decreased compared to Wsh animals (**Figure 3.10B**). Mast cells were not detected in the E0771 TME by flow cytometry. These data, taken together, suggest that mast cell reconstitution enhances memory CD4+ T cell activation in the E0771 TME, which coincides with an overall decrease in tumour size. Neutrophil infiltration was also significantly decreased after mast cell reconstitution in Recon Wsh compared to Wsh controls, suggesting that infiltration of both innate and adaptive immune cell populations are impacted by the presence of mast cells in this tumour model. Mast cell reconstitution

also enhances CD8+ T cell activation in the spleen, suggesting that local reconstitution has a systemic impact. Interestingly, these data would also suggest that mast cells do not have intra-tumoural localization in this model of mammary cancer given they were not detected in the tumour site. Gating strategies for the classification of individual lymphocyte and myeloid cell populations can be found in **Appendix Figure 3**.

3.5 Genetic modification of BMMCs by transduction with inducible IFN-λ2

3.5.1 Testing IFN-λ2 induction of target genes and protein production in U2-OS cells

In vitro genetic modification of immune cells to enhance their anti-tumour responses is a well-documented strategy for cancer immunotherapy. The use of both type I and III IFNs for cancer immunotherapy has gained notable attention and has been taken to clinical trials[78]. After characterizing the impact of mast cells in E0771 mammary cancer, we sought to determine how a combined approach of mast cell-mediated IFN delivery would effect tumour growth in this model. IFN-λ2 was selected to genetically modify mast cells, given that it has been used previously in analogous experiments[164]. Two different IFN-λ2 transcripts, V1 and V2, were used during the initial cloning, generation of lentiviral particles, and transduction process. The V1 transcript was used in a study that modified B16 cells to express IFN-λ2 and is known to induce mRNA expression and produce functional IFN protein[164]. V2 was selected as it possesses an extended signal peptide sequence to the V1 sequence, which has unknown effects on mRNA expression and protein production. The DNA vector, pLJM1_Bla_TRE_ IFN-λ2, was cloned, transfected into HEK293T cells to generate lentiviral particles, and subsequently transduced into U2-OS cells *in vitro* to evaluate production of the two IFN-λ2 variants. A GFP construct was

used to determine efficiency of transfection and transduction, and to act as a negative control for IFN-λ2 induction.

To confirm successful induction of IFN-λ2 mRNA and protein from transduced U2OS cells expressing IFN-λ2 (IFN-λ2-U2-OS), cells were stimulated with 0.5 μg/mL of doxycycline added every 24 hours. Cells and their respective supernatants were harvested at 6, 24, 48, and 72 hours after induction. RNA was isolated from cells for examination of IFN-λ2 gene expression by RT-qPCR and IFN-λ2 protein production was determined in cell supernatants by ELISA (**Figure 3.11**). Unstimulated cells were used as a negative control. The results showed that both IFN-λ2 variants induced mRNA expression in a doxycycline-dependent manner, which increased over time for V1 and plateaued at 48 hours post-induction for V2 (**Figure 3.11A, B)**. Doxycycline induction of transduced cells also resulted in IFN-λ2 protein production for both tested variants, which increased over 72 hours (**Figure 3.11D, E**). Cells transduced with pLJM1_Bla_TRE_GFP showed no detectable gene expression or protein production of IFN-λ2. Interestingly, IFN-λ2 V1 sustained gene expression after 72 hours of doxycycline induction unlike V2, which was statistically significant (**Appendix Figure 4**). V1 produced more protein than V2-transduced cells, however this was not statistically significant at any time point (**Appendix Figure 4**). These findings suggested that the IFN-λ2 V1 transcript would be an appropriate target transcript to transduce BMMCs, given its sustained gene expression.

3.5.2 Assessing production of target genes by transduced BMMCs

To ensure that BMMCs could successfully produce IFN-λ2 after transduction with pLJM1_Bla_TRE_ IFN-λ2_V1, transduced-BMMCs (IFN-λ2-BMMCs) were stimulated

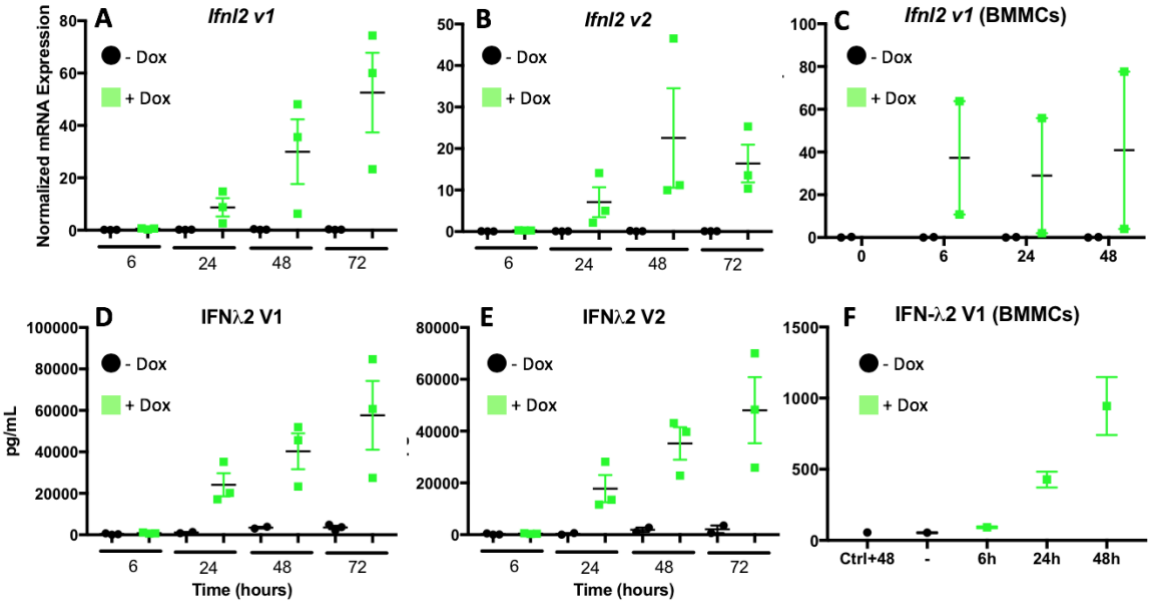

Figure 3.11: U2-OS cells and BMMCs transduced with IFN-λ2 showed successful doxycycline-dependent induction of IFN-λ2 mRNA expression and protein production *in vitro*. U2-OS cells were transduced with one of two transcripts, either *Ifnl2 v1* (N = 3) and *Ifnl2 v2* (N = 3), and treated with 0.5 µg/mL of doxycycline every 24 hours. Cells and supernatants were collected at four different time points (6, 24, 48, and 72 hours) to measure IFN-λ2 mRNA expression (**A, B**) and protein production (**D, E**) by RT-qPCR and ELISA, respectively**.** The experiment was repeated using IFN-λ2 V1-transduced-BMMCs (N = 2) to determine IFN-λ2 mRNA expression (**C**) and protein production (**F**). Protein production in IFN-λ2-BMMCs was compared to normal WT BMMCs left in culture for 48hrs (Ctrl+48) and transduced BMMCs in the absence of doxycycline (-). Experiments testing induction of IFN-λ2 by BMMCs were performed by Dr. Ian Haidl and Nong Xu. Gene expression was normalized to human *HPRT* and *GUSB* in experiments with U2-OS cells and mouse *Hprt* and *Gusb* for experiments using BMMCs. Data are shown as mean ± SEM.

with 0.5 μg/mL doxycycline every 24 hours and harvested at 0, 6, 24, and 48 hours, to analyze for IFN-λ2 gene expression and protein production. Unstimulated cells were used to determine IFN-λ2 V1 production in the absence of doxycycline in BMMCs and WT BMMCs stimulated with doxycycline for 48 hours to examine if IFN-λ2 production occurs in the absence of transduction. IFN-λ2-BMMCs exhibited a doxycycline-dependent upregulation in IFN-λ2 V1 gene expression over 48 hours (**Figure 3.11C**). This translated to a doxycycline-dependent protein production that increased over time (**Figure 3.11F**). There was a striking difference in the level of protein produced between IFN-λ2-U2-OS cells 48 hours post-induction (~40,000 pg/mL) compared to IFN-λ2-BMMCs (~1000 pg/mL) (**Figure 3.11D, F**). Despite these differences in production, IFN-λ2-BMMCs displayed a successful doxycycline-dependent induction of IFN-λ2 mRNA and protein, confirming the efficacy of this genetic modification system of BMMCs to produce inducible IFN.

3.6 Transduced-BMMC reconstitution of mast cell-deficient mice to determine IFN-λ2 induction and survival *in vivo*

After confirming that cultured BMMCs can be genetically modified to produce IFN-λ2 mRNA and protein upon induction *in vitro*, we sought to confirm that these findings could be reproduced *in vivo*. It was important to determine that IFN-λ2 production using this modification system produced functional protein, assessed by measuring ISG induction. IFN-λ2-BMMCs were injected into the peritoneum of male Wsh mice and rested for 6 weeks to fully reconstitute peritoneal tissue sites (IFN-λ2-BMMC Recon). After reconstitution, doxycycline was administered through chow for 4 or 14 days to

induce IFN-λ2 production. Control groups included mice reconstituted with WT BMMCs (WT Recon) and administered doxycycline and IFN-λ2-BMMC Recon mice that were not administered doxycycline. Peritoneal cells were harvested from mouse groups upon sacrifice to determine IFN-λ2 gene expression and induction of *Cxcl10* and *Ifit1* by RT-qPCR as a surrogate for functional protein production (**Figure 3.12**). Peritoneal cells collected from IFN-λ2-BMMC Recon mice showed a trend towards doxycycline-dependent upregulation of *Ifnl2* expression, which was absent in WT Recon groups administered doxycycline and IFN-λ2-BMMC Recon mice in the absence of doxycycline (**Figure 3.12A**). *Cxcl10* and *Ifit1* showed no trend towards an increase in expression from IFN-λ2-BMMC Recon mice administered doxycycline compared to those without (**Figure 3.12B, C**). Similarly, IFN-λ2 was undetectable in the peritoneal lavage fluid by ELISA (data not shown). These findings indicated that IFN-λ2-BMMCs survived reconstitution *in vivo* and produced *Ifnl2* mRNA upon doxycycline induction. Consequently, the data would suggest that either 1) induction did not translate to IFN-λ2 protein production or 2) that not enough IFN-λ2 was produced to elicit a detectable response considering type III IFNs are less potent, which resulted in no detectable ISG induction at either measured time point. To further investigate this issue, we wanted confirmation that type I and III IFN responses *in vivo* were detectable using our technical methods.

3.7 Characterization of *in vivo* type I and III IFN responses through injection of recombinant protein

Type III IFNs are known for less potent ISG induction that is sustained over longer

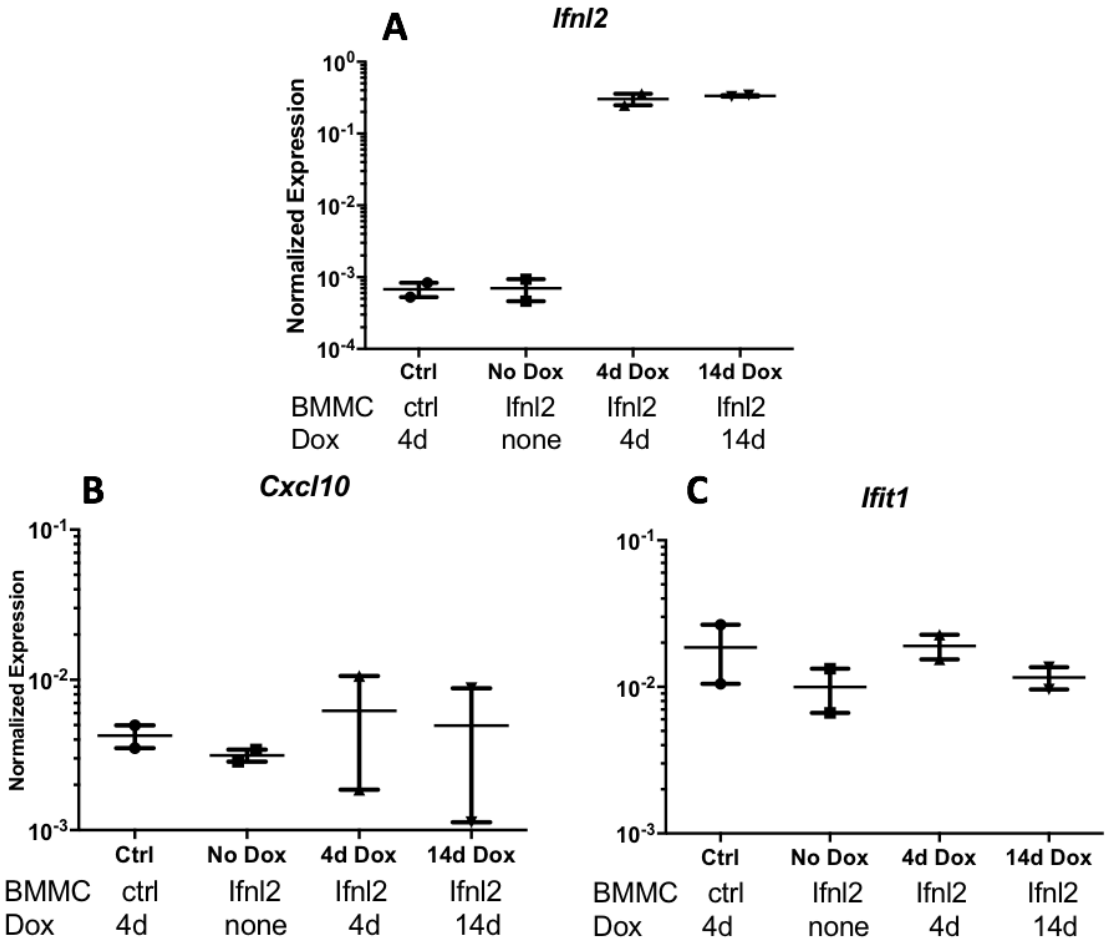

Figure 3.12: IFN-λ2-BMMC reconstitution of Wsh mice showed induction of *Ifnl2* mRNA, but no induction of ISGs in peritoneal cells harvested after 4 or 14 days of continuous doxycycline administration. IFN-λ2-BMMCs were injected i.p. into Wsh mice and rested for 6 weeks to fully reconstitute the peritoneum. Doxycycline was then administered continuously via chow for 4 or 14 days and animals were sacrificed to harvest peritoneal cells by lavage. A group of mice were reconstituted with WT BMMCs and given doxycycline, while another group of mice were reconstituted with IFN-λ2-BMMCs but not fed doxycycline as controls. RNA was isolated for peritoneal cells to analyze *Ifnl2* expression and ISG induction through *Cxcl10* and *Ifit1* mRNA expression by RT-qPCR (**A-C**). Experiment was performed by Dr. Ian Haidl. Data are shown as mean ± SEM. N = 2.

periods compared to type I IFNs[56]. IFN signaling is tightly regulated and signaling can change drastically over time[65]. Considering our previous data in which we were unable to detect ISG induction or IFN-λ2 production in Wsh mice reconstituted with IFN-λ2-BMMCs, we investigated whether our technical methods of analysis were suitable to detect recombinant IFN signaling *in vivo*. To investigate this, female C57BL/6 mice were injected intraperitoneally with 1 μg IFN-α, 5 μg IFN-λ2, 1 μg IFN-λ2 or saline. Mice were sacrificed after 4 or 24 hours to analyze for protein in the peritoneal lavage fluid and ISG induction (using *Cxcl10, Mx1,* and *Ifit1* mRNA analysis) in the peritoneal lining (**Figure 3.13.1**). IFN-dependent changes in innate and adaptive immune cell infiltration in the peritoneum were also characterized by flow cytometry (**Figure 3.13.2**). Recombinant IFN-λ2 at both doses was detectable in the lavage fluid by ELISA after 4 hours and was statistically significant for mice injected with 5 μg IFN-λ2 compared to saline injection (**Figure 3.13.1A**). This signal decreased to background levels 24 hours post-injection (**Figure 3.13.1A**). IFN-α injection had no impact on downstream IFN-λ2 measurements, but showed significant induction of all measured ISGs 4 hours post-injection compared to saline-injected controls (**Figure 3.13.1A-D**). Mice injected with 5 μg IFN-λ2 also significantly induced *Mx1* and *Ifit1*, but not *Cxcl10*, upregulation 4 hours post-injection compared to saline control mice (**Figure 3.13.1B-D**). Strikingly, the ISG upregulation observed in all IFN-injected animals was largely abolished 24 hours after IFN-λ2 injection (**Figure 3.13.1B-D**). IFN-α-injected mice showed significant *Ifit1* induction after 24 hours, suggesting these responses *in vivo* were detectable over multiple timepoints. These findings suggest that our collection methods were suitable to detect IFN-λ2 protein in the lavage fluid and injection of recombinant protein showed

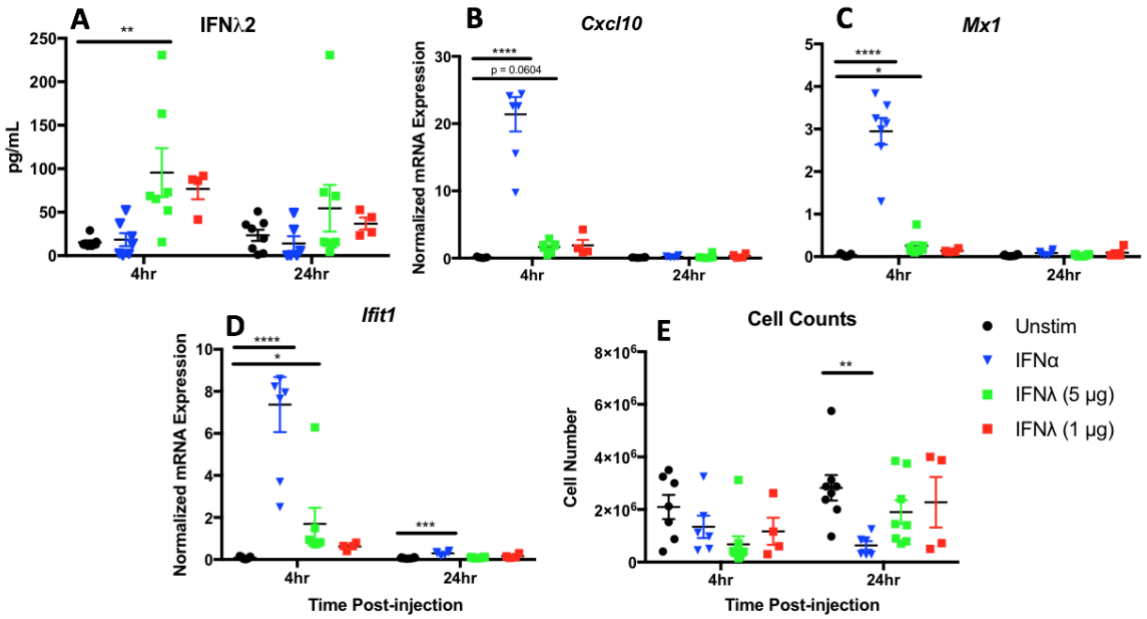

Figure 3.13.1: Intraperitoneal injection of IFN-λ2 induces short-lived ISG expression and is detectable in lavage fluid. C57BL/6 mice were injected intraperitoneally with 1 μg IFN-α (N = 6 – 7), 5 μg IFN-λ2 (N = 7 – 8), 1 μg IFN-λ2 (N = 4), or saline (N = 7 – 8). Mice were sacrificed 4 and 24 hours post-injection. Peritoneal lavage was collected to determine IFN-λ2 levels by ELISA (**A**) and a portion of the peritoneal lining was collected to isolate mRNA to assess ISG induction (**B-D**)**.** Cells were counted to determine any effect on cell number in the peritoneum (**E**). Statistical significance was determined by one-way ANOVA followed by Dunnett's multiple comparisons test, comparing IFN treatment groups to unstimulated controls at each time point. Data are shown as mean ± SEM. * = $p < 0.05$, ** = $p < 0.01$, *** = $p < 0.001$, **** = $p < 0.0001$.

significant, observable enhancement of ISGs *in vivo* from harvested tissue. Although positive signals were detected, the data suggests that type I and III IFN responses are fast and transient responses when administered to healthy mice that may only be detectable over a short period.

In addition to the detection of proper IFN signaling *in vivo*, we characterized the impact of IFN overexpression on immune infiltration at the site of injection. Peritoneal cells were stained to characterize either myeloid cells (neutrophils, DCs, macrophages, monocytes) or lymphocytes (NK cells, B cells, $CD4^+$ and $CD8^+$ T cells). Mice injected with either type of IFN exhibited a trend towards reduction in overall cell number in the peritoneal lavage fluid compared to saline-injected control mice (**Figure 3.13.1E**). IFN-α injection resulted in a statistically significant reduction in peritoneal cell number after 24 hours (**Figure 3.13.1E**). IFN-α injection significantly decreased $CD8^+$ T cell populations in the peritoneum after 4 hours, while B cell, resting macrophage, and DC numbers in the peritoneum were significantly reduced after 24 hours (**Figure 3.13.2A-D**). IFN-λ2 significantly decreased $CD8^+$ T cell and DC populations after 4 hours post-injection and negatively affected B cell infiltration after 24 hours (**Figure 3.13.2A-D**). Overall, these data suggest that injection of recombinant IFN protein in healthy mice have negative effects on immune cell numbers in the peritoneum, affecting both innate and adaptive immune populations.

These results shifted interest in our choice of IFN to be used in a mast cell delivery system. There are certain advantages in the use of IFN-α over IFN-λ2, given our *in vivo* injection data, considering 1) a smaller dose was required to achieve effects that were easily detectable *in vivo* and 2) *in vivo* ISG induction was sustained at longer time

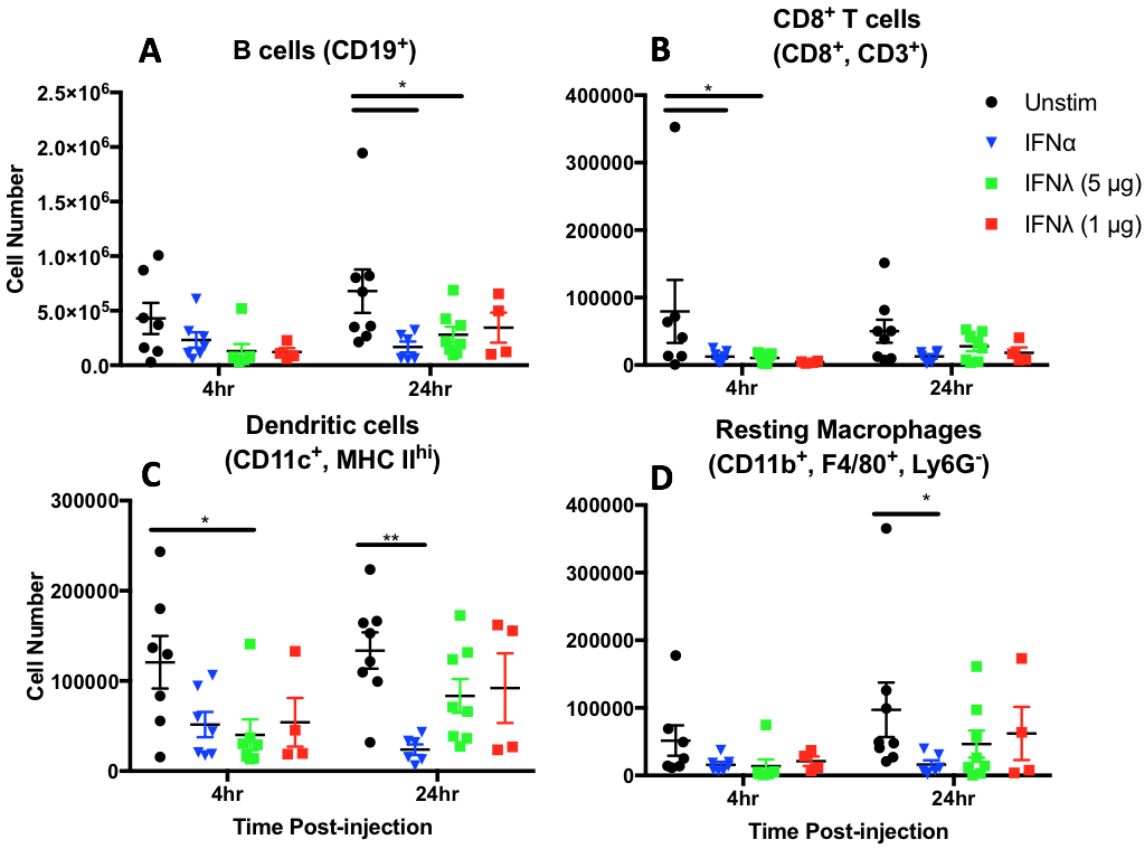

Figure 3.13.2: Intraperitoneal injection of IFN-α and IFN-λ2 reduces immune infiltration in the peritoneal cavity, impacting B cell, CD8+ T cell, DC, and resting macrophage populations at different time points. C57BL/6 mice were injected intraperitoneally with 1 μg IFN-α (N = 6 – 7), 5 μg IFN-λ2 (N = 7 – 8), 1 μg IFN-λ2 (N = 4), or saline (N = 7 – 8). Mice were sacrificed 4 and 24 hours post-injection to collect peritoneal cells by lavage. Cells suspended in the lavage fluid were stained with Panel D and E to analyze innate and adaptive immune infiltrate in the peritoneum as outlined in **Table 1.2** and were assessed by flow cytometry **(A-D).** Outliers were removed prior to determining significance, which was analyze by two-way ANOVA comparing treatment groups to the saline control in each timepoint. Data are shown as mean ± SEM. * = $p < 0.05$, ** = $p < 0.01$.

points, despite reports that IFN-λ generally provides more sustained signaling[56]. Therefore, we sought to determine how mast cell delivery of IFN-α would impact tumour growth. Considering there was difficulty in properly characterizing the ID8 model in mast cell-deficient animals, our experiments focused on the E0771 model.

3.8 *In vivo* reconstitution with IFN-α1-BMMCs and the impact on E0771 tumour growth and inflammation

3.8.1 Effect of type I IFN expression on E0771 tumour growth and survival

To assess the effects of mast cell-mediated IFN-α delivery on breast tumour growth, BMMCs were transduced with IFN-α1 (IFN-α1-BMMCs) and tested for successful mRNA gene expression and protein production *in vitro* and *in vivo* (**Appendix Figure 5**). Female Wsh mice were reconstituted with IFN-α1-BMMCs through subcutaneous injection into the mammary fat pad and rested for 6 weeks to reconstitute. E0771 cells were then inoculated into the same site. Mice were fed doxycycline via chow to induce IFN-α1 production on Day 4 and continued until experimental endpoint. Tumour volume and survival were monitored over 21 days (**Figure 3.14.1**). A group of C57BL/6 and non-reconstituted Wsh mice were fed doxycycline to control for any effects on E0771 tumour growth. IFN-α1-Recon Wsh mice were also fed normal chow to control for the effect of IFN-α1 expression on tumour growth. Mice fed doxycycline showed no differences mammary tumour volume in C57BL/6 animals compared to those without doxycycline and Wsh mice fed doxycycline (**Figure 3.14.1A**). IFN-α1-Recon Wsh mice fed doxycycline exhibited similar tumour volumes compared to unfed reconstituted controls during the early stages of tumour growth, before showing a trend towards an increase in

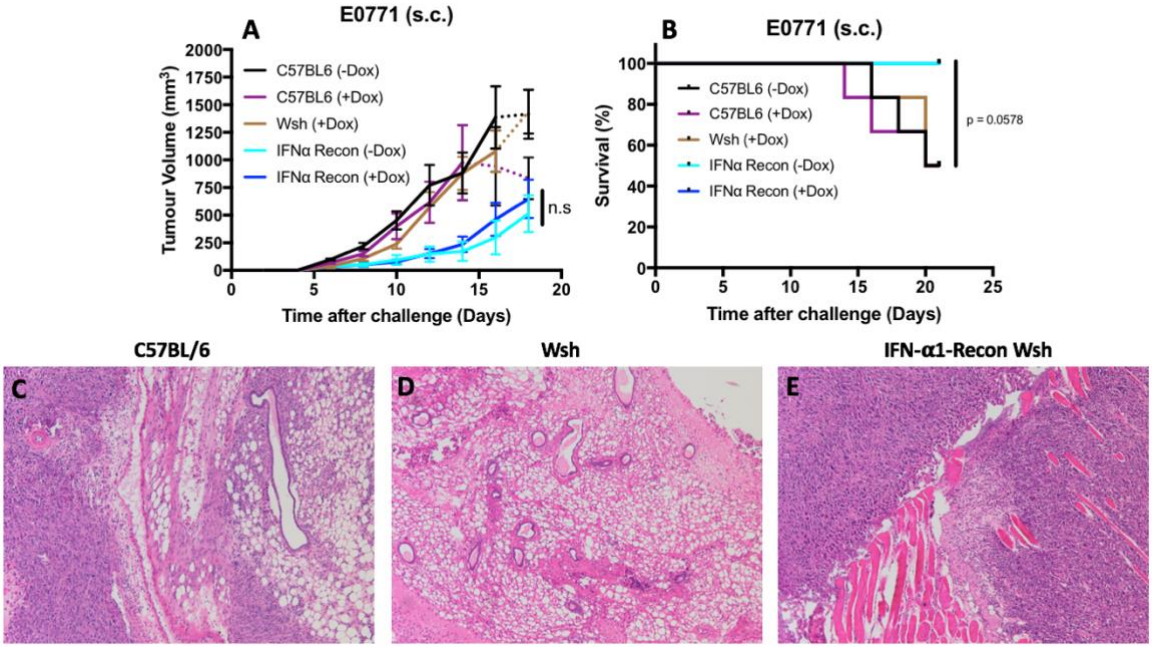

Figure 3.14.1: Induction of IFN-α1 after reconstitution of Wsh mammary fat pads with IFN-α1-BMMCs showed no significant change in E0771 mammary tumour growth upon doxycycline induction, compared to uninduced controls. A group of Wsh mice were injected subcutaneously with $2.0x10_6$ IFN-α1-BMMCs into the mammary fat pad and rested for 6 weeks to allow for local reconstitution (IFN-α1-Recon Wsh). After 6 weeks, C57BL/6 mice (N = 6), non-reconstituted Wsh mice (N = 6), and IFN-α1-Recon Wsh (N = 6) were challenged with $2.0x10_5$ E0771 cells and tumour volume (**A**) and overall survival (**B**) were assessed for 21 days. Mice were fed doxycycline via chow from Day 4 until the experimental endpoint (+Dox). A control group of C57BL/6 and IFN-α1-Recon Wsh were not fed doxycycline (-Dox) to determine how the drug impacted tumour growth in WT animals and to control for IFN-α1 induction. Dotted segments for tumour volume data represent groups in which sacrifice of single animals occurred before humane endpoint, which impacted the mean of their respective groups at time points after sacrifice. Tumours were harvested upon sacrifice and were fixed in Carnoy's solution for 24 hours and subsequently paraffin embedded. Tumours were sectioned into 5 μM longitudinal sections and stained with H&E to visualize general immune infiltrate at the tumour site. Images were taken at 100x total magnification and represent tumours harvested from C57BL/6, Wsh, and IFN-α1-Recon Wsh mice (**C-E**). Statistical significance for tumour volume was determined by determining the area under the curve and comparing the area of each line by one-way ANOVA followed by Sidak's multiple comparisons test. Overall survival is represented through Kaplan-Meier survival curves, using Log-Rank (Mantel-Cox) Test to determine significance. Data are shown as mean ± SEM. n.s. = not significant.

later stage tumour growth, which was not statistically significant (**Figure 3.14.1A**). Both IFN-α1-Recon Wsh mice showed improved survival rates compared to all C57BL/6 and Wsh control groups, however this was not statistically significant (**Figure 3.14.1B**). These findings imply that induction of IFN-α1 after reconstitution with IFN-α1-BMMCs did not further reduce E0771 tumour growth compared to those without IFN induction. Doxycycline administration did not appear to impact tumour growth in control mice in the absence of transduced cells.

Although induction of IFN-α1 showed no further reduction of E0771 breast tumours, tumour tissue was harvested to determine general inflammation via H&E staining (**Figure 3.14.1C-E**). Tumours harvested from C57BL/6 mice showed infiltrating of leukocytes, ranging from mononuclear immune cells, to polymorphonuclear cells and eosinophils (**Figure 3.14.1C**). Wsh mice showed a reduced of immune infiltration around the tumour periphery, based on observation alone (**Figure 3.14.1D**). IFN-α1-Recon Wsh tumours showed an observable increase in infiltrating immune cells compared to Wsh mice, suggesting mast cell reconstitution enhanced inflammatory infiltration into the tumour site (**Figure 3.14.1D, E**).

Despite a lack of differences in tumour phenotype from IFN-α1-BMMC reconstitution, it was crucial to confirm that IFN-α1 induction occurred *in vivo*, given the difficulty observed with IFN-λ2-BMMCs.

3.8.2 Impact of type I IFN production on type I and III IFN expression in the TME

To assess for induction of IFN-α1 by IFN-α1-BMMCs *in vivo*, tumour tissue was harvested and RNA was isolated to measure ISG induction, *Tpsb2* expression, and type I

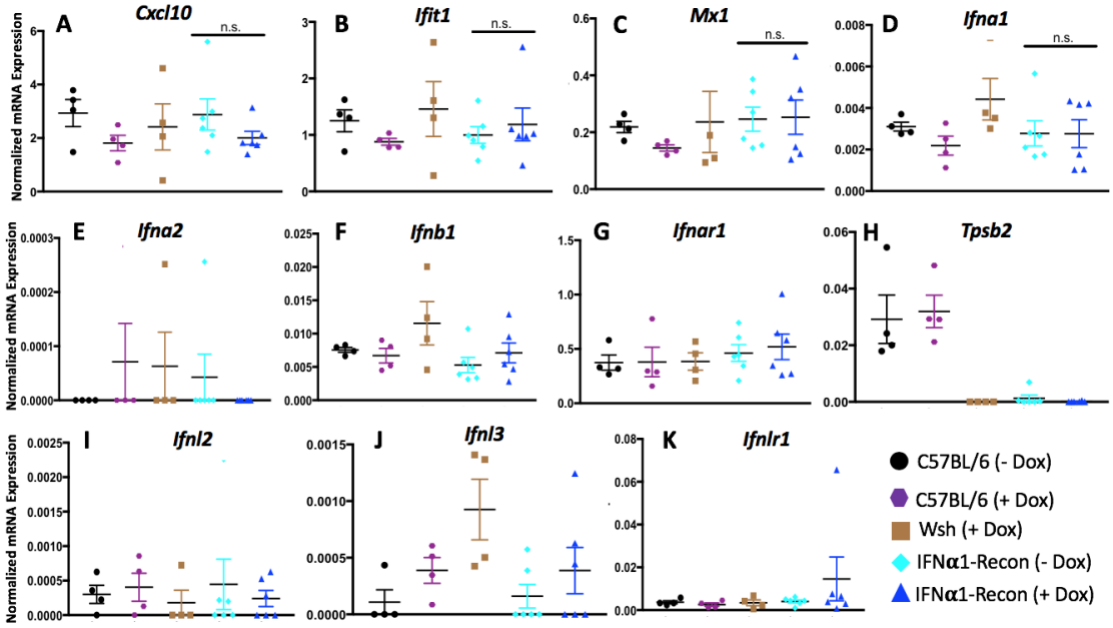

Figure 3.14.2: IFN-α1-Recon Wsh animals fed doxycycline show no substantial upregulation of ISGs in the E0771 TME upon induction, with IFN-α1 gene expression unaffected by doxycycline administration. A group of Wsh mice were injected subcutaneously with 2.0x10$_6$ IFN-α1-BMMCs into the mammary fat pad and rested for 6 weeks to allow for local reconstitution (IFN-α1-Recon Wsh). After 6 weeks, C57BL/6 mice, non-reconstituted Wsh mice, and IFN-α1-Recon Wsh were challenged with 2.0x10$_5$ E0771 cells and were monitored for 21 days. C57BL/6 (N = 4), Wsh (N = 4), and IFN-α1-Recon Wsh (N = 6) groups were fed doxycycline via chow on Day 4 through to experimental endpoint to induce IFN-α1 production from IFN-α1-Recon groups. Control groups included C57BL/6 (N = 4) and IFN-α1-Recon Wsh mice (N = 6) that were not fed doxycycline to determine any impact on gene expression. Tumours were harvested to isolate RNA before assessing induction of ISGs (*Cxcl10, Mx1,* and *Ifit1*) (**A-C**), *Tpsb2* expression (**H**) and the expression of type I IFN-related genes (*Ifna1, Ifna2, Ifnb1, Ifnar1*) (**D-G**) and type III IFN-related genes (*Ifnl2, Ifnl3,* and *Ifnlr1*) (**I-K**) by RT-qPCR. Gene expression data is representative of mice sacrificed on Days 20-21. Data are shown as mean ± SEM. n.s. = not significant.

and III IFN gene expression by RT-qPCR (**Figure 3.14.2**). These tumours were harvested on Day 21 after experimental endpoint was reached. There were no significant changes in expression of any of the measured ISGs between IFN-α1-Recon Wsh groups with and without doxycycline administration (**Figure 3.14.2A-C**). *Ifna1* expression was also unaffected by doxycycline induction at the tumour site between IFN-α1-BMMC Recon groups (**Figure 3.14.2D**). E0771 tumours expressed mRNA for *Ifnlr1* and *Ifnar1* (**Figure 3.14.2G, K**). However, all measured type I and III IFN cytokine genes (*Ifna2, Ifnb1, Ifnl2, Ifnl3*) were not affected by IFN-α1-BMMC reconstitution and doxycycline administration (**Figure 3.14.2E, F, I, J**). Interestingly, when *Tpsb2* expression was measured to assess the presence of mast cells in the E0771 TME, signals were very low or absent in Wsh and IFN-α1-Recon Wsh groups compared to C57BL/6 mouse group (**Figure 3.14.2H**). These findings suggest that IFN-α1-BMMCs do not reside in the tumour after engraftment. Additionally, the lack of ISG expression in the tumour site would suggest that IFN-α1-BMMCs may not be secreting functional protein on Day 21 after continuous doxycycline administration.

CHAPTER 4: DISCUSSION

Cancer remains the second leading cause of death in the modern age and continues as a global health threat as incidence rates and mortality continue to rise[2]. Immunotherapy is a novel approach to cancer treatment that has emerged with promising results. Mast cells are an aspect of the immune system that are rarely targeted in disease therapies, especially in the context of cancer, given their many pro-tumourigenic functions. Although pro-tumourigenic features are well-documented, current research lacks investigation into the use of anti-tumour mediators secreted by mast cells, including IFNs. We set out to investigate the feasibility of mast cell-mediated IFN delivery into tumours as a potential cancer immunotherapy. We hypothesized that the localization of mast cells around the TME, combined with the abilities of IFNs to directly kill tumour cells and enhance anti-tumour immunity could result in elimination of macroscopic tumours from mice. To investigate the therapeutic efficacy of this approach, we genetically modified BMMCs isolated from C57BL/6 mice using a DNA vector expressing a type I or III IFN gene under the control of an inducible tetracycline promoter system, allowing for controlled secretion of IFN protein by modified mast cells. Reconstitution of mast cell-deficient mice resulted in reduced mammary tumour growth. These results were corroborated when mast cell-sufficient mice were enriched with mast cells locally at the mammary fat pad. However, induction of type I IFNs did not further reduce macroscopic tumours as expected. This research highlighted the use of mast cells in reducing breast tumours, identifying their natural therapeutic efficacy in mediating reduction. However, this has also suggested that further work is required to optimize production of type I IFNs through the inducible system.

4.1 Results in the context of established literature and cancer immunotherapy

4.1.1 The role of mast cells in combating breast tumour growth

To date, there has been little investigation into utilizing the anti-tumorigenic properties and functions of mast cells in the context of cancer. Similarly, characterizing the impact of mast cell populations in different cancer types must be further investigated, specifically in mouse models. Preliminary studies conducted on the relationship between mast cell number, tumour grade and growth in human breast cancer patients have shown contrasting findings[176,177]. In this investigation, we showed that administering mast cells locally around the site of orthotopic mammary cancer implantation in mouse models prior to tumour cell injection decreased tumour growth and improved overall survival compared to mice lacking mast cell populations. These results were corroborated in two models of mast cell-deficiency, further implicating anti-tumourigenic role of mast cells in this tumour model. Related results have been observed in human studies, as Rajput *et al.* documented that increased mast cell number correlated favourably with survival in 4,444 breast cancer patients, with a variety of different molecular subtypes of breast cancer, classifying mast cells as a positive prognostic biomarker in this disease[147]. The role of mast cells in breast cancer is theorized to be affected by the presence of hormone receptor expression patterns on breast tumour cells. These receptors include progesterone receptor (PR), ER, and human epidermal growth factor receptor 2 (HER-2)[178]. One study by Sange *et al.* showed that human breast cancer patients with ER^+ or PR^+ expression genotypes had higher mast cell densities around the tumour site, which was associated with lower rates of tumour progression[178]. The model used in this study, E0771, is a TNBC model lacking expression of all aforementioned receptors. Studies comparing mast

cell numbers in TNBC to other breast cancer types revealed that mast cell numbers were decreased in TNBC patients[179]. TNBC is known to have more aggressive growth rates compared to other types of breast cancer, which is associated with poorer prognosis[180]. Given our results, it could be suggested that mast cells are an important potential therapeutic target for TNBC and increasing their number at the tumour site could improve the poor prognosis associated with this disease. This was highlighted through our analysis of E0771 tumours administered to C57BL/6 mice that were locally enriched with mast cells. Such treatment resulted in a transient reduction in tumour growth occurring between Day 10-12 post-injection compared to control mice at our standard dose of tumour cells and provided significant suppression of tumour growth when a lower dose of tumour cells was employed in this experiment, confirming that increasing local mast cells can reduce mammary tumour growth even in WT mice. To our knowledge, these investigations are the first to study the impact of adoptive mast cell transfer into the mammary tissue of WT mice. Our data suggest two possible explanations, either 1) mast cells either remain resident and impact local immune responses or 2) have a lasting impact on the immune microenvironment, locally or in the draining lymph node. Notably we detected no significant differences in tryptase gene expression in mammary fat pads harvested from both groups, suggesting that the number of mast cells at this site are very low. This suggests that mast cells may be distributed in other anatomical tissue sites at the injection site, such as the inguinal lymph node or surrounding connective tissue. The observed differences in tumour growth would suggest that increasing mast cell numbers locally in the mammary fat pad prior to tumour growth reduces tumour size in the E0771 TNBC model. Mast cells may directly mediate this reduction through the secretion of

cytotoxic mediators, such as TNF, which has been observed to induce apoptosis in HER-2+ breast tumour cells *in vitro*[144]. Considering that ER and PR are important prognostic markers for survival in human patients, and are associated with increased mast cell numbers at the tumour site, the molecular subtype of breast cancer may dictate the nature or extent of mast cell populations residing within, or peripheral to, the solid mass.

Another important factor to consider when investigating mast cell function during tumour growth is their localization at the tumour site. During our study, we were unable to detect mast cells in the TME of E0771 tumours by flow cytometry, RT-qPCR or histology in Recon Wsh tumours, suggesting that mast cells were localized in the peritumoural tissue rather than residing intratumourally. The localization of mast cells can have polarizing effects on tumour progression depending on the type of cancer. In one study analyzing mast cell function in prostate cancer, Johansson *et al.* found that peritumoural mast cells were associated with angiogenesis and increased tumour growth, while intratumoural mast cell numbers correlated negatively with the occurrence of metastasis, tumour stage and tumour cell proliferation[181]. In breast cancer research, Dabiri *et al.* observed that increased mast cell infiltration of the peritumoural stroma was associated with smaller tumour size and improved survival rates in human patients[182]. Our investigations corroborated these latter findings in the E0771 model of murine mammary cancer. Considering there was no detectable expression of tryptase in the mammary fat pad of local Recon Wsh mice, this suggests that mast cells reconstituted the lymph node or connective tissue surrounding the fat pad, and therefore were localized in the tumour periphery after tumour cell injection. It is well known that mast cell engraftment of mast cell-deficient animals does not directly follow anatomical

distribution of mast cells in WT animals, and injection may have localized to tissues outside of the mammary fat pad[172].

4.1.2 Mast cell modulation of the TME in breast cancer

Although previous literature has documented some instances of mast cells modulating immune cell infiltration and activation in the TME, this has been limited to immunosuppressive cells types such as MDSCs and T_{regs}. Investigations by Yang *et al.* showed that mast cells recruit MDSCs in murine hepatocarcinoma, which initiated downstream T_{reg} recruitment and production of IL-17, resulting in enhancement of mast cells immunosuppressive functions [122]. To our knowledge, there has been little systemic assessment of how mast cells impact the phenotype of innate and adaptive immune cell infiltrates the TME of mouse mammary tumours. We investigated whether mast cell recruitment of anti-tumour effector cells was associated with mammary tumour reduction. Tumours harvested from C57BL/6 and IFN-α1-Recon Wsh mice showed increased mononuclear and polymorphonuclear leukocyte immune infiltrate at the tumour periphery via histology compared to mast cell knockout conditions. Specific analysis of the E0771 tumours in C57BL/6, Wsh, and Recon Wsh by flow cytometry showed that mast cell reconstitution of Wsh mice exhibited a trend towards the number of tumour-associated $CD4^+$ and $CD8^+$ effector memory T cells, while significantly reducing infiltrating naïve $CD4^+$ populations. Activation of T cells showed a trend towards enhancement, as measured through CD69 expression. While no significant trend was observed in the tumour, mast cell reconstitution significantly enhanced CD69 expression on $CD8^+$ T cells in the spleen, suggesting reconstitution mediated systemic T cell activation. These data

taken together suggest that mast cells may directly or indirectly mediate T cell recruitment and activation in mammary cancer, enhancing T cell immunity against tumour cells.

Outside the context of cancer, mast cell-mediated recruitment and activation of T cell populations has been well-documented. Ott *et al.* showed that mast cells can induce migration of effector memory CD8+ T cell populations *in vitro*[121]. In a separate study, Mantri *et al.* showed that mast cells enhanced CD69 expression on CD8+ and CD4+ T cells in the draining lymph nodes of dengue virus-infected Wsh mice[183]. Our results would corroborate that mast cells have potential actions in enhancing activation of memory T cell populations, through reduction of infiltrating naïve CD4+ T cell populations observed in E0771 tumours. Karkeni *et al.* showed that CD8+ effector memory T cells are important for reducing E0771 tumours, as depletion of this population results in more aggressive tumour growth[184]. When considering CD4+ T cells, Meng *et al.* observed that CD4 expression in breast tumours was associated with positive outcomes in human patients[185]. This group similarly determined that HER-2+ and TNBC tumours had increased infiltration of CD4+ T cells compared to luminal subtypes[185]. Considering that mast cell reconstitution had no effect on infiltrating or systemic DC numbers, this may suggest that mast cells in the tumour periphery directly mediate T cell migration and activation, although this must be confirmed in future experiments. Mast cell reconstitution also did not significantly impact NK cell infiltration in the E0771 TME, suggesting that the reduction in tumour growth observed was not NK cell-mediated. Mast cells possess the ability to directly present antigen and induce activation of both CD4+ and CD8+ T cell populations through the OX40/OX40L axis as reviewed

by Bulfone-Paus and Bahri[120]. Our results would implicate mast cells as important mediators of anti-tumour T cell responses in this model of TNBC, however further research would be necessary to define potential mechanisms of action. Initial experiments could target systemic depletion of $CD4^+$ and $CD8^+$ T cell populations using mAbs after mast cell reconstitution and tumour challenge, to determine if this abolishes tumour reduction.

Mast cell reconstitution of Wsh mice also affected the innate immune infiltrate of the TME in E0771 mammary tumours. Neutrophil infiltration was significantly decreased in Recon Wsh groups compared to control Wsh mice. Currently, interactions between mast cells and neutrophils in the context of neoplasia are not well defined. Our data would suggest that lower neutrophil numbers are associated with reduced tumour size and better overall survival in E0771-challenged mice. Neutrophils are known to secrete pro-angiogenic mediators, such as VEGF-A and CXCL8, and may be associated with pro-tumorigenic outcomes in this model[186]. It is important to note that in addition to mast cell-deficiency, Wsh mice have neutrophilia as a result of the inversion of c-kit, which may explain elevated neutrophil infiltration in control Wsh mice[172]. In breast cancer, the presence of neutrophil extracellular traps has been reported to contribute to increased disease progression and metastasis[187]. It is possible that mast cells promote neutrophil efflux from the E0771 TME, given that mast cell-sufficient mice had decreased neutrophil infiltration. Fewer neutrophils may inhibit tumour growth given the pro-tumourigenic functions of neutrophils. Future studies will be necessary to uncover mast cell-neutrophil interactions in the TME to better define their functions in breast cancer.

Future experiments could target systemic depletion of neutrophils by injection of mAbs into Wsh mice to determine if this exhibits a reduction in E0771 tumour growth.

4.1.3 IFN expression in the TME

While there is a current understanding of how IFNs can be used clinically in cancer treatment, there is little characterization of endogenous IFN expression during tumour growth. Our observations in a mouse model of breast cancer showed that IFN-α1, IFN-α2, IFN-λ2, and IFN-λ3 were poorly expressed or absent in the TME across all measured time points. The relationship between type I IFN expression and breast cancer progression has been controversial. In inflammatory breast cancer, IFN-α gene signatures are upregulated. Similarly Ahmed *et al.* observed that 63% of human breast cancers expressed IFN-α2 in the TME[188,189]. Interestingly, these studies suggest that sustained endogenous IFN-α production enhanced pro-tumourigenic effects, including increased metastasis and resistance to DNA damage and subsequent cell death[188,189]. Only IFN-β1 expression was observed in the E0771 TME across all measured timepoints. Previous studies have shown that TNBC patients with higher STAT1 expression signatures were more susceptible to chemotherapies and was associated with lower instances of recurrences[190]. Doherty *et al.* observed that IFN-β gene signatures correlated with patient survival and improved recurrence-free survival in TNBC patients[190]. Our data did not corroborate this trend, as IFN-β expression was generally lowest in the Recon groups of each model of mast cell-deficiency. Alternatively, IFN-β1 could be constitutively expressed by some of the cellular components of the TME via constant IRF7 interaction with the IFN-β promoter, a phenomenon that has been documented in the absence of

infection or disease[191]. Less is known about type III IFN expression signatures in breast tumours, however, the downregulation of type III cytokine expression in the E0771 TME may be due to an intrinsic ability of tumour cells to downregulate IFN signaling pathways through upregulation of negative feedback mechanisms, such as the SOCS proteins[57]. This has been documented for type I IFNs, and as type III IFN share some regulatory features, this may explain the lack of expression of type III IFNs at the tumour site[57]. Expression of both type I and III IFN receptors were detectable across all mouse models, suggesting that cells in the TME would respond to IFN-based therapies. Although the signals could not distinguish which cells would express the receptors, it is likely that all players in the TME would respond to type I IFN given the ubiquitous expression of its receptors. In contrast, only infiltrating immune cells would likely respond to type III IFNs, considering E0771 cells showed no expression of the type III IFN receptor *in vitro*, and neither fibroblasts nor endothelial cells are known to express the type III IFN receptor[192].

To our knowledge, there have been no studies that characterized mast cell IFN responses during tumour development *in vivo*. Given that we did not observe any differences in type I and III IFN gene expression in tumours harvested from mast cell-sufficient, mast cell-deficient and mast cell-reconstituted groups across any measured timepoint between our selected mouse models, the data suggests that mast cells do not substantially impact IFN expression in this model of mammary cancer.

4.1.4 Feasibility of mast cell-mediated IFN delivery as an immunotherapy

Genetic modification of immune cells to enhance their targeting of tumour cells is a popular area of interest in cancer treatment research. Current research has largely focused on utilizing T cell-based therapies, with a lack of immunomodulation of some innate immune system components, such as mast cells. Conversely, the use of IFNs in cancer immunotherapies has been well-documented and has reached human clinical trials for many type I IFN-based therapies[193]. Mast cells are an ideal target to mediate controlled IFN delivery into the tumour site as they reside close to the tumour periphery and possess radioresistant properties, which could be used in combination therapy approaches with radiation treatment[194,152]. In this project, we genetically modified mast cells to express type I or III IFNs under the control of an inducible tetracycline "ON" promoter system.[195]. Mast cells were transduced with a DNA vector containing the IFN gene downstream of the tetracycline "ON" promoter and tested for induction of IFN mRNA and protein *in vitro*. Cells were then implanted into mast cell-deficient mice to determine whether IFN induction would help eliminate mammary tumours. Interestingly, before transduced BMMCs were tested *in vivo*, we observed a striking difference in the level of IFN-λ2 produced by IFN-λ2-BMMCs compared to IFN-λ2-U2-OS cells, in which U2-OS cells produced numerically higher levels of IFN-λ2 protein. These observations could be attributed to differences between transcriptional or translational machinery between BMMCs and U2-OS cells that result in protein production disparities, as research has suggested that protein production in tumour cells correlates with proliferation rates[196]. U2-OS cells have a doubling rate of ~29 hours, while primary murine BMMCs are known to double at rates between 20 hours to 4 days[197,198]. Alternatively, BMMCs

possess cytoplasmic granules that can store cytokines and may be directing the storage of IFNs upon doxycycline induction into these granules rather than direct secretion. Future directions will target confirming if IFN-λ2-BMMCs are storing IFN upon induction through performing degranulation assays. This lack of protein production favoured the use of IFN-α1 as the therapeutic target over IFN-λ2 in tumour-challenged mice, since lower doses of type I IFNs elicit more potent effects than type III IFNs.

When utilizing this system *in vivo*, we showed that induction of IFN-α1 from IFN-α1-BMMCs yielded no further reduction in mammary tumour size compared to non-induced mast cells. Further analysis on ISG induction in E0771 tumours showed that doxycycline induction had no effect on gene expression compared to control mice reconstituted with IFN-α1-BMMCs. IFN-α1-BMMC reconstitutions were tested *in vivo* in the peritoneum, and results showed cells survived and produced *Ifna1* mRNA and elicited ISG induction upon doxycycline administration, suggesting these cells were able to induce protein. Taken together, these data imply three possible explanations: 1) induction of IFN-α1 for 17 continuous days triggered possible negative regulatory mechanisms that suppressed signaling pathways measured for detection, 2) continuous IFN-α1 expression induced apoptosis of BMMCs, or 3) IFN-α1-BMMCs resided in a tissue site outside of the mammary fat pad or tumour site after reconstitution. Our data with recombinant IFN suggests that *in vivo* IFN responses are time-limited as injection of IFN-α resulted in early upregulation of ISGs in the peritoneal lining, a signal that was decreased after 20 hours. Considering IFN responses were cleared early after one administration, continuous induction of type I IFNs may elicit negative regulatory pathways that shut down production or induce cell death. Administering doxycycline in a

staggered manner may be more appropriate to elicit a more optimal immune-stimulating IFN response.

IFN-α1-Recon Wsh administered doxycycline showed a trend towards increased tumour growth from Day 16 onward. This would corroborate previous theories that sustained IFN-α production is associated with tumour progression[188,189]. Considering there was no detectable mast cell signal present intratumourally after mammary fat pad reconstitution and subsequent tumour challenge, it is possible that mast cells reside in lymph node or connective tissue surrounding the fat pad after reconstitution and during tumour growth. This would explain the lack of detection of *Tpsb2* or *Ifna1* in the tumour site, both of which would be markers for transduced mast cells. Until the IFN-α1-BMMCs can be located after reconstitution and successful mRNA induction and protein production can be detected, it is difficult to firmly assess the feasibility of mast cell-mediated IFN delivery, however continuous doxycycline administration is not optimal when using IFN-α1.

4.2 Critiques and Limitations

Although the use of *in vivo* tumour models is advantageous as it reproduces the TME in proper biological context, the use of genetically modified mouse models has limitations that should be considered before translating the knowledge to practice. Wsh and HK (fl/fl) mice are valuable for exploring mast cell function *in vivo*, however, their genetic mutations create immune-related abnormalities outside of mast cell-deficiency. For example, the mutation of c-kit in the Wsh model can lead to enhanced basophil populations, neutrophilia and enlarged spleens, containing increased myeloid cell and

megakaryocyte populations [199,200]. Other investigations have observed that Wsh mice have increased proportions of T_{regs}, findings important to consider in the context of cancer[201]. In the c-kit-independent HK mouse model, there are reports of incomplete mast cell depletion in multiple tissues sites, including 92-100% reduction of connective tissue mast cells and mucosal mast cells in the skin, trachea, lung, peritoneum, and digestive tract, and no reduction in splenic mast cells[175]. The deletion of Mcl-1 also reduced basophil numbers in the spleen, blood, and bone marrow, demonstrating that this mutation also has pleiotropic effects on mouse immune cells[175]. Reconstitution of these mast cell-deficient mouse models also results in altered anatomical engraftment compared to WT mice, which is influenced by the route of injection and the number of mast cells injected. In our study, we detected lower *Tpsb2* levels in the mammary fat pad of locally reconstituted Wsh mice compared to C57BL/6 controls, suggesting that the number of surviving mast cells was lower at this site compared to WT. Therefore, it is possible that the subcutaneous injection of mast cells reconstituted other connective tissue sites rather than the primary target, the mammary fat pad, or that mast cells did not survive at this site. Considering that $2x10^6$ BMMCs were injected locally, it remains possible that the collective mast cell number in these animals is greater than the number in WT animals, however this must be more thoroughly investigated.

Another limitation of this research is associated with the lentiviral transduction process used to create IFN-BMMCs. The use of a third generation lentivirus transduction system means that BMMCs infected with lentivirus undergo integration of the IFN-DNA vector into the mast cell genome at active transcription sites[202]. Selection of surviving mast cells creates a heterogenous population of transduced-BMMCs that have non-

specific site interruptions of active genes that will vary between independent transduction trials. These interruptions, depending on the site of insertion, may inactivate mast cell genes important for tumour control. Importantly, this also means that independent transductions will result in heterogeneous populations with interruptions of different subsets of genes, and result in deficiencies in mast cell populations that may have longstanding effects during *in vivo* experiments.

4.3 Clinical Implications

Our animal experiments indicate that mast cells have anti-tumourigenic effects on E0771 tumours and that increasing mast cell number around the tumour site can reduce tumour size. Although there are differences between the mouse and human immune systems, our results corroborate human studies that associate increased mast cells around the tumour site with better prognosis in breast cancer. During this investigation, our results suggested that mast cells may either survive or modify the microenvironment following reconstitution of WT mice and can act to reduce mammary tumours, depending on the dosage of tumour cells used for challenge. These results imply that locally increasing mast cell numbers in breast cancer patients may have therapeutic efficacy, especially in those with TNBC. There is evidence to suggest that mast cells can directly induce apoptosis of breast cancer cells, however our data suggests that mast cells may reduce naïve $CD4^+$ T cell numbers, which was associated with a trend towards increased effector memory and $CD69^+$ expression. T cell activation has been associated with E0771 tumour reduction in mice[144,184]. Future experiments will be required to determine whether the mechanism of tumour reduction by mast cells is direct or indirect, and identification of

this mechanism will be critical in devising treatment strategies for human clinical trials moving forward. To our knowledge, this is the first investigation to identify mast cell-mediated reduction of mouse mammary tumours and their modulation of T cell activation in the context of cancer. Our studies support the investigation of mast cells as a therapeutic target in human breast cancers and further explore their anti-tumourigenic effects.

4.4 Future Research Directions

These investigations into therapeutic applications for mast cells in a tumour setting have opened many avenues for future explorations. Given the evidence suggesting functional roles of mast cells in TNBC, this would require corroboration in another mouse model of mammary cancer to confirm whether similar results occur in other molecular subtypes of breast cancer. The 4T1 mammary adenocarcinoma model would be an ideal target for future experiments given its metastatic potential could determine how mast cell reconstitution affects metastasis[203]. Future experiments would also target administering mast cells after established tumour growth, around the periphery, to determine if this also mediates reduction. These findings would provide more clinically translatable applications for mast cell adoptive transfer as an immunotherapy.

To improve our understanding of the mechanism behind mast cell-mediated tumour reduction, future work would follow up on the trend of $CD4^+$ and $CD8^+$ effector memory T cell activation enhancement, which occurred after mast cell reconstitution. Considering the enhanced effector memory T cell populations showed large variability, repeated experiments must be carried out to determine if these trends are significant.

Investigations should better define these potential mast cell-T cell interactions to determine a mechanism of action in a tumour setting. Ott *et al.* previously showed that mast cell-mediated LTB_4 was crucial for effector $CD8^+$ T cell recruitment in the context of allergic asthma[121]. A separate study by Chheda *et al.* showed that LTB_4 receptor knockout mice had significantly enhanced E0771 tumour growth compared to WT animals, suggesting this pathway was important in mediating tumour control[204]. Considering that LTB_4 is also important in mast cell-mediated $CD8^+$ T cell activation, this would be an area to explore to identify a potential mechanism[120].

Despite a visible difference in tumour growth across two models of mast cell-deficiency and occurring in WT animals at lower doses of tumour cells, our efforts to detect local mast cell populations after mammary fat pad reconstitution was inconclusive. *Tpsb2* expression was not detectable in RNA isolated from fat pads via ddPCR, although mast cells were observed via histology through Alcian blue staining. Given the limited number of animals, we were unable to a explore a plethora of sites surrounding the mammary fat pad that could also contain mast cells after reconstitution. Other sites such as the draining lymph node, peritoneal lining around the fat pad or the surrounding connective tissue should be examined for mast cells after reconstitution. Identifying other tissue sites containing mast cells would help identify potential areas transferred BMMCs localize to during tumour growth. This information would also help to determine whether IFN-α1-BMMCs survived continuous induction of IFN-α1.

Future studies will also aim to optimize the production of target IFN by transduced-BMMCs, considering that IFN-λ2-BMMCs produced numerically less IFN-λ2 compared to U2-OS cells. Future experiments would analyze whether BMMCs stored

IFN in their cytoplasmic granules after doxycycline induction, to determine if this accounts for the observed differences in production. Characterization of IFN production by transduced-BMMCs would be critical in further optimizing their use in tumour models *in vivo*.

Another potential investigation could revise the treatment regimen for doxycycline administration. Continuous IFN-α1 induction may induce apoptosis in non-specific targets and result in negative feedback inhibition, which may counteract any anti-tumour effects. Future experiments would administer doxycycline every other day or every 2 days to determine whether staggering treatment has a more beneficial effect.

Due to time constraints, we were unable to fully explore IFN overexpression by mast cells in other cancer models, such as the ID8 ovarian cancer model. Upon further optimization of IFN induction *in vivo*, future studies could target other models of cancer to determine potential impact. Further research into the use of IFN-λ2-BMMCs as an immunotherapy would also be explored *in vivo* once production was further optimization.

Addressing these future experiments would help define how mast cells reduce mammary cancer and better determine the feasibility of mast cell-mediated IFN delivery.

4.5 Concluding Remarks

Despite a surge in cancer immunotherapy research, the use of mast cells as a therapeutic target remains understudied. During this project, we characterized mast cell function as anti-tumourigenic in a mouse TNBC model and successfully produced genetically modified mast cells to allow for inducible type I and III IFN production. These studies have further defined how mast cells function in mouse mammary cancer and deduced the

potential impact of mast cells on infiltrating immune composition in these tumours. These findings may have clinical implications in targeting mast cells to enhance tumour clearance. Currently, breast cancer remains a major public health concern, as it is the second leading cause of death amongst females with cancer in Canada. Mast cell numbers have correlated with better prognosis in human disease, yet little has been done to therapeutically target these cells to enhance their anti-tumour functions. Our observations provide insight into how mast cells mediate reduction of mammary tumours and have implicated mast cell-T cell interactions as a potential target for further investigations. Furthermore, genetically modified mast cells can be used as vehicles to produce any type I or III IFNs, although further work is required to identify mast cell localization and optimize IFN production. Ultimately the use of mast cells as therapeutic targets has merit, and further understanding of their role and underlying mechanisms in cancer will inspire their investigations in other models of cancer.

REFERENCES

1. Cancer. https://www.who.int/news-room/fact-sheets/detail/cancer.

2. Bray, F. *et al.* Global cancer statistics 2018: GLOBOCAN estimates of incidence and mortality worldwide for 36 cancers in 185 countries. *CA. Cancer J. Clin.* **6,** 394-426 (2018).

3. Smith, L. *et al.* Members of the Canadian Cancer Statistics Advisory Committee Analytic leads. (2019).

4. McDaniel, J. T., Nuhu, K., Ruiz, J. & Alorbi, G. Social determinants of cancer incidence and mortality around the world: an ecological study. *Glob. Health Promot.* **1,** 41-9 (2019).

5. Pandya, P. H., Murray, M. E., Pollok, K. E. & Renbarger, J. L. The Immune System in Cancer Pathogenesis: Potential Therapeutic Approaches. *J. Immunol. Res.* (2016) doi:10.1155/2016/4273943.

6. Chen, D. S. & Mellman, I. Oncology meets immunology: The cancer-immunity cycle. *Immunity.* **1,** 1-10 (2013).

7. Dunn, G. P., Bruce, A. T., Ikeda, H., Old, L. J. & Schreiber, R. D. Cancer immunoediting: From immunosurveillance to tumor escape. *Nature Immunology.* **11,** 991-8 (2002).

8. Swann, J. B. & Smyth, M. J. Immune surveillance of tumors. *Journal of Clinical Investigation.* **5,** 1137-1146 (2007).

9. Hanahan, D. & Weinberg, R. A. Hallmarks of cancer: The next generation. *Cell.* **5,** 646-74 (2011).

10. Hanahan, D. & Weinberg, R. A. The hallmarks of cancer. *Cell.* **1,** 57-70 (2000).

11. Wang, M. *et al.* Role of tumor microenvironment in tumorigenesis. *Journal of Cancer.* **8,** 761-773 (2017).

12. Gonzalez, H., Hagerling, C. & Werb, Z. Roles of the immune system in cancer: From tumor initiation to metastatic progression. *Genes and Development* (2018) doi:10.1101/GAD.314617.118.

13. Mantovani, A., Marchesi, F., Malesci, A., Laghi, L. & Allavena, P. Tumour-associated macrophages as treatment targets in oncology. *Nature Reviews Clinical Oncology.* **14,** 399-416 (2017).

14. Fridlender, Z. G. *et al.* Polarization of Tumor-Associated Neutrophil Phenotype by TGF-β: 'N1' versus 'N2' TAN. *Cancer Cell.* **16,** 183-94 (2009).

15. Veglia, F. & Gabrilovich, D. I. Dendritic cells in cancer: the role revisited. *Current Opinion in Immunology.* **45,** 43-51 (2017).

16. Budhwar, S., Verma, P., Verma, R., Rai, S. & Singh, K. The Yin and Yang of myeloid derived suppressor cells. *Frontiers in Immunology.* **9,** 2776 (2018).

17. Li, Q., Teitz-Tennenbaum, S., Donald, E. J., Li, M. & Chang, A. E. In Vivo Sensitized and In Vitro Activated B Cells Mediate Tumor Regression in Cancer Adoptive Immunotherapy. *J. Immunol.* **183,** 3195-203 (2009).

18. Lai, Y.-P., Jeng, C.-J. & Chen, S.-C. The Roles of CD4 + T Cells in Tumor Immunity. *Int. Sch. Res. Netw. ISRN Immunol.* **27**, 37-48 (2011).

19. Clemente, C. G. *et al.* Prognostic value of tumor infiltrating lymphocytes in the vertical growth phase of primary cutaneous melanoma. *Cancer.* **77**, 1303-10 (1996).

20. Oldford, S. A. *et al.* Tumor cell expression of HLA-DM associates with a Th1 profile and predicts improved survival in breast carcinoma patients. *Int. Immunol.* **18**, 1591-602 (2006).

21. Hodi, F. S. *et al.* Improved survival with ipilimumab in patients with metastatic melanoma. *N. Engl. J. Med.* **363**, 711-23 (2010).

22. Sharma, P. & Allison, J. P. Immune checkpoint targeting in cancer therapy: Toward combination strategies with curative potential. *Cell.* **161,** 205-14 (2015).

23. Galluzzi, L. *et al.* Classification of current anticancer immunotherapies. *Oncotarget.* **5**, 12472-508 (2014).

24. Maus, M. V. *et al.* Adoptive Immunotherapy for Cancer or Viruses. *Annu. Rev. Immunol.* **32**, 189-225 (2014).

25. Venstrom, J. M. *et al.* HLA-C-dependent prevention of leukemia relapse by donor activating KIR2DS1. *N. Engl. J. Med.* **367**, 805-816 (2012).

26. Sabado, R. L., Balan, S. & Bhardwaj, N. Dendritic cell-based immunotherapy. *Cell Research.* **27**, 74-95 (2017).

27. Maio, M. Melanoma as a model tumour for immuno-oncology. in *Annals of Oncology.* (2012). doi:10.1093/annonc/mds257.

28. Lamers, C. H. J. *et al.* Treatment of metastatic renal cell carcinoma with CAIX CAR-engineered T cells: Clinical evaluation and management of on-target toxicity. *Mol. Ther.* **21**, 904-12 (2013).

29. Lee Ventola, C. Cancer immunotherapy, part 3: Challenges and future trends. *P T.* **42**, 514-521 (2017).

30. Tartari, F. *et al.* Economic sustainability of anti-PD-1 agents nivolumab and pembrolizumab in cancer patients: Recent insights and future challenges. *Cancer Treatment Reviews.* **48**, 20-4 (2016).

31. Alatrash, G., Jakher, H., Stafford, P. D. & Mittendorf, E. A. Cancer immunotherapies, their safety and toxicity. *Expert Opinion on Drug Safety.* **12**, 631-45 (2013).

32. Frese, K. K. & Tuveson, D. A. Maximizing mouse cancer models. *Nature Reviews Cancer.* **7**, 645-58 (2007).

33. Zhang, Y. *et al.* Establishment of a murine breast tumor model by subcutaneous or orthotopic implantation. *Oncol. Lett.* **15**, 6233-6240 (2018).

34. Pearce, J. V. *et al.* E0771 and 4T1 murine breast cancer cells and interleukin 6 alter gene expression patterns but do not induce browning in cultured white adipocytes. *Biochem Biophys Reports.* **18** (2019).

35. Johnstone, C. N. *et al.* Functional and molecular characterisation of EO771.LMB tumours, a new C57BL/6-mouse-derived model of spontaneously metastatic mammary cancer. *DMM Dis. Model. Mech.* **8**, 237–251 (2015).

36. Ewens, A., Mihich, E. & Ehrke, M. J. Distant metastasis from subcutaneously grown E0771 medullary breast adenocarcinoma. *Anticancer Res.* **25**, 3905-15 (2005).

37. Hart, I. R. The selection and characterization of an invasive variant of the B16 melanoma. *Am. J. Pathol.* **97**, 587-600 (1979).

38. Fong, M. Y. & Kakar, S. S. Ovarian cancer mouse models: A summary of current models and their limitations. *Journal of Ovarian Research.* **28**, (2009).

39. Cheon, D.-J. & Orsulic, S. Mouse Models of Cancer. *Annu. Rev. Pathol. Mech. Dis.* **6**, 95-119 (2011).

40. Stanifer, M. L., Pervolaraki, K. & Boulant, S. Differential regulation of type I and type III interferon signaling. *International Journal of Molecular Sciences.* **20**, (2019).

41. Lazear, H. M., Schoggins, J. W. & Diamond, M. S. Shared and Distinct Functions of Type I and Type III Interferons. *Immunity.* **50**, 907-923 (2019).

42. Lee, A. J. & Ashkar, A. A. The dual nature of type I and type II interferons. *Frontiers in Immunology.* **9**, 2061 (2018).

43. Bach, E. A., Aguet, M. & Schreiber, R. D. THE IFNγ RECEPTOR:A Paradigm for Cytokine Receptor Signaling. *Annu. Rev. Immunol.* **15**, 563-91 (1997).

44. Valente, G. *et al.* Distribution of interferon-γ receptor in human tissues. *Eur. J. Immunol.* **12**, 195-202 (1992).

45. Kotenko, S. V. *et al.* IFN-λs mediate antiviral protection through a distinct class II cytokine receptor complex. *Nature Immunology.* **4**, 69-77 (2003).

46. Prokunina-Olsson, L. *et al.* A variant upstream of IFNL3 (IL28B) creating a new interferon gene IFNL4 is associated with impaired clearance of hepatitis C virus. *Nat. Genet.* **45**, 164-71 (2013).

47. Durbin, R. K., Kotenko, S. V. & Durbin, J. E. Interferon induction and function at the mucosal surface. *Immunological Reviews.* **255**, 25-39 (2013).

48. Randall, R. E. & Goodbourn, S. Interferons and viruses: An interplay between induction, signalling, antiviral responses and virus countermeasures. *Journal of General Virology.* **89**, 1-47 (2008).

49. Hoffmann, H. H., Schneider, W. M. & Rice, C. M. Interferons and viruses: An evolutionary arms race of molecular interactions. *Trends in Immunology.* **36**, 124-38 (2015).

50. Ivashkiv, L. B. & Donlin, L. T. Regulation of type i interferon responses. *Nature Reviews Immunology.* **14**, 36-49 (2014).

51. Platanias, L. C. Mechanisms of type-I- and type-II-interferon-mediated signalling. *Nature Reviews Immunology.* **5**, 375-86 (2005).

52. Mesev, E. V., LeDesma, R. A. & Ploss, A. Decoding type I and III interferon signalling during viral infection. *Nature Microbiology.* **4**, 914-924 (2019).

53. Donnelly, R. P. & Kotenko, S. V. Interferon-lambda: A new addition to an old family. *Journal of Interferon and Cytokine Research.* **30**, 555-564 (2010).

54. Doyle, S. E. *et al.* Interleukin-29 uses a type 1 interferon-like program to promote antiviral responses in human hepatocytes. *Hepatology.* **44**, 896-906 (2006).

55. Zhou, Z. *et al.* Type III Interferon (IFN) Induces a Type I IFN-Like Response in a Restricted Subset of Cells through Signaling Pathways Involving both the Jak-STAT Pathway and the Mitogen-Activated Protein Kinases. *J. Virol.* **81**, 7749-58 (2007).

56. Jilg, N. *et al.* Kinetic differences in the induction of interferon stimulated genes by interferon-α and interleukin 28B are altered by infection with hepatitis C virus. *Hepatology.* **59**, 1250-61 (2014).

57. Tomita, S. *et al.* Suppression of SOCS3 increases susceptibility of renal cell carcinoma to interferon-α. *Cancer Sci.* **102**, 57-63 (2011).

58. Kagan, J. C. *et al.* TRAM couples endocytosis of Toll-like receptor 4 to the induction of interferon-β. *Nat. Immunol.* **9**, 681-8 (2008).

59. Odendall, C. *et al.* Diverse intracellular pathogens activate type III interferon expression from peroxisomes. *Nat. Immunol.* **15**, 717-726 (2014).

60. Kotenko, S. V. & Durbin, J. E. Contribution of type III interferons to antiviral immunity: Location, location, location. *Journal of Biological Chemistry.* **292**, 7295-7303 (2017).

61. Suresh Kumar, K. G. *et al.* Site-specific ubiquitination exposes a linear motif to promote interferon-α receptor endocytosis. *J. Cell Biol.* **179**, 935-50 (2007).

62. Chmiest, D. *et al.* Spatiotemporal control of interferon-induced JAK/STAT signalling and gene transcription by the retromer complex. *Nat. Commun.* **7**, 13476 (2016).

63. Jiang, H., Lu, Y., Yuan, L. & Liu, J. Regulation of interleukin-10 receptor ubiquitination and stability by beta-TrCP-containing ubiquitin E3 ligase. *PLoS One.* **6,** (2011) doi:10.1371/journal.pone.0027464.

64. Sen, A., Sharma, A. & Greenberg, H. B. Rotavirus Degrades Multiple Interferon (IFN) Type Receptors To Inhibit IFN Signaling and Protects against Mortality from Endotoxin in Suckling Mice. *J. Virol.* **92,** (2017) doi:10.1128/jvi.01394-17.

65. Song, M. M. & Shuai, K. The suppressor of cytokine signaling (SOCS) 1 and SOCS3 but not SOCS2 proteins inhibit interferon-mediated antiviral and antiproliferative activities. *J. Biol. Chem.* **273**, 35056-62 (1998).

66. Fenner, J. E. *et al.* Suppressor of cytokine signaling 1 regulates the immune response to infection by a unique inhibition of type I interferon activity. *Nat. Immunol.* **7**, 33-9 (2006).

67. Liu, B., Chen, S., Guan, Y. & Chen, L. Type III interferon induces distinct SOCS1 expression pattern that contributes to delayed but prolonged activation of Jak/STAT signaling pathway: Implications for treatment non-response in HCV patients. *PLoS One.* **10**, (2015).

68. Sarasin-Filipowicz, M. *et al.* Alpha Interferon Induces Long-Lasting Refractoriness of JAK-STAT Signaling in the Mouse Liver through Induction of USP18/UBP43. *Mol. Cell. Biol.* **29**, 4841–4851 (2009).

69. Blumer, T., Coto-Llerena, M., Duong, F. H. T. & Heim, M. H. SOCS1 is an inducible negative regulator of interferon λ (IFN-λ)-induced gene expression in vivo. *J. Biol. Chem.* **292**, 17928-17938 (2017).

70. Romero-Weaver, A. L. *et al.* Resistance to IFN-α-induced apoptosis is linked to a loss of STAT2. *Mol. Cancer Res.* **8**, 80-92 (2010).

71. Li, W., Lewis-Antes, A., Huang, J., Balan, M. & Kotenko, S. V. Regulation of apoptosis by type III interferons. *Cell Prolif.* **41**, 960-979 (2008).

72. Chawla-Sarkar, M. *et al.* Apoptosis and interferons: Role of interferon-stimulated genes as mediators of apoptosis. *Apoptosis.* **8**, 237-49 (2003).

73. Kotredes, K. P. & Gamero, A. M. Interferons as inducers of apoptosis in malignant cells. *Journal of Interferon and Cytokine Research.* **33**, 162-170 (2013).

74. Medrano, R. F. V., Hunger, A., Mendonça, S. A., Barbuto, J. A. M. & Strauss, B. E. Immunomodulatory and antitumor effects of type I interferons and their application in cancer therapy. *Oncotarget.* **8**, 71249-71284 (2017).

75. Dvorak, H. F. & Gresser, I. Microvascular injury in pathogenesis of interferon-induced necrosis of subcutaneous tumors in mice. *J. Natl. Cancer Inst.* **81**, 497-502 (1989).

76. von Marschall, Z. *et al.* Effects of interferon alpha on vascular endothelial growth factor gene transcription and tumor angiogenesis. *J. Natl. Cancer Inst.* **95**, 437-48 (2003).

77. Tagawa, M. *et al.* A possible anticancer agent, type III interferon, activates cell death pathways and produces antitumor effects. *Clinical and Developmental Immunology.* (2011) doi:10.1155/2011/479013.

78. Lasfar, A., Gogas, H., Zloza, A., Kaufman, H. L. & Kirkwood, J. M. IFN-λ cancer immunotherapy: New kid on the block. *Immunotherapy.* **8**, 877-88 (2016).

79. Baldo, P. *et al.* Interferon-alpha for maintenance of follicular lymphoma. *Cochrane Database Syst. Rev.* **20,** (2010) doi:10.1002/14651858.cd004629.pub2.

80. Lasfar, A. *et al.* Characterization of the mouse IFN-λ ligand-receptor system: IFN-λs exhibit antitumor activity against B16 melanoma. *Cancer Res.* **66**, 4468-77 (2006).

81. Numasaki, M. *et al.* IL-28 Elicits Antitumor Responses against Murine Fibrosarcoma. *J. Immunol.* **178**, 5086-98 (2007).

82. Abushahba, W. *et al.* Antitumor activity of Type i and Type III interferons in BNL hepatoma model. *Cancer Immunol. Immunother.* **59**, 1059-71 (2010).

83. Lasfar, A. *et al.* Concerted action of IFN-α and IFN-γ induces local NK cell immunity and halts cancer growth. *Oncotarget.* **7**, 49259-49267 (2016).

84. Müller, L., Aigner, P. & Stoiber, D. Type I interferons and natural killer cell regulation in cancer. *Frontiers in Immunology.* **8**, 304 (2017).

85. Müller, E. *et al.* Both type I and type II interferons can activate antitumor M1 macrophages when combined with TLR stimulation. *Front. Immunol.* **9**, 2520 (2018).

86. Gessani, S., Conti, L., Del Cornò, M. & Belardelli, F. Type I interferons as regulators of human antigen presenting cell functions. *Toxins.* **6**, 1696-1723 (2014).

87. Parlato, S. *et al.* Expression of CCR-7, MIP-3β, and Th-1 chemokines in type I IFN-induced monocyte-derived dendritic cells: Importance for the rapid acquisition of potent migratory and functional activities. *Blood.* **98**, 3022-9 (2001).

88. Diamond, M. S. *et al.* Type I interferon is selectively required by dendritic cells for immune rejection of tumors. *J. Exp. Med.* **208**, 1989-2003 (2011).

89. Knutson, K. L. & Disis, M. L. Tumor antigen-specific T helper cells in cancer immunity and immunotherapy. *Cancer Immunology, Immunotherapy.* **54**, 721-8 (2005).

90. Hervas-Stubbs, S. *et al.* Effects of IFN-α as a signal-3 cytokine on human naïve and antigen-experienced CD8+ T cells. *Eur. J. Immunol.* **40**, 3389-402 (2010).

91. Fink, K. *et al.* Early type I interferon-mediated signals on B cells specifically enhance antiviral humoral responses. *Eur. J. Immunol.* **36**, 2094-105 (2006).

92. Broggi, A., Tan, Y., Granucci, F. & Zanoni, I. IFN-λ suppresses intestinal inflammation by non-translational regulation of neutrophil function. *Nat. Immunol.* **18**, 1084-1093 (2017).

93. Zanoni, I., Granucci, F. & Broggi, A. Interferon (IFN)-λ takes the helm: Immunomodulatory roles of type III IFNs. *Frontiers in Immunology.* **8**, 1661 (2017).

94. Finotti, G., Tamassia, N. & Cassatella, M. A. Synergistic production of TNFα and IFNα by human pDCs incubated with IFNλ3 and IL-3. *Cytokine.* **86**, 124-131 (2016).

95. Koltsida, O. *et al.* IL-28A (IFN-λ2) modulates lung DC function to promote Th1 immune skewing and suppress allergic airway disease. *EMBO Mol. Med.* **3**, 348-361 (2011).

96. Ank, N. *et al.* An Important Role for Type III Interferon (IFN-λ/IL-28) in TLR-Induced Antiviral Activity. *J. Immunol.* **180**, 2474–2485 (2008).

97. Souza-Fonseca-Guimaraes, F. *et al.* NK cells require IL-28R for optimal in vivo activity. *Proc. Natl. Acad. Sci. U. S. A.* **112**, E2376-84 (2015).

98. Wongthida, P. *et al.* Type III IFN interleukin-28 mediates the antitumor efficacy of oncolytic virus VSV in immune-competent mouse models of cancer. *Cancer Res.* **70**, 4539-49 (2010).

99. Witte, K. *et al.* Despite IFN- receptor expression, blood immune cells, but not keratinocytes or melanocytes, have an impaired response to type III interferons: Implications for therapeutic applications of these cytokines. *Genes Immun.* **10**, 702-14 (2009).

100. Kelly, A. *et al.* Immune Cell Profiling of IFN-λ Response Shows pDCs Express Highest Level of IFN-λR1 and Are Directly Responsive via the JAK-STAT Pathway. *J. Interf. Cytokine Res.* **36**, 671-680 (2016).

101. de Groen, R. A., Groothuismink, Z. M. A., Liu, B.-S. & Boonstra, A. IFN-λ is able to augment TLR-mediated activation and subsequent function of primary human B cells. *J. Leukoc. Biol.* **98**, 623-630 (2015).

102. Varricchi, G. *et al.* Are mast cells MASTers in cancer? *Frontiers in Immunology.* **8**, 424 (2017).

103. Krystel-Whittemore, M., Dileepan, K. N. & Wood, J. G. Mast cell: A multi-functional master cell. *Frontiers in Immunology.* **6**, 620 (2016).

104. Jamur, M. C. *et al.* Identification and characterization of undifferentiated mast cells in mouse bone marrow. *Blood.* **105**, 4282-9 (2005).

105. da Silva, E. Z. M., Jamur, M. C. & Oliver, C. Mast Cell Function: A New Vision of an Old Cell. *Journal of Histochemistry and Cytochemistry.* **62**, 698-738 (2014).

106. Rao, K. N. & Brown, M. A. Mast cells: Multifaceted immune cells with diverse roles in health and disease. *Annals of the New York Academy of Sciences.* **1143**, 83-104 (2008).

107. Caughey, G. H. Mast cell tryptases and chymases in inflammation and host defense. *Immunological Reviews.* **217**, 141-54 (2007).

108. Gri, G. *et al.* Mast cell: An emerging partner in immune interaction. *Frontiers in Immunology.* **3**, 120 (2012).

109. Moon, T. C. *et al.* Advances in mast cell biology: New understanding of heterogeneity and function. *Mucosal Immunology.* **3**, 111-28 (2010).

110. Dahl, C., Hoffmann, H. J., Saito, H. & Schiøtz, P. O. Human mast cells express receptors for IL-3, IL-5 and GM-CSF; a partial map of receptors on human mast cells cultured in vitro. *Allergy Eur. J. Allergy Clin. Immunol.* **59**, 1087-96 (2004).

111. Abraham, S. N. & St. John, A. L. Mast cell-orchestrated immunity to pathogens. *Nature Reviews Immunology.* **10**, 440-52 (2010).

112. Supajatura, V. *et al.* Differential responses of mast cell Toll-like receptors 2 and 4 in allergy and innate immunity. *J. Clin. Invest.* **109**, 1351-9 (2002).

113. St. John, A. L. & Abraham, S. N. Innate Immunity and Its Regulation by Mast Cells. *J. Immunol.* **109**, 4458-63 (2013).

114. Kumar, V. & Sharma, A. Mast cells: Emerging sentinel innate immune cells with diverse role in immunity. *Molecular Immunology.* **48**, 14-25 (2010).

115. Applequist, S. E. Variable expression of Toll-like receptor in murine innate and adaptive immune cell lines. *Int. Immunol.* **14**, 1065-74 (2002).

116. Kulka, M., Alexopoulou, L., Flavell, R. A. & Metcalfe, D. D. Activation of mast cells by double-stranded RNA: Evidence for activation through Toll-like receptor 3. *J. Allergy Clin. Immunol.* **114**, 174-82 (2004).

117. Urb, M. & Sheppard, D. C. The role of mast cells in the defence against pathogens. *PLoS Pathog.* **8**, (2012) doi:10.1371/journal.ppat.1002619.

118. Heib, V. *et al.* Mast cells are crucial for early inflammation, migration of Langerhans cells, and CTL responses following topical application of TLR7 ligand in mice. *Blood.* **110**, 946-53 (2007).

119. Suto, H. *et al.* Mast Cell-Associated TNF Promotes Dendritic Cell Migration. *J. Immunol.* **176**, 4102-12 (2006).

120. Bulfone-Paus, S. & Bahri, R. Mast cells as regulators of T cell responses. *Frontiers in Immunology.* **6**, 394 (2015).

121. Ott, V. L., Cambier, J. C., Kappler, J., Marrack, P. & Swanson, B. J. Mast cell-dependent migration of effector CD8+ T cells through production of leukotriene B4. *Nat. Immunol.* **4**, 974-81 (2003).

122. Yang, Z. *et al.* Mast cells mobilize myeloid-derived suppressor cells and Treg cells in tumor microenvironment via IL-17 pathway in murine hepatocarcinoma model. *PLoS One.* **5,** (2010) doi:10.1371/journal.pone.0008922.

123. Galli, S. J., Nakae, S. & Tsai, M. Mast cells in the development of adaptive immune responses. *Nature Immunology.* **6**, 135-42 (2005).

124. Suurmond, J. *et al.* Communication between human mast cells and CD4+ T cells through antigen-dependent interactions. *Eur. J. Immunol.* **43**, 1758-68 (2013).

125. Stelekati, E. *et al.* Mast Cell-Mediated Antigen Presentation Regulates CD8+ T Cell Effector Functions. *Immunity.* **31**, 665-76 (2009).

126. Gaudenzio, N., Laurent, C., Valitutti, S. & Espinosa, E. Human mast cells drive memory CD4+ T cells toward an inflammatory IL-22+ phenotype. *J. Allergy Clin. Immunol.* **131**, 1400-7 (2013).

127. Frandji, P. *et al.* Antigen-dependent stimulation by bone marrow-derived mast cells of MHC class II-restricted T cell hybridoma. *J. Immunol.* **151**, 6318–6328 (1993).

128. Malaviya, R., Ikeda, T., Ross, E. & Abraham, S. N. Mast cell modulation of neutrophil influx and bacterial clearance at sites of infection through TNF-α. *Nature.* **381**, 77-80 (1996).

129. Siebenhaar, F. *et al.* Control of Pseudomonas aeruginosa skin infections in mice is mast cell-dependent. *Am. J. Pathol.* **170**, 1910-6 (2007).

130. Shelburne, C. P. *et al.* Mast Cells Augment Adaptive Immunity by Orchestrating Dendritic Cell Trafficking through Infected Tissues. *Cell Host Microbe.* **6**, 331-42 (2009).

131. Sutherland, R. E., Olsen, J. S., McKinstry, A., Villalta, S. A. & Wolters, P. J. Mast Cell IL-6 Improves Survival from Klebsiella Pneumonia and Sepsis by Enhancing Neutrophil Killing. *J. Immunol.* **181**, 5598-5605 (2008).

132. Maurer, M. *et al.* Skin mast cells control T cell-dependent host defense in Leishmania major infections. *FASEB J.* **20**, 2460-7 (2006).

133. Orinska, Z. *et al.* TLR3-induced activation of mast cells modulates CD8+ T-cell recruitment. *Blood.* **106**, 978-87 (2005).

134. Piliponsky, A. M., Acharya, M. & Shubin, N. J. Mast cells in viral, bacterial, and fungal infection immunity. *Int. J. Mol. Sci.* **20**, 2851 (2019).

135. McAlpine, S. M., Enoksson, M., Lunderius-Andersson, C. & Nilsson, G. The effect of bacterial, viral and fungal infection on mast cell reactivity in the allergic setting. *Journal of Innate Immunity.* **3**, 120-30 (2011).

136. Al-Afif, A. *et al.* Respiratory syncytial virus infection of primary human mast cells induces the selective production of type i interferons, CXCL10, and CCL4. *J. Allergy Clin. Immunol.* **136**, 1346-54 (2015).

137. Graham, A. C., Hilmer, K. M., Zickovich, J. M. & Obar, J. J. Inflammatory Response of Mast Cells during Influenza A Virus Infection Is Mediated by Active Infection and RIG-I Signaling. *J. Immunol.* **190**, 4676-84 (2013).

138. Portales-Cervantes, L., Haidl, I. D., Lee, P. W. & Marshall, J. S. Virus-infected human mast cells enhance natural killer cell functions. *J. Innate Immun.* **9**, 94–108 (2017).

139. Portales-cervantes, L., Crump, O. M. & Dada, S. IL-4 Enhances Interferon Production by Virus-Infected Human Mast Cells. *J. Allergy Clin. Immunol.* (2020) doi:10.1016/j.jaci.2020.02.011.

140. Portales-Cervantes, L., Haidl, I. D., Lee, P. W. & Marshall, J. S. Virus-Infected Human Mast Cells Enhance Natural Killer Cell Functions. *J. Innate Immun.* **9**, 94–108 (2017).

141. Sellge, G. *et al.* Interferon-γ regulates growth and controls Fcγ receptor expression and activation in human intestinal mast cells. *BMC Immunol.* **15**, 27 (2014).

142. Crivellato, E., Nico, B. & Ribatti, D. Mast cells and tumour angiogenesis: New insight from experimental carcinogenesis. *Cancer Letters.* **269**, 1-6 (2008).

143. Gooch, J. L., Lee, A. V. & Yee, D. Interleukin 4 inhibits growth and induces apoptosis in human breast cancer cells. *Cancer Res.* **58**, 4199-205 (1998).

144. Plotkin, J. D. *et al.* Human mast cells from adipose tissue target and induce apoptosis of breast cancer cells. *Front. Immunol.* **10**, 138 (2019).

145. Maciel, T. T., Moura, I. C. & Hermine, O. The role of mast cells in cancers. *F1000Prime Rep.* **7**, 09 (2015).

146. Rigoni, A., Colombo, M. P. & Pucillo, C. The Role of Mast Cells in Molding the Tumor Microenvironment. *Cancer Microenviron.* **8**, 167-176 (2015).

147. Rajput, A. B. *et al.* Stromal mast cells in invasive breast cancer are a marker of favourable prognosis: A study of 4,444 cases. *Breast Cancer Res. Treat.* **107**, 249-57 (2008).

148. Chan, J. K. *et al.* Mast cell density, angiogenesis, blood clotting, and prognosis in women with advanced ovarian cancer. *Gynecol. Oncol.* **99**, 20-5 (2005).

149. Ruoss, S. J., Hartmann, T. & Caughey, G. H. Mast cell tryptase is a mitogen for cultured fibroblasts. *J. Clin. Invest.* **88**, 493-9 (1991).

150. Komi, D. E. A. & Redegeld, F. A. Role of Mast Cells in Shaping the Tumor Microenvironment. *Clinical Reviews in Allergy and Immunology.* (2019) doi:10.1007/s12016-019-08753-w.

151. Ribatti, D. & Crivellato, E. Mast cells, angiogenesis, and tumour growth. *Biochimica et Biophysica Acta - Molecular Basis of Disease.* **1822**, 2-8 (2012).

152. Aponte-López, A., Fuentes-Pananá, E. M., Cortes-Muñoz, D. & Muñoz-Cruz, S. Mast Cell, the Neglected Member of the Tumor Microenvironment: Role in Breast Cancer. *Journal of Immunology Research.* (2018) doi:10.1155/2018/2584243.

153. Rabenhorst, A. *et al.* Mast cells play a protumorigenic role in primary cutaneous lymphoma. *Blood.* **120**, 2042-2054 (2012).

154. Welsh, T. J. *et al.* Macrophage and mast-cell invasion of tumor cell islets confers a marked survival advantage in non-small-cell lung cancer. *J. Clin. Oncol.* **23**, 8959-67 (2005).

155. Samoszuk, M. & Corwin, M. A. Acceleration of tumor growth and peri-tumoral blood clotting by imatinib mesylate (Gleevectm). *Int. J. Cancer.* **106**, 647-52 (2003).

156. Oldford, S. A. & Marshall, J. S. Mast cells as targets for immunotherapy of solid tumors. *Molecular Immunology.* **63**, 113-24 (2015).

157. Soucek, L. *et al.* Modeling pharmacological inhibition of mast cell degranulation as a therapy for insulinoma. *Neoplasia.* **13**, 1093-110 (2011).

158. Melillo, R. M. *et al.* Mast cells have a protumorigenic role in human thyroid cancer. *Oncogene.* **29**, 6203-15 (2010).

159. Pittoni, P. *et al.* Mast cell targeting hampers prostate adenocarcinoma development but promotes the occurrence of highly malignant neuroendocrine cancers. *Cancer Res.* **71**, 5987-97 (2011).

160. Öhrvik, H. *et al.* Mast cells promote melanoma colonization of lungs. *Oncotarget* **7**, 68990-69001 (2016).

161. Oldford, S. A. *et al.* A Critical Role for Mast Cells and Mast Cell-Derived IL-6 in TLR2-Mediated Inhibition of Tumor Growth. *J. Immunol.* **185**, 7067-76 (2010).

162. Drobits, B. *et al.* Imiquimod clears tumors in mice independent of adaptive immunity by converting pDCs into tumor-killing effector cells. *J. Clin. Invest.* **122**, 575-85 (2012).

163. Soule, B. P. *et al.* Effects of Gamma Radiation on FcεRI and TLR-Mediated Mast Cell Activation. *J. Immunol.* **179**, 3276-86 (2007).

164. Sato, A., Ohtsuki, M., Hata, M., Kobayashi, E. & Murakami, T. Antitumor Activity of IFN-λ in Murine Tumor Models. *J. Immunol.* **176**, 7686-94 (2006).

165. Steen, H. C. & Gamero, A. M. Interferon-lambda as a potential therapeutic agent in cancer treatment. *Journal of Interferon and Cytokine Research.* **30**, 597-602 (2010).

166. Dull, T. *et al.* A Third-Generation Lentivirus Vector with a Conditional Packaging System. *J. Virol.* **72**, 8463-71 (1998).

167. Li, Q. *et al.* Interferon-λ induces G1 phase arrest or apoptosis in oesophageal carcinoma cells and produces anti-tumour effects in combination with anti-cancer agents. *Eur. J. Cancer.* **46**, 180-90 (2010).

168. Staker, B. L. *et al.* The mechanism of topoisomerase I poisoning by a camptothecin analog. *Proc. Natl. Acad. Sci. U. S. A.* **99**, 15387-92 (2002).

169. Vestergaard, A. L., Knudsen, U. B., Munk, T., Rosbach, H. & Martensen, P. M. Transcriptional expression of type-I interferon response genes and stability of housekeeping genes in the human endometrium and endometriosis. *Mol. Hum. Reprod.* **17**, 243-54 (2011).

170. Wolters, P. J. *et al.* Tissue-selective mast cell reconstitution and differential lung gene expression in mast cell-deficient KitW-sh/KitW-sh sash mice. *Clin. Exp. Allergy.* **35**, 82–88 (2005).

171. Dickensheets, H., Sheikh, F., Park, O., Gao, B. & Donnelly, R. P. Interferon-lambda (IFN- λ) induces signal transduction and gene expression in human hepatocytes, but not in lymphocytes or monocytes. *J. Leukoc. Biol.* **93**, 377-385 (2013).

172. Reber, L. L., Marichal, T. & Galli, S. J. New models for analyzing mast cell functions in vivo. *Trends in Immunology.* **33**, 613-25 (2012).

173. Gujar, S. *et al.* Multifaceted therapeutic targeting of ovarian peritoneal carcinomatosis through virus-induced immunomodulation. *Mol. Ther.* **21**, 338-347 (2013).

174. Rutkowski, M. R. *et al.* Microbially driven TLR5-dependent signaling governs distal malignant progression through tumor-promoting inflammation. *Cancer Cell.* **27**, 27-40 (2015).

175. Lilla, J. N. *et al.* Reduced mast cell and basophil numbers and function in Cpa3-Cre; Mcl-1 fl/fl mice. *Blood.* **118**, 6930–6938 (2011).

176. Fakhrjou, A. *et al.* The relationship between histologic grades of invasive carcinoma of breast ducts and mast cell infiltration. *South Asian J. Cancer.* **5**, 5-7 (2016).

177. Della Rovere, F. *et al.* Mast cells in invasive ductal breast cancer: Different behavior in high and minimum hormone-receptive cancers. *Anticancer Res.* **27,** 2465-71 (2007).

178. Sang, J., Yi, D., Tang, X., Zhang, Y. & Huang, T. The associations between mast cell infiltration, clinical features and molecular types of invasive breast cancer. *Oncotarget.* **7,** 81661-81669 (2016).

179. Glajcar, A. *et al.* The relationship between breast cancer molecular subtypes and mast cell populations in tumor microenvironment. *Virchows Arch.* **470,** 505-515 (2017).

180. Reddy, S. M. *et al.* Long-term survival outcomes of triple-receptor negative breast cancer survivors who are disease free at 5 years and relationship with low hormone receptor positivity. *Br. J. Cancer.* **118,** 17-23 (2018).

181. Johansson, A. *et al.* Mast cells are novel independent prognostic markers in prostate cancer and represent a target for therapy. *Am. J. Pathol.* **177,** 1031-1041 (2010).

182. Dabiri, S. *et al.* The presence of stromal mast cells identifies a subset of invasive breast cancers with a favorable prognosis. *Mod. Pathol.* **17,** 690-5 (2004).

183. Mantri, C. K. & St. John, A. L. Immune synapses between mast cells and γδ T cells limit viral infection. *J. Clin. Invest.* **129,** 1094-1108 (2019).

184. Karkeni, E. *et al.* Vitamin D controls tumor growth and CD8+ T Cell infiltration in breast cancer. *Front. Immunol.* **10,** 1307 (2019).

185. Meng, S. *et al.* Distribution and prognostic value of tumor-infiltrating T cells in breast cancer. *Mol. Med. Rep.* **18**, 4247–4258 (2018).

186. De Palma, M., Biziato, D. & Petrova, T. V. Microenvironmental regulation of tumour angiogenesis. *Nature Reviews Cancer.* **17**, 457–474 (2017).

187. Snoderly, H. T., Boone, B. A. & Bennewitz, M. F. Neutrophil extracellular traps in breast cancer and beyond: Current perspectives on NET stimuli, thrombosis and metastasis, and clinical utility for diagnosis and treatment. *Breast Cancer Research.* **21,** (2019).

188. Provance, O. K. & Lewis-Wambi, J. Deciphering the role of interferon alpha signaling and microenvironment crosstalk in inflammatory breast cancer. *Breast Cancer Research.* **21,** (2019).

189. Ahmed, F. *et al.* Mutations in Human Interferon α2b Gene and Potential as Risk Factor Associated with Female Breast Cancer. *Cancer Biother. Radiopharm.* **31**, 199-208 (2016).

190. Doherty, M. R. *et al.* Interferon-beta represses cancer stem cell properties in triple-negative breast cancer. *Proc. Natl. Acad. Sci. U. S. A.* **114**, 13792-13797 (2017).

191. Gough, D. J., Messina, N. L., Clarke, C. J. P., Johnstone, R. W. & Levy, D. E. Constitutive Type I Interferon Modulates Homeostatic Balance through Tonic Signaling. *Immunity.* **36**, 166-74 (2012).

192. Sommereyns, C., Paul, S., Staeheli, P. & Michiels, T. IFN-lambda (IFN-λ) is expressed in a tissue-dependent fashion and primarily acts on epithelial cells in vivo. *PLoS Pathog.* **4,** (2008) doi:10.1371/journal.ppat.1000017.

193. Bracarda, S. *et al.* Randomized prospective phase II trial of two schedules of sorafenib daily and interferon-α2a (IFN) in metastatic renal cell carcinoma (RAPSODY): GOIRC Study 0681. *J. Clin. Oncol.* **25**, 5100 (2007).

194. Murakami, S. *et al.* Effects of ionizing radiation on differentiation of murine bone marrow cells into mast cells. *J. Radiat. Res.* **56**, 865-871 (2015).

195. Gossen, M. *et al.* Transcriptional activation by tetracyclines in mammalian cells. *Science.* **268**, 1766-9 (1995).

196. Forero, A. *et al.* Differential Activation of the Transcription Factor IRF1 Underlies the Distinct Immune Responses Elicited by Type I and Type III Interferons. *Immunity.* **51,** 451-464 (2019).

197. Musa, M. Cell Proliferation Study of Human Osteosarcoma Cell Line (U2OS) using Alamar Blue Assayand Live Cell Imaging. *IOSR J. Dent. Med. Sci.* (2013) doi:10.9790/0853-0826065.

198. Young, J. D., Liu, C. C., Butler, G., Cohn, Z. A. & Galli, S. J. Identification, purification, and characterization of a mast cell-associated cytolytic factor related to tumor necrosis factor. *Proc. Natl. Acad. Sci. U. S. A.* **84,** 9175-9 (1987).

199. Piliponsky, A. M. *et al.* Mast cell-derived TNF can exacerbate mortality during severe bacterial infections in C57BL/6-KitW-sh/W-sh mice. *Am. J. Pathol.* **176,** 926-38 (2010).

200. Nigrovic, P. A. *et al.* Genetic inversion in mast cell-deficient Wsh mice interrupts corin and manifests as hematopoietic and cardiac aberrancy. *Am. J. Pathol.* **173,** 1693-1701 (2008).

201. Tunis, M. C., Dawicki, W., Carson, K. R., Wang, J. & Marshall, J. S. Mast cells and IgE activation do not alter the development of oral tolerance in a murine model. *J. Allergy Clin. Immunol.* **130,** 705-715 (2012).

202. Desfarges, S. & Ciuffi, A. Retroviral integration site selection. *Viruses.* **2,** 111-130 (2010).

203. Fantozzi, A. & Christofori, G. Mouse models of breast cancer metastasis. *Breast Cancer Research.* **8,** 212 (2006).

204. Chheda, Z. S., Sharma, R. K., Jala, V. R., Luster, A. D. & Haribabu, B. Chemoattractant Receptors BLT1 and CXCR3 Regulate Antitumor Immunity by Facilitating CD8 + T Cell Migration into Tumors. *J. Immunol.* **197,** 2016-26 (2016).

APPENDIX

Table 1. Effect of local mast cell reconstitution of the mammary fat pad on immune populations in the spleen in tumour-bearing mice

	Mean ± SEM (Cell number)			P value	
Immune cell subset	**C57BL/6**	**Wsh**	**Recon Wsh**	**C57BL/6 vs. Wsh**	**Wsh vs. Recon Wsh**
B cells	64313392 ± 4836196	37080059 ± 5141757	49837919 ± 5141757	0.0083**	0.4124
Follicular B cells	50470420 ± 3524806	28572802 ± 3962878	39053589 ± 7237754	0.01**	0.5692
Marginal Zone B cells	5425801 ± 712285	3840151 ± 725685	4343344 ± 817369	0.2879	>0.9999
NK cells	4206426 ± 1067482	3878755 ± 1293529	2714211 ± 663494	0.7488	>0.9999
Inflammatory Monocytes	2551735 ± 161818	2919197 ± 679524	2487147 ± 706218	>0.9999	>0.9999
Neutrophils	6793012 ± 1136763	11726091 ± 3293821	7733397 ± 1899615	0.5781	0.6787
Resting Macrophages	4603622 ± 304655	5152422 ± 1125750	5057614 ± 932758	>0.9999	>0.9999
DCs	1968720 ± 210600	1379653 ± 247383	1798713 ± 364197	0.2172	0.6877
$CD4_+$ T cells	17152520 ± 1242689	12267965 ± 1770128	16090855 ± 2740428	0.1172	0.4793
$CD69_+$ $CD4_+$ T cells	1917970 ± 314063	926659 ± 196858	1240045 ± 200809	0.0119*	0.5229
Effector memory $CD4_+$ T cells	3156387 ± 357213	1832475 ± 291636	2619267 ± 420657	0.0234	0.3640
Central memory $CD4_+$ T cells	1442052 ± 181072	872088 ± 191136	1143884 ± 174116	0.1931	0.6581
Naïve $CD4_+$ T cells	10993736 ± 762291	7757160 ± 1072678	10512293 ± 1942682	0.0898	0.4339
T_{regs}	1387012 ± 111827	832615 ± 125710	1048036 ± 205184	0.0234*	0.8009
$CD8_+$ T cells	12007740 ± 896452	7891249 ± 1283473	10190540 ± 1703826	0.0348*	0.5105
$CD69_+$ $CD8_+$ T cells	337301 ± 59092	174133 ± 28020	269122 ± 35567	0.01**	0.0271*
Effector memory $CD8_+$ T cells	358801 ± 59892	242858 ± 41810	410883 ± 107063	0.5276	>0.9999

Central memory CD8+ T cells	2237296 ± 160518	1410851 ± 211817	1901709 ± 253767	0.0130*	0.0652
Naïve CD8+ T cells	8915447 ± 717009	5501701 ± 838477	7065586 ± 1509104	0.0376*	0.8076

Statistical significance was assessed by assessed by one-way ANOVA followed by a Kruskal-Wallis multiple comparisons test* = $p > 0.05$, ** = $p > 0.01$.

Table 2. Effect of local mast cell reconstitution of the mammary fat pad on immune populations in the non-reconstituted inguinal lymph node in tumour-bearing mice

	Mean ± SEM (Cell number)			P value	
Immune cell subset	**C57BL/6**	**Wsh**	**Recon Wsh**	**C57BL/6 vs. Wsh**	**Wsh vs. Recon Wsh**
B cells	1126752 ± 777949	396578 ± 62518	399933 ± 75537	>0.9999	>0.9999
NK cells	17817 ± 6729	18783 ± 7420	47628 ± 26891	>0.9999	0.95
CD4+ T cells	543555 ± 143859	455377 ± 117719	652586 ± 158050	>0.9999	0.8754
CD69+ CD4+ T cells	321089 ± 146523	186052 ± 40356	261700 ± 91708	>0.9999	>0.9999
Effector memory CD4+ T cells	40572 ± 12908	31111 ± 8240	42824 ± 10660	>0.9999	>0.9999
Central memory CD4+ T cells	47046 ± 24870	20518 ± 5425	31875 ± 7937	0.6599	0.6817
Naïve CD4+ T cells	430420 ± 108785	368955 ± 104495	543389 ± 133934	0.9833	0.7493
T_{regs}	57491 ± 21096	44322 ± 11120	59837 ± 14597	>0.9999	>0.9999
CD8+ T cells	579078 ± 155393	437710 ± 105684	589967 ± 144319	>0.9999	>0.9999
CD69+ CD8+ T cells	27425 ± 7657	21557 ± 5946	28986 ± 8340	0.9833	>0.9999
Effector memory CD8+ T cells	11058 ± 2544	7646 ± 1232	12326 ± 3270	>0.9999	>0.9999
Central memory CD8+ T cells	90507 ± 27709	69586 ± 17076	91609 ± 24703	>0.9999	>0.9999
Naïve CD8+ T cells	439812 ± 123217	322941 ± 92525	447589 ± 115261	0.812	0.8999

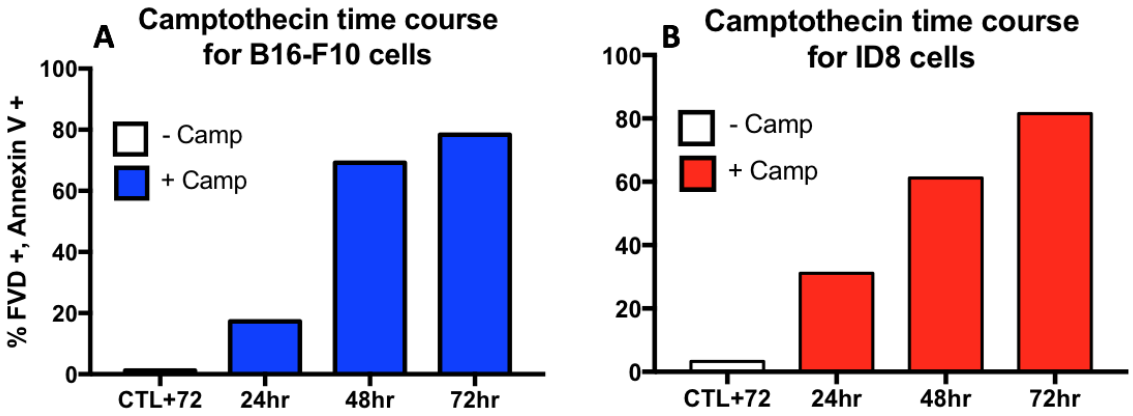

Appendix Figure 1. Camptothecin induces apoptosis in B16-F10 and ID8 cells, which increases over time. B16-F10 and ID8 cells were seeded on a 6 well plate and treated with 12 μM camptothecin to assess the induction of apoptosis measured by expression of annexin V and FVD by flow cytometry. Cells were harvested at 3 different time points, 24, 48, and 72 hours post-treatment. A control group of cells was left untreated and was harvested after 72 hours to assess induction of apoptosis in the absence of camptothecin (CTL+72). N = 1.

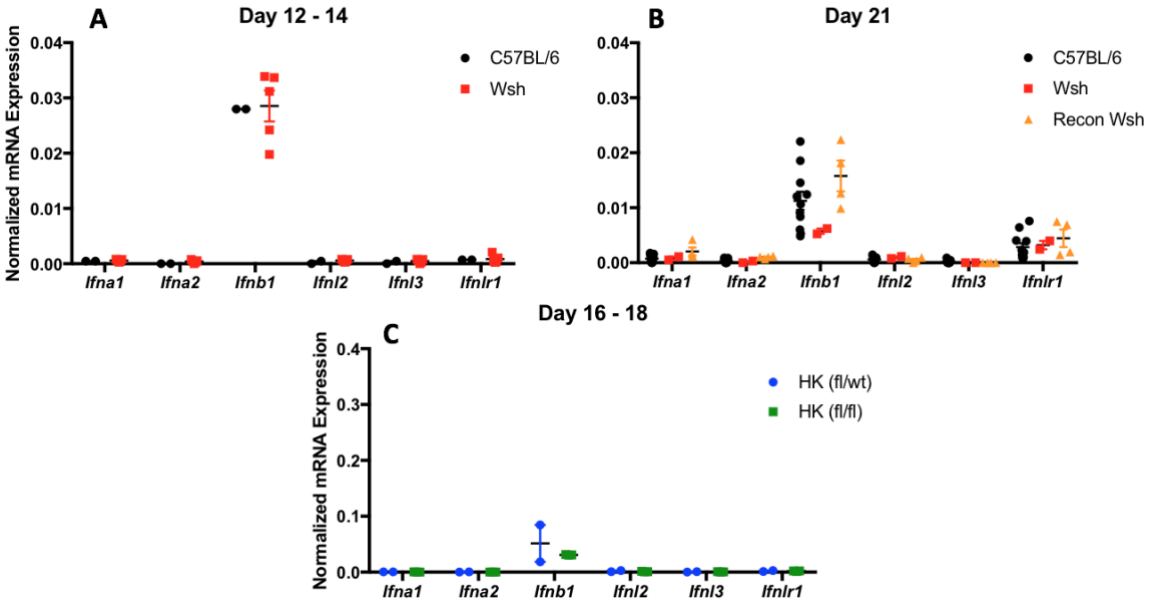

Appendix Figure 2. Type I and III IFN expression in the E0771 TME shows no consistent trends in both models of mast cell-deficiency across all other measured timepoints during tumour growth. A group of Wsh mice were subcutaneously injected with 2.0x10$_6$ WT BMMCs into the mammary fat pad and rested for 6 weeks to allow for mast cell reconstitution (Recon Wsh). These mice were challenged in parallel with age-matched C57BL/6 and control Wsh mice with 2.0x10$_5$ E0771 cells suspended in Matrigel injected subcutaneously into the mammary fat pad to monitor tumour growth over 21 days. If tumours reached >2000 mm$_3$, mobility was affected, the mice lost 15% or more of their initial body weight, or the tumour ulcerated, the mice were sacrificed and tumour tissue was harvested to perform RNA isolation. An array of type I and III IFN genes were assessed by RT-qPCR, which included *Ifna1, Ifna2, Ifnb1, Ifnl2, Ifnl3,* and *Ifnlr1*. RNA data was collected in groups, organized in increments based on day of sacrifice to account for changes in gene expression occurring over time. This data was collected with data shown in **Figure 3.6**. Data represents gene expression from C57BL/6, Wsh, and Recon Wsh sacrificed on Day 12 -14 (**A**) or Day 21 (**B**) or HK (fl/wt) or HK (fl/fl) mice sacrificed on Day 16 – 18 (**C**). Data are shown as mean ± SEM.

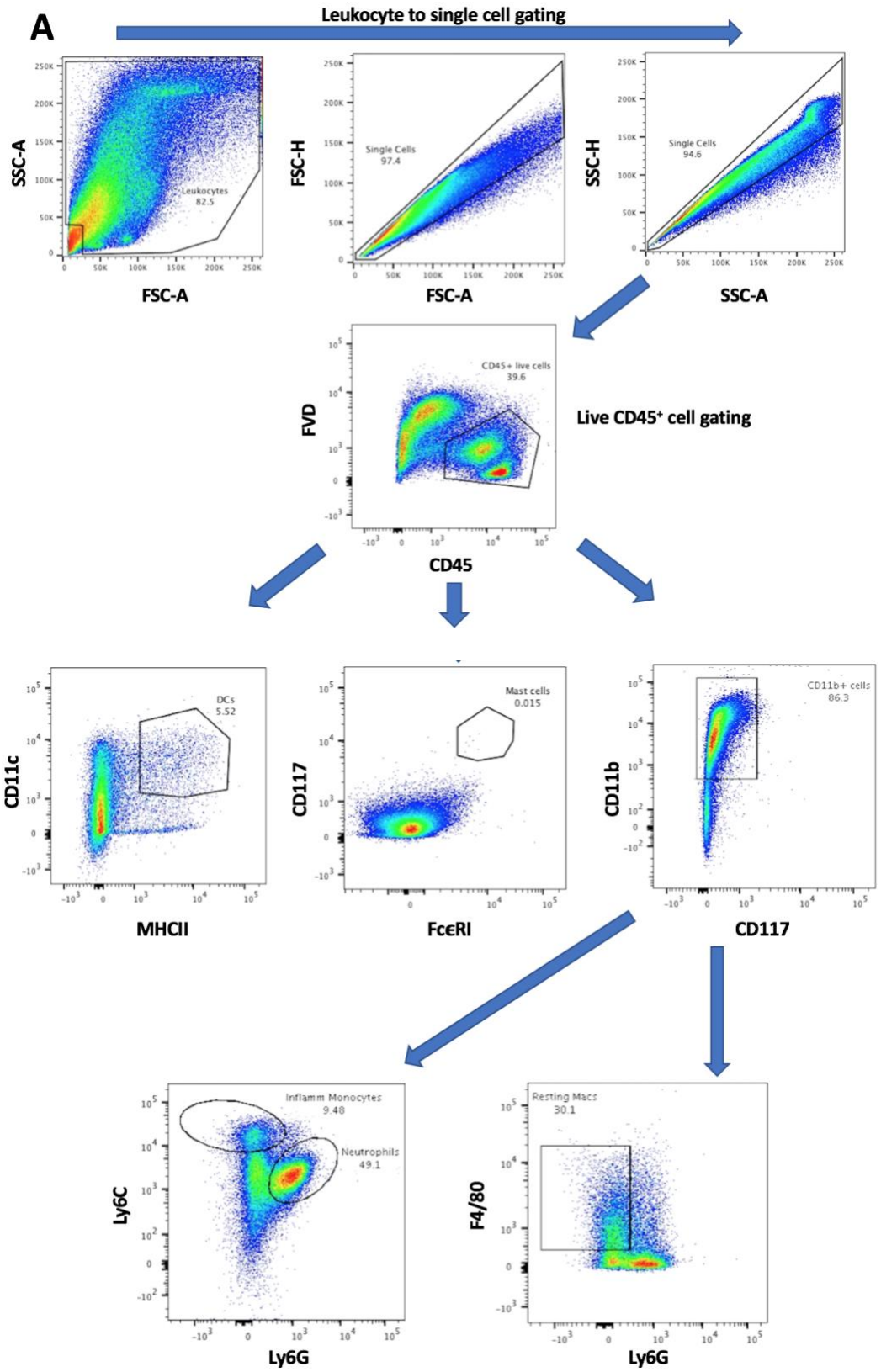
A
Leukocyte to single cell gating
SSC-A
FSC-A
Leukocytes
82.5
FSC-H
FSC-A
Single Cells
97.4
SSC-H
SSC-A
Single Cells
94.6
FVD
CD45
CD45+ live cells
39.6
Live CD45+ cell gating
CD11c
MHCII
DCs
5.52
CD117
FcεRI
Mast cells
0.015
CD11b
CD117
CD11b+ cells
86.3
Ly6C
Ly6G
Inflamm Monocytes
9.48
Neutrophils
49.1
F4/80
Ly6G
Resting Macs
30.1

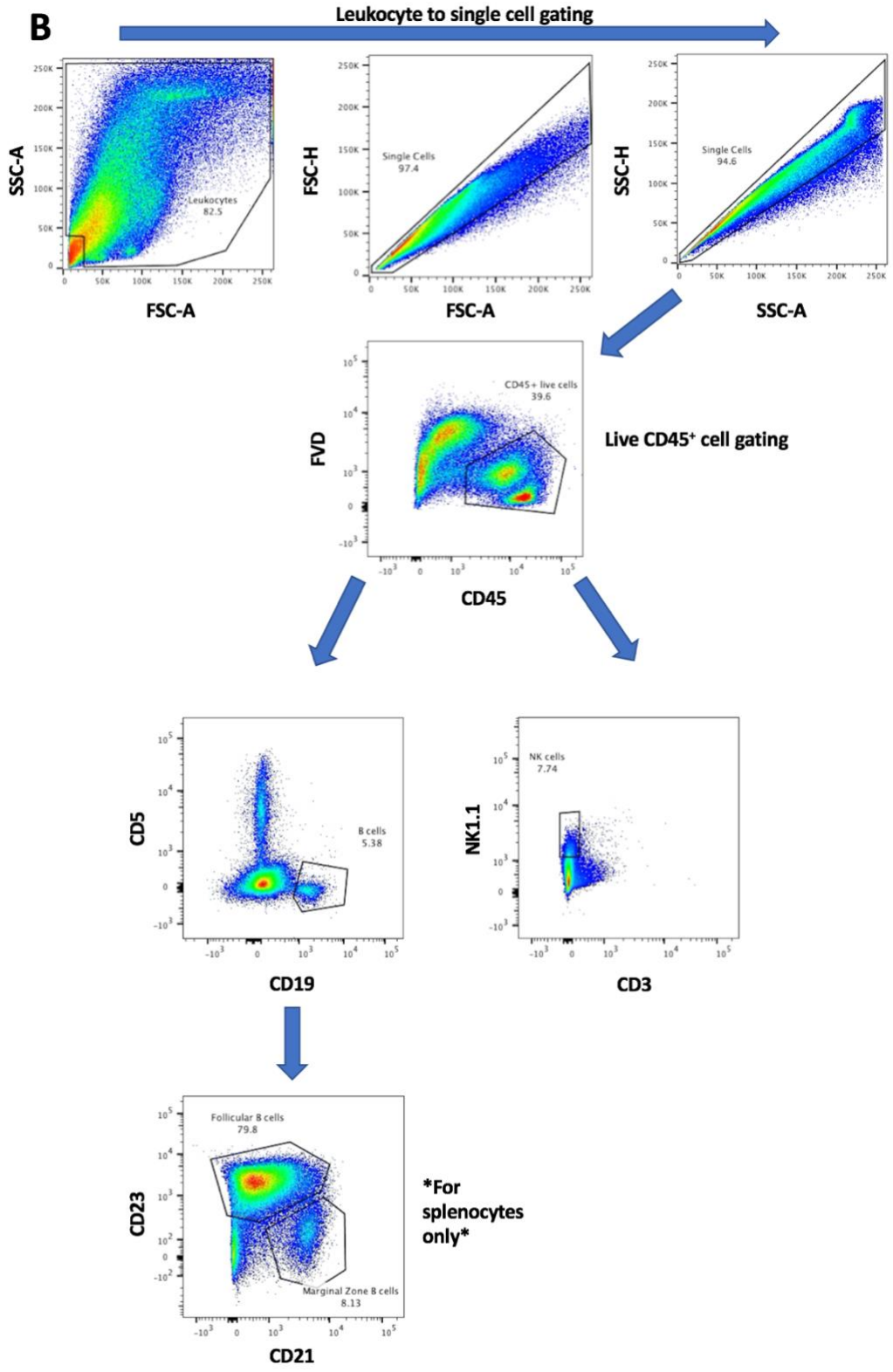
B
Leukocyte to single cell gating
SSC-A
FSC-A
Leukocytes
82.5
FSC-H
FSC-A
Single Cells
97.4
SSC-H
SSC-A
Single Cells
94.6
FVD
CD45
CD45+ live cells
39.6
Live CD45+ cell gating
CD5
CD19
B cells
5.38
NK1.1
CD3
NK cells
7.74
CD23
CD21
Follicular B cells
79.8
Marginal Zone B cells
8.13
*For
splenocytes
only*

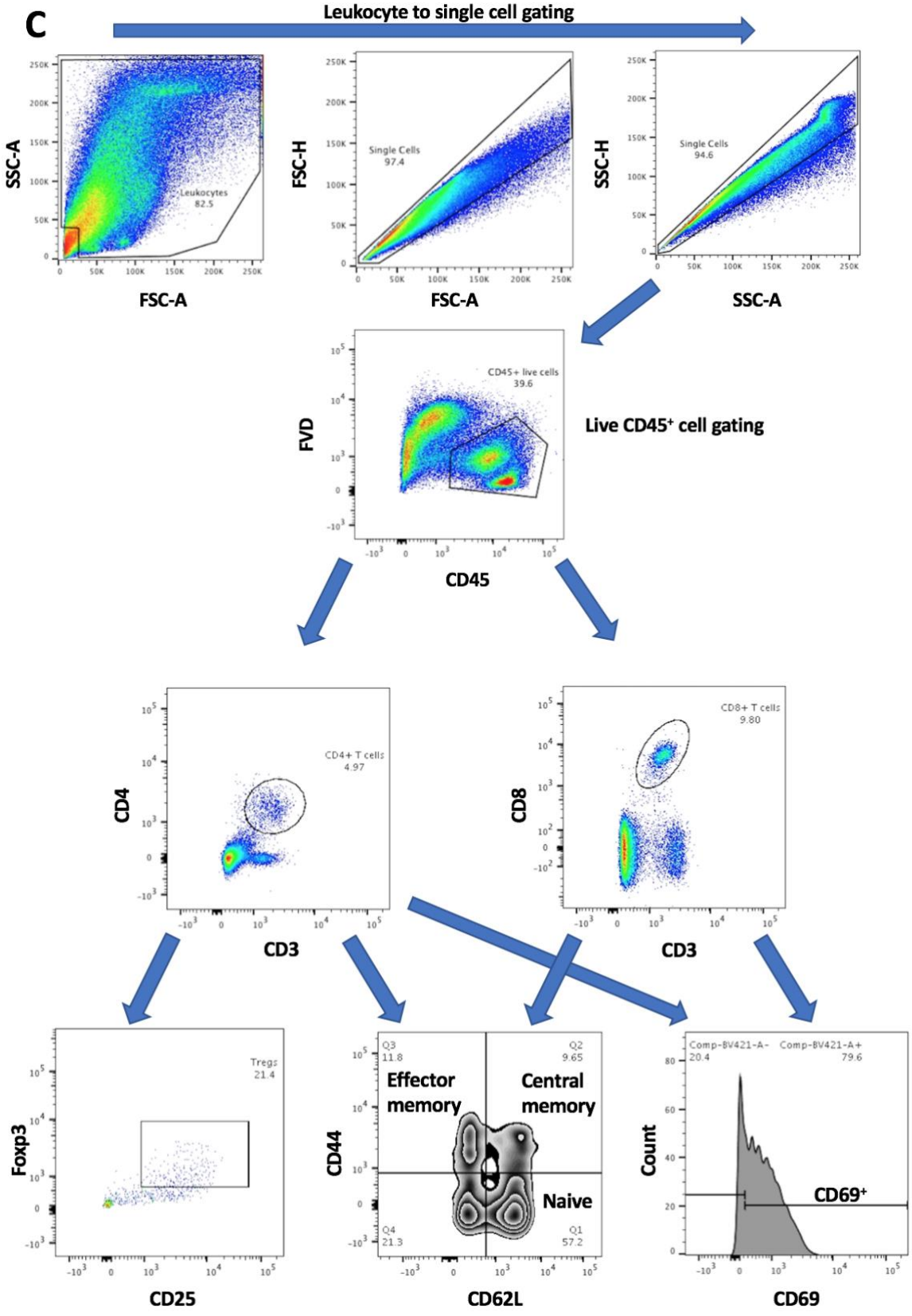
C
Leukocyte to single cell gating
SSC-A
FSC-A
Leukocytes
82.5
FSC-H
FSC-A
Single Cells
97.4
SSC-H
SSC-A
Single Cells
94.6
FVD
CD45
CD45+ live cells
39.6
Live CD45+ cell gating
CD4
CD3
CD4+ T cells
4.97
CD8
CD3
CD8+ T cells
9.80
Foxp3
CD25
Tregs
21.4
CD44
CD62L
Q3
11.8
Effector memory
Q2
9.65
Central memory
Naive
Q4
21.3
Q1
57.2
Count
CD69
Comp-BV421-A-
20.4
Comp-BV421-A+
79.6
CD69+

Appendix Figure 3. Gating strategy for immune cell subsets. Innate and adaptive immune cell numbers were analyzed to determine the impact of mast cell reconstitution or of recombinant IFN injection at different tissue sites, which included tumour, spleen, lymph nodes and the peritoneal cavity. Harvested cells were stained antibodies for immune cell markers depicted in **Table 2.2** and were analyzed by flow cytometry. The gating strategy for identifying myeloid cell subsets (**A**), B and NK cells (**B**) and T cells (**C**) are depicted above.

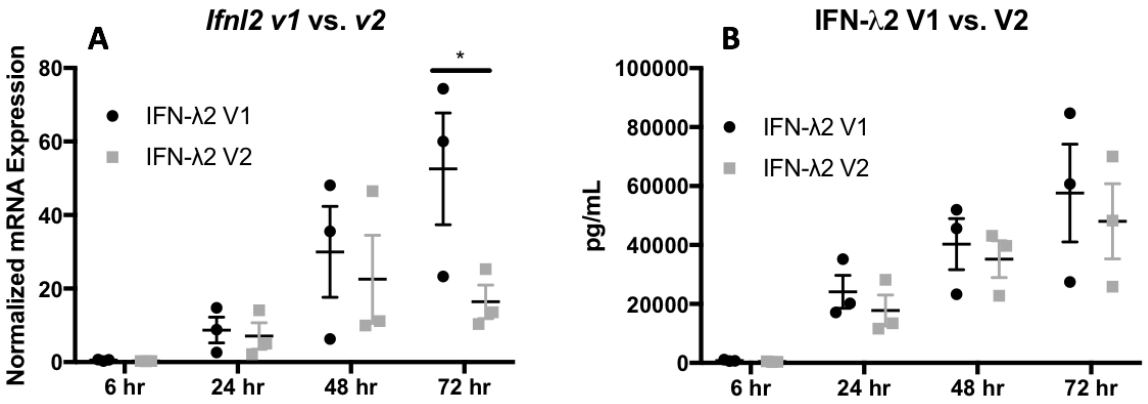

Appendix Figure 4. IFN-λ2-U2-OS cells significantly upregulated IFN-λ2 V1 mRNA expression compared to IFN-λ2 V2 mRNA after 72 hours of doxycycline administration, however this did not translate to a significant difference in IFN-λ2 protein production at this time point. U2-OS cells transduced with IFN-λ2 V1 or V2 were activated with 0.5 μg/mL doxycycline every 24 hours. Cells and supernatant were collected at four different time points, 6, 24, 48, and 72 hours, to assess the level of IFN-λ2 mRNA expression (**A**) and protein production (**B**) by RT-qPCR and ELISA, respectively. This data represents a comparison between only doxycycline-activated U2-OS cells transduced with either IFN-λ2 V1 or V2 and is represented individually with unstimulated controls in **Figure 3.11**. Statistical significance was determined using a two-way ANOVA comparing IFN-λ2 V1 and V2 mRNA expression and protein production at each individual time point. Data are shown as mean ± SEM. N = 3. * = $p > 0.05$.

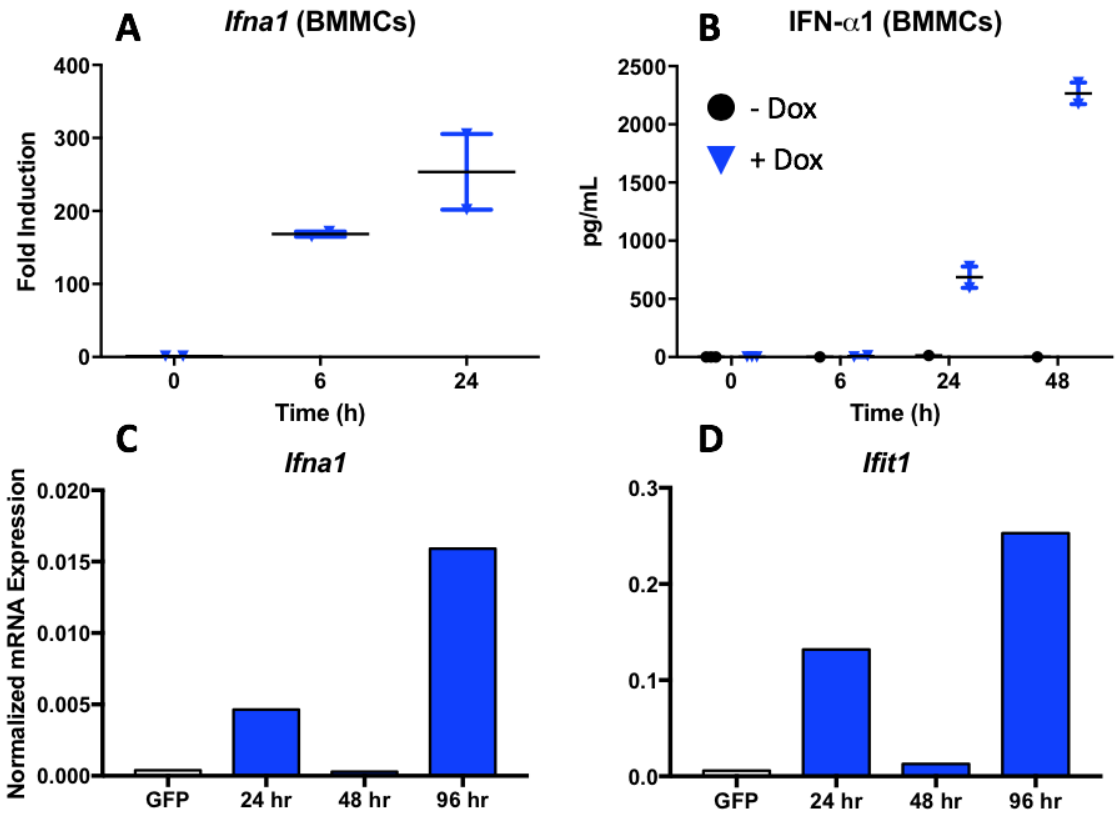

Appendix Figure 5. IFN-α1-BMMCs produce doxycycline-dependent IFN-α1 mRNA and protein *in vitro* and *in vivo*. IFN-α1-BMMCs (N = 2) were cultured *in vitro* and stimulated with 0.5 ug/mL doxycycline. Cells were harvested after 0, 6, 24, and 48 hours to analyze for IFN-α1 gene expression (**A**) and protein production (**B**) by RT-qPCR and ELISA, respectively. Male Wsh mice were injected intraperitoneally with 3.0x10$_6$ BMMCs transduced with GFP or IFN-α1 (N = 1) and rested for 6 weeks to allow for reconstitution. Mice were fed doxycycline via chow and peritoneal cells were harvested after 24, 48, and 96 hours to determine *Ifna1* (**C**) and *Ifit1* (**D**) expression by RT-qPCR. RT-qPCR data is represented as fold induction for *in vitro* analysis compared to unstimulated controls. *In vivo* gene expression data was normalized to *Hprt* and *Gusb*. Experiments were performed by Dr. Ian Haidl and Nong Xu. Data are shown as mean ± SEM.